Quantifying and Comparing the Pattern of Thalamic and Cortical Projections to the Posterior Auditory Field in Hearing and Deaf Cats

Blake E. Butler,[1,2,4] Nicole Chabot,[1,2,4] and Stephen G. Lomber[1,2,3,4,5]*

[1]Cerebral Systems Laboratory, University of Western Ontario, London, Ontario, Canada N6A 5C2
[2]Department of Physiology and Pharmacology, University of Western Ontario, London, Ontario, Canada N6A 5C1
[3]Department of Psychology, University of Western Ontario, London, Ontario, Canada N6A 5C2
[4]Brain and Mind Institute, University of Western Ontario, London, Ontario, Canada N6A 5B7
[5]National Centre for Audiology, University of Western Ontario, London, Ontario, Canada N6G 1H1

ABSTRACT

Following sensory loss, compensatory crossmodal reorganization occurs such that the remaining modalities are functionally enhanced. For example, behavioral evidence suggests that peripheral visual localization is better in deaf than in normal hearing animals, and that this enhancement is mediated by recruitment of the posterior auditory field (PAF), an area that is typically involved in localization of sounds in normal hearing animals. To characterize the anatomical changes that underlie this phenomenon, we identified the thalamic and cortical projections to the PAF in hearing cats and those with early- and late-onset deafness. The retrograde tracer biotinylated dextran amine was deposited in the PAF unilaterally, to label cortical and thalamic afferents. Following early deafness, there was a significant decrease in callosal projections from the contralateral PAF. Late-deaf animals showed small-scale changes in projections from one visual cortical area, the posterior ectosylvian field (EPp), and the multisensory zone (MZ). With the exception of these minor differences, connectivity to the PAF was largely similar between groups, with the principle projections arising from the primary auditory cortex (A1) and the ventral division of the medial geniculate body (MGBv). This absence of large-scale connectional change suggests that the functional reorganization that follows sensory loss results from changes in synaptic strength and/or unmasking of subthreshold intermodal connections. J. Comp. Neurol. 000:000–000, 2016.

INDEXING TERMS: anatomical connectivity; auditory deprivation; BDA; crossmodal plasticity; RRID: AB_2336249; RRID: AB_10123643; RRID: AB_10120127; RRID: AB_2315331; RRID: nif-0000-10294

Neural plasticity refers to the capacity of the brain to undergo experience-dependent adaptation to best perceive those stimuli most frequently encountered by an organism. In the case of sensory deprivation, compensatory changes take place such that brain regions that typically respond to the missing modality are reorganized to contribute to the remaining senses. For example, in deaf animals, areas that normally respond to sound are activated by visual (Neville et al., 1983; Finney et al., 2001, 2003; Lee et al., 2001; Lambertz et al., 2005; Pekkola et al., 2005; Lomber et al., 2010; Meredith et al., 2011; Karns et al., 2012) or somatosensory stimuli (Levänen et al., 1998; Levänen and Hamdorf, 2001; Allman et al., 2009; Bhattacharjee et al., 2010; Meredith and Lomber, 2011; Karns et al., 2012). This crossmodal reorganization is often considered to be beneficial, as it has been shown to result in functional enhancement of the remaining sensory modalities. For example, deaf individuals demonstrate greater accuracy in identifying and localizing peripheral visual stimuli than individuals with normal hearing (e.g., Neville et al., 1983; Stevens and Neville, 2006). This

Grant sponsor: Canadian Institutes of Health Research; Grant sponsor: Natural Sciences and Engineering Research Council of Canada; Grant sponsor: Canada Foundation for Innovation.

*CORRESPONDENCE TO: Stephen G. Lomber, The University of Western Ontario, Medical Sciences Building, Room 216, 1151 Richmond Street North, London, Ontario, N6A 5C1, Canada. E-mail:steve.lomber@uwo.ca

Received December 4, 2015; Revised March 21, 2016;
Accepted March 24, 2016.
DOI 10.1002/cne.24005
Published online Month 00, 2016 in Wiley Online Library (wileyonlinelibrary.com)

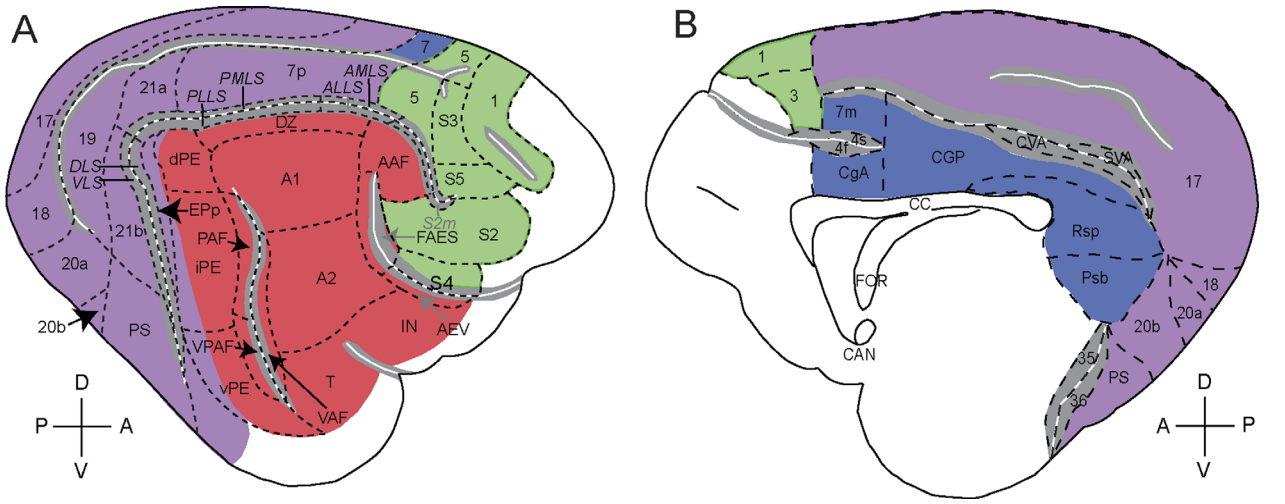

Figure 1. Lateral (**A**) and medial (**B**) depictions of the cat brain. The auditory (red), visual (purple), somatomotor (green), and other (blue) cortical areas analyzed in this study are highlighted. The bottom of each sulcus is represented by a white line, and the cortex in the bank is gray. Dashed lines indicate cortical area borders. Dorsoventral and anteroposterior axes are indicated at bottom left. For abbreviations, see list.

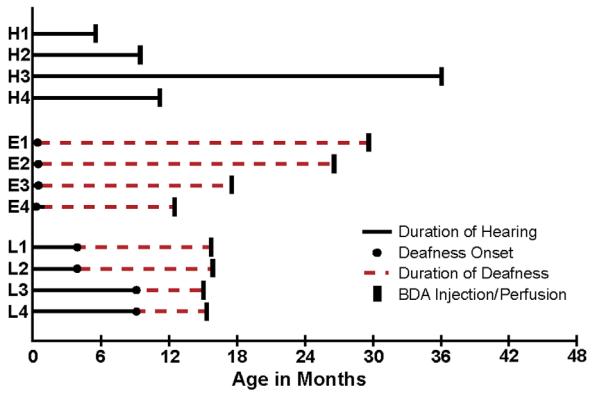

Figure 2. Experimental timeline for the 12 cats examined. The duration of hearing is illustrated in solid black lines, and deafness onset is indicated by solid black circles. The duration of deafness is represented by dashed red lines. After a period of deafness lasting at least 6 months, or after at least 6 months of age in hearing animals, retrograde BDA injections were made in the PAF, and animals were perfused (vertical lines). The age at the onset of deafness (early vs. late) was significantly different ($t(6) = 3.7172$, $P < 0.01$).

reorganization occurs, at least in part, through the recruitment of areas of cortex that would normally process sound. Interestingly, investigations using animal models have demonstrated that reassigned cortical areas change the sensory modality to which they respond, but contribute to the same function in the replacement modality. For example, while sound localization is impaired following reversible deactivation of the posterior auditory field (PAF) in hearing cats (Malhotra et al., 2004; Malhotra and Lomber, 2007; Lomber and Malhotra, 2008), the same manipulation affects peripheral visual localization in deaf animals (Lomber et al., 2010).

The evidence that behavioral changes following sensory loss result from crossmodal plasticity between sensory brain structures is compelling. However, the extent of change following sensory loss has repeatedly been shown to depend upon the time at which deprivation began (Cohen et al., 1999; Sadato et al., 2002; Sadato, 2006; Chabot et al., 2007, 2015; Kok et al., 2014). The capacity for reorganization is widely understood to be greatest in the developing brain, particularly during windows of heightened plasticity, referred to as critical periods (Hensch, 2004; Sharma et al., 2005, 2009). However, some degree of plasticity remains throughout adulthood and likely facilitates changes in the aged brain; for example, crossmodal reorganization results in somatosensory processing in the auditory cortex of the ferret even following late-onset hearing loss (Allman et al., 2009). Thus, while neural plasticity provides the basis for crossmodal compensation following sensory loss, the areas that undergo change, and the degree to which they are reorganized, is expected to depend on the age at which sensory input is lost.

In addition to developmental factors, the degree to which an area of sensory cortex is susceptible to crossmodal reorganization appears to depend on its position within the hierarchy of processing. Primary sensory cortices have been shown to contain fewer crossmodal projections than nonprimary fields (Budinger et al., 2000). This pattern appears to be reflected in the

TABLE 1.
Milestones in Cat Auditory Development

Milestone	Supporting evidence	Postnatal age	Reference
External auditory meatus opens	Ear canal visible	10–15 days	Webster and Martin, 1991 Chabot et al., 2015
Cochlear maturation	Adult-like patterns of discharge from cochlear nucleus neurons	2 weeks (high frequency) 4 weeks (low frequency)	Brugge et al., 1978
	Frequency-specific 2-DG labeling	35 days	Webster and Martin, 1991
Auditory cortex maturation	Adult-like wave VII latency	3 months	Walsh et al., 1985
	Adult-like laminar organization and midlatency evoked potential amplitudes	4 months	Kral et al., 2005
	Adult-like long latency potential amplitudes	6 months	
Sexual maturity	Onset of estrous cycle in females and fertile ejaculate in males	6 months	Concannon, 1991

degree to which these fields are altered following sensory loss, with primary fields undergoing minimal crossmodal reorganization. For example, electrophysiological studies of the cat primary auditory cortex (A1) fail to demonstrate crossmodal activity (Stewart and Starr, 1970; Kral et al., 2003), or find that reorganization takes place only when the onset of deafness occurs within the first postnatal week (Rebillard et al., 1977). Indeed, an anatomical examination of the changes in projections to A1 following the onset of hearing loss shows only small-scale crossmodal changes that depend on age at deafness onset (Chabot et al., 2015). In contrast, the anterior auditory field (AAF) is also considered to be a core field of the cat auditory cortex, but has been shown to undergo considerable crossmodal reorganization (Meredith and Lomber, 2011) and changes in connectivity to nonauditory cortical areas in the deaf (Wong et al., 2015).

Anatomical studies have placed the PAF just above the core areas of the auditory cortex (A1 and AAF) in the hierarchy of processing (Lee and Winer, 2011). This organization is reinforced by electrophysiological studies demonstrating that response latencies of PAF neurons exceed those of neurons in A1 and AAF, and that deactivation of A1 results in a decrease in the response strength of PAF neurons (Carrasco and Lomber, 2009, 2013). Indeed, there is behavioral evidence that crossmodal reorganization occurs in the PAF following hearing loss; deaf animals show superior localization in the peripheral visual field compared with normal hearing controls—an advantage that is lost following deactivation of the PAF (Lomber et al., 2010). Thus, visual localization in the deaf is mediated by an auditory cortical field (the PAF), presumably due to the enhanced crossmodal processing that occurs following the loss of auditory input. A recent anatomical study also noted that the mean fractional volume of the auditory cortex occupied by the PAF is increased relative to normal hearing animals following both early- and late-onset hearing loss (Wong et al., 2014). While it is possible that reorganization following sensory loss may arise, at least in part, from altered thalamocortical circuits (Antonini et al., 1999), the changes in connectivity to thalamic and other cortical areas that underlie

Abbreviations

A1	primary auditory cortex
A2	second auditory cortex
AAF	anterior auditory field
ABR	auditory brainstem response
AES	anterior ectosylvian sulcus
AEV	anterior ectosylvian visual area
ALLS	anterolateral lateral suprasylvian visual area
BDA	biotinylated dextran amine
BOLD	blood oxygen-level-dependent
dB nHL	decibels normal hearing level
DLS	dorsal lateral suprasylvian area
dPE	dorsal posterior ectosylvian gyrus
DZ	dorsal zone of auditory cortex
EEG	electroencephalography
EPp	posterior ectosylvian field
fAES	auditory field of the anterior ectosylvian sulcus
HRP	horseradish peroxidase
IN	insular auditory area
iPE	intermediate division of the posterior ectosylvian auditory cortex
LP	lateral posterior nucleus
MGB	medial geniculate body
MGBd	dorsal division of the medial geniculate body
MGBm	medial division of the medial geniculate body
MGBv	ventral division of the medial geniculate body
MZ	multisensory zone
PAF	posterior auditory field
PES	posterior ectosylvian sulcus
PLLS	posterolateral lateral suprasylvian visual area
S2	secondary somatosensory area
S4	fourth somatosensory area
T	temporal area
V1	primary visual cortex
VAF	ventral auditory field
VLS	ventral lateral suprasylvian area
VPAF	ventroposterior auditory field
vPE	ventral posterior ectosylvian gyrus

functional and volumetric changes remain unknown. Thus, the goals of this study were to quantify the thalamocortical and corticocortical projections (Fig. 1) to the PAF in hearing animals, and to compare this pattern with those of animals that experienced early- and late-onset hearing loss.

MATERIALS AND METHODS

A total of 12 adult cats were obtained from a U.S. Department of Agriculture–licensed commercial breeding facility (Liberty Laboratories, Waverly, NY). An illustrated timeline for all three groups (four normal hearing controls, four early-deaf, and four late-deaf) is presented in Figure 2, and a list of developmental milestones in the cat is provided in Table 1. The kitten cochlea is immature at birth, and undergoes maturation throughout the first 4 weeks of postnatal life (Brugge et al., 1978; Webster and Martin, 1991). Moreover, aminoglycosides have been shown to be ineffective at elevating thresholds if administered prior to the onset of hearing (Shepherd and Martin, 1995). Thus, bilateral hearing loss was induced in the four early-deaf animals shortly after hearing onset (mean age of 23.5 days) to provide a model of hearing loss during the critical period for normal development of auditory function, when the potential for neural plasticity is greatest (Lewis and Maurer, 2009). In the four late-deaf animals, hearing loss was induced at no earlier than 3.7 months of age (late-deaf), to provide a model in which auditory input is removed from a normally developed auditory system near or following the closure of this critical period. The exact point at which auditory cortex is considered fully developed depends upon the measure of development chosen. For example, Kral and colleagues (2005) have suggested that laminar properties and response amplitudes of midlatency evoked potentials are mature by 4 months of age, while longer latency potentials continue to mature up to an age of 6 months. However, the latency of wave 7 in the cat evoked potential (a cortical component corresponding to the midlatency wave P_a in humans; Erwin and Buchwald,) matures before 3 months of age (Walsh et al., 1985). In the current study, late-deaf animals were deafened at a mean age of 6.3 months, shortly after the suggested age of sexual maturity (6 months; Concannon, 1991). All surgical and experimental procedures were conducted in accordance with the Canadian Council on Animal Care's *Guide to the Care and Use of Experimental Animals* (Olfert, 1993) and were approved by the University of Western Ontario Animal Use Subcommittee of the University Council on Animal Care.

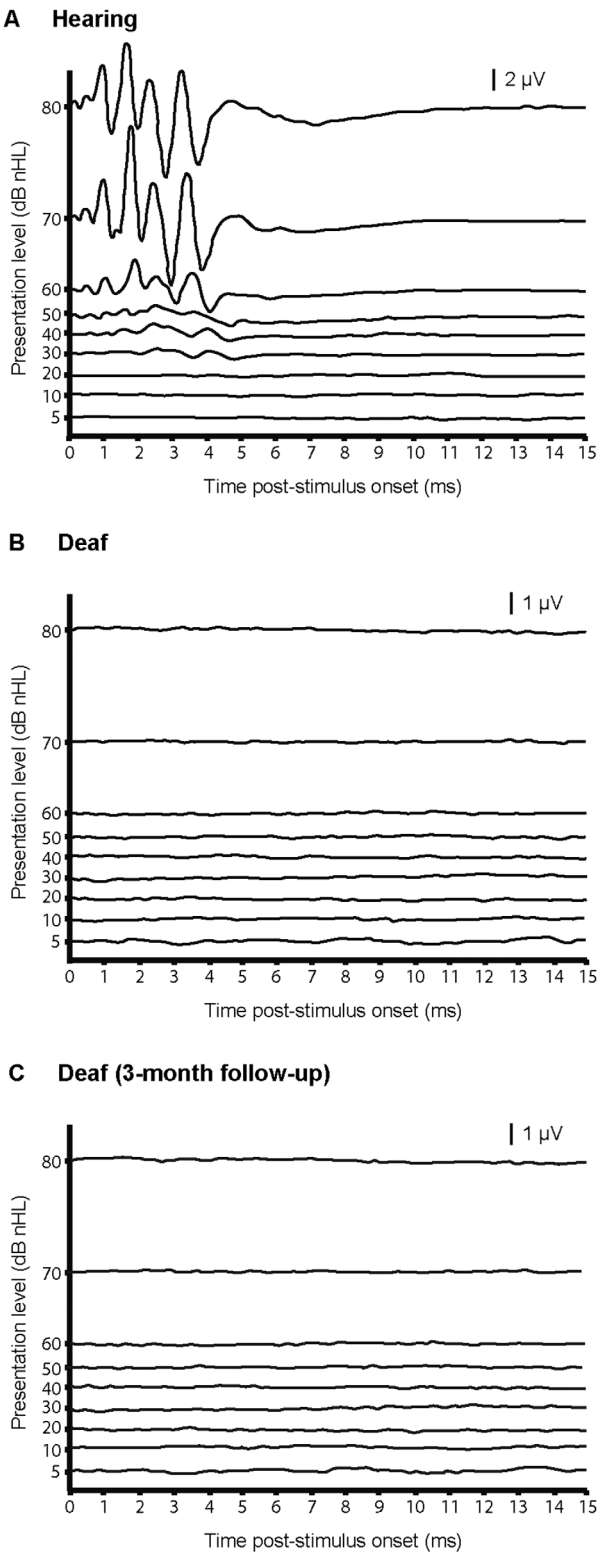

Figure 3. Auditory brainstem responses (ABRs) to click stimuli of increasing sound intensities up to 80 dB nHL. **A:** In the hearing cat, typical responses were observed with peaks that decreased in amplitude and increased in latency with decreasing stimulus intensity. **B:** Representative ABR from a cat immediately after deafness onset. **C:** A 3-month post deafness onset follow-up ABR from the same animal in B. Scale bars are provided in each panel.

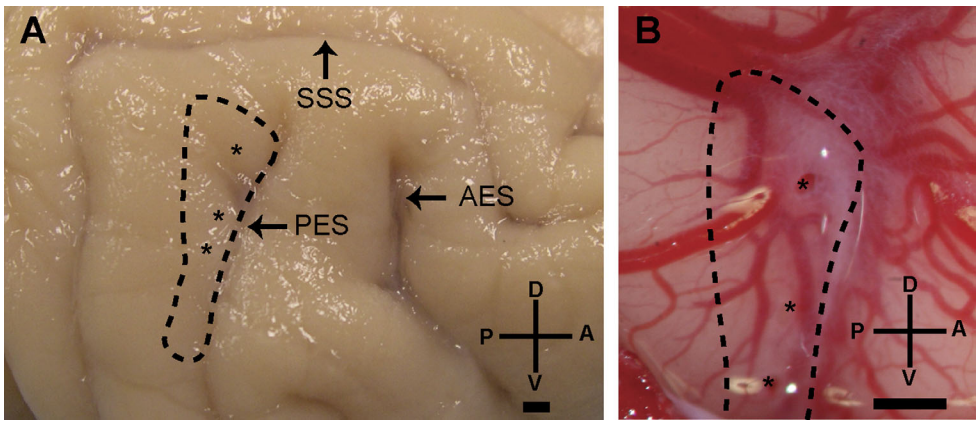

Figure 4. Injection locations in the PAF. **A:** Lateral view of the right hemisphere post perfusion (H1). The asterisks indicate the locations of the three penetrations. **B:** Enlargement of the exposed PAF from the same animal following craniotomy and BDA injection. The perimeter of the PAF is noted by a black dashed line. AES, anterior ectosylvian sulcus; PES, posterior ectosylvian sulcus; SSS, suprasylvian sulcus. Scale bar = 1 mm in A&B. A, anterior; D, dorsal; P, posterior; V, ventral.

Onset of deafness

Permanent threshold shifts were induced ototoxically in all deaf animals through the coadministration of kanamycin (300 mg/kg) and ethacrynic acid (10 mg/ml to effect; Valeant Pharmaceuticals, Laval, Quebec). In combination, these drugs cause hair cell destruction in the cochlea, resulting in a permanent profound hearing loss (Xu et al. 1993). Prior to the procedure, anesthesia was induced through the spontaneous inhalation of oxygen (1 L/min) and isoflurane (5% to effect for induction followed by 1.5–2% for maintenance). In all cases, baseline hearing thresholds (Fig. 3A) were measured, and hearing status was determined to be normal using auditory brainstem responses (ABRs) elicited by click stimuli (0.1 ms squarewave; normal hearing confirmed by the presence of an ABR signal at or below 20 dB nHL) presented through ER3A foam insert headphones (Etymotic Research, Elk Grove Village, IL). Electroencephalography (EEG) leads were placed subdermally behind the right and left ears, with a reference lead at the vertex, and a ground at the lower back. Animals received a subcutaneous injection of kanamycin (300 mg/kg), and an infusion of ethacrynic acid was delivered via an intravenous catheter placed in the cephalic vein of the forelimb (to effect: 35–60 mg/kg). ABR measurements were repeated continuously until waveforms were no longer present in response to bilaterally presented 80 dB nHL clicks (Fig. 3B). Since click-evoked ABRs have been shown to reflect audiometric thresholds across a wide frequency range (Picton et al., 1977; Munnerley et al., 1991), the absence of an evoked response to bilateral stimulation provided evidence of successful bilateral deafening. At this point, the ethacrynic acid infusion was stopped, and was replaced by an infusion of lactated Ringer's solution (4 ml/kg IV). Following this, the catheter was removed, and the animals were allowed to recover from the anesthetic. Follow-up ABRs were measured 3 months after the onset of deafness to confirm a permanent threshold shift (Fig. 3C).

Tracer deposits

At least 6 months following the onset of deafness, or at a minimum of 6 months of age in hearing animals, injections of BDA were made into the right hemisphere. Approximately 18 hours prior to surgery, cats were fasted and lightly anesthetized with ketamine (4 mg/kg IM) and dexdomitor (0.05 mg/kg IM). An antiinflammatory medication was administered (dexamethasone, 0.05 mg/kg IM), and a catheter was inserted into the cephalic vein to allow for administration of anesthetic during surgery; the catheter was flushed with heparinized saline. On the day of surgery, each animal received doses of atropine (0.02 mg/kg SC) to minimize respiratory and alimentary secretions, acepromazine (0.02 mg/kg SC), dexamethasone (0.5 mg/kg IV), and buprenorphine (0.01 mg/kg SC). General anesthesia was then induced using sodium pentobarbital (25 mg/kg to effect IV). Animals were intubated following the application of Cetecaine (a topical anesthetic) onto the pharyngeal walls to inhibit the gag reflex. Each animal had its head shaved and was stabilized in a stereotaxic apparatus. The cats were then prepared for surgery using antiseptic procedures. Vital signals including respiration rate, blood pressure, and heart rate were monitored throughout the procedure, and body temperature was maintained at 37°C using water-filled heating pads (Gaymar, Orchard Park, NY).

TABLE 2.
Primary Antibody Used

Antibody	Immunogen	Source, host species, cat#, RRID	Concentration
SMI-32	Dephosphorylated epitope on medium- and high-molecular-weight subunits of the neurofilament triplet	Covance Research, mouse monoclonal, cat# SMI-32, RRID:AB_2315331	0.05 μg/ml

A midline incision was made, and the right temporalis muscle was reflected laterally. A craniotomy was made that extended from the anterior ectosylvian sulcus (AES) to the posterior suprasylvian sulcus, and from the middle suprasylvian sulcus to the ventral border of the PAF. The piece of bone was removed and the dura was reflected laterally. Biotinylated dextran amine (BDA; 3,000 MW [10%]; Vector, Burlingame, CA, cat# SP-1140; RRID:AB_2336249) was pressure-injected (Nanoliter 2000, World Precision Instruments, Sarasota, FL) through a glass pipette. While BDA 3k does provide some anterograde labeling, it is principally a robust retrograde pathway tracer (Reiner et al., 2000) that is more sensitive than horseradish peroxidase (HRP), and has been shown to label afferent projections more reliably than biocytin or neurobiotin (Lapper and Bolam, 1991). The PAF is a large field, typically extending in the dorsoventral plane from the dorsal tip of the posterior ectosylvian sulcus (PES), to its ventral limit approximately halfway along the length of PES. In the anterior-posterior plane, the PAF extends from the fundus of the PES, up the posterior bank of the PES, and includes the anterior 1/3 of the posterior ectosylvian gyrus. Thus, to label a substantial subsection of this area and ensure that the tracer spread was confined to the PAF, injections were made at three pipette penetrations spanning the length of the PAF in the right hemisphere (Fig. 4). In each case, the pipette tip was placed just posterior to the PES, and the angle of insertion was perpendicular to the cortical surface. At each penetration, a 150-nl deposit was made at a depth of 1200 μm from the cortical surface to target deep cortical layers, and a second 150-nl deposit was made 500 μm from the cortical surface to target more superficial layers. Three minutes passed after each injection before the pipette was moved. When all three penetrations (six injections total) were completed, the brain was photographed to provide a record of the location of injection sites (Fig. 4B), and the craniotomy was closed with dental acrylic anchored to stainless steel skull screws. Once the acrylic had hardened, cats were transitioned to isoflurane anesthesia (via spontaneous inhalation; 1.5%). Finally, lidocaine was subcutaneously injected around the incision margin, and the incision was closed.

Postsurgical procedures

When a swallowing reflex was evident, cats were extubated, venous catheters were removed, and a subcutaneous bolus of lactated Ringer's solution was given. Vital signs continued to be monitored until the animal was sternally recumbent. Buprenorphine (0.01 mg/kg SC) was administered every 6 hours for the first 24 hours after surgery, and every 12 hours for the subsequent 72 hours. Animals also received dexamethasone every 24 hours after the surgery (0.05 mg/kg on day 1, decreasing by 0.01 mg/kg each day thereafter). In all cases, recovery was uneventful.

Perfusion and tissue processing

Two weeks after BDA deposits were made, a catheter was placed in the cephalic vein, and each animal was deeply anesthetized with sodium pentobarbital (30 mg/kg IV), and heparin (1 cc; anticoagulant) and 1% sodium nitrite (1 cc; vasodilator) were administered. Animals were then intracardially perfused through the ascending aorta with 1 L of physiological saline, followed by 2 L of fixative solution (4% paraformaldehyde), and 2 L of 10% sucrose solution to cryoprotect the tissue. Each solution was buffered to a pH of 7.4 with 0.1 M Sorenson's buffer and infused at a rate of 100 ml/min. Once perfused, heads were mounted in a stereotaxic frame, and brains were exposed and blocked in the coronal plane at Horsley–Clarke (Horsley and Clarke, 1908) level A27. Brains were then removed from the cranium, photographed (Fig. 4A), and immersed in a 30% sucrose solution to cryoprotect them for histological processing.

Brains were frozen, and 60-μm serial sections were cut in the coronal plane using a Leica CM 3050s cryostat (Leica Microsystems, Nussloch, Germany). Six series of sections at 360-μm intervals were collected in total. One series was immunohistochemically processed to reveal the presence of BDA using the avidin–biotin peroxidase method (Covance Research, Cumberland, VA, cat# SMI-32R-100; RRID: AB_10123643; Covance Research, cat# SMI-5010C-2000; RRID: AB_10120127), with nickel-cobalt intensification (Veenman et al., 1992). To assist with laminar and other border distinctions, three of the remaining series were processed using the monoclonal antibody SMI-32 (Covance

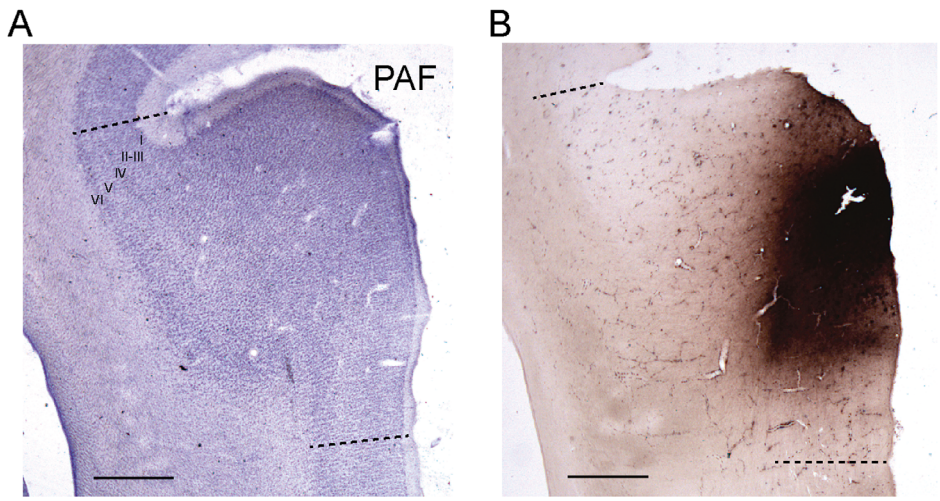

Figure 5. Photomicrographs of coronal sections through the posterior auditory field (PAF) showing a representative injection site (H4). **A:** Section stained with Nissl. **B:** Adjacent section processed for BDA and showing the injection spread. The tracer was limited to the boundaries of the PAF, while spanning all six layers of the neocortex. Nissl, along with SMI-32 and cytochrome oxidase (CO) (not shown), were used to identify the boundaries of cortical areas. Scale bar = 1 mm in A,B.

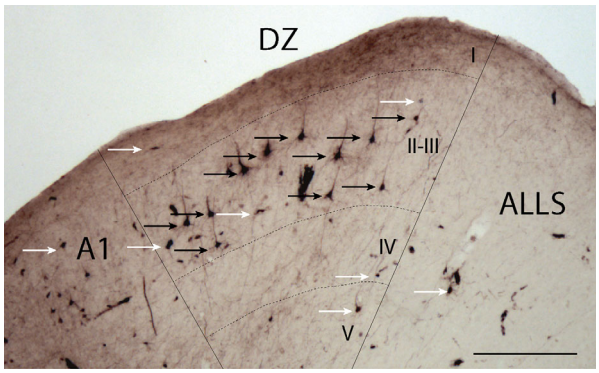

Figure 6. Labeled neurons in the auditory cortex (dorsal zone) following injections in the PAF. The black arrows indicate labeled neurons. For a neuron to be counted, the nucleus had to be visible and the entirety of the somatic membrane had to be present. The white arrows point to neurons that are too faintly labeled to be counted, or to artifactual staining. For abbreviations, see list. Scale bar = 50 μm. Right is medial.

Research, cat# SMI-32; RRID: AB_2315331; Table 2), cytochrome oxidase (Payne and Lomber, 1996), or cresyl violet stain to label Nissl bodies. The remaining series were retained as spares and were processed using the above methods when necessary. All tissue was mounted onto gelatin-coated slides, air-dried, cleared, and coverslipped.

Antibody characterization

The monoclonal antibody SMI-32 has an affinity for a dephosphorylated epitope on the medium- and high-molecular-weight subunits of neurofilament proteins (Sternberger and Sternberger, 1983), results in robust labeling of pyramidal cells and dendrites in the cat sensory cortices (van der Gucht et al., 2001; Mellott et al., 2010), and allows for the identification of subdivisions in the cat thalamus (Bickford et al., 1998).

Data analysis

Neurons labeled with BDA were examined using a Nikon E600 microscope equipped with Nomarski DIC imaging and mounted with a DXM 1200 digital camera. Tissue and injection sites were outlined, and neurons were labeled using a PC-driven motorized stage controlled by Neurolucida software (MBF Bioscience, Williston, VT; RRID: nif-0000-10294). A representative visualization of tracer spread in the current study is illustrated in Figure 5. To obtain an unbiased and comprehensive sample, the Neurolucida 'Meander Scan' paradigm was used to systematically mark and count labeled cells. Using the criteria of Kok and colleagues (2014), neurons were counted only if the entirety of the soma was labeled; partial cell bodies or dendritic branches alone were not quantified, to exclude artifacts of the reaction process, and thus a conservative estimate of neuronal projections was measured (Fig. 6). Neurons within the injection site or within the lateral extent of the injection were not counted, to avoid inclusion of labeled neurons located within the PAF. The full thickness of each slice was examined by taking focal levels throughout the z-plane. Importantly, differences between groups cannot be attributed to the age of the animal at injection/perfusion, as retrograde labeling

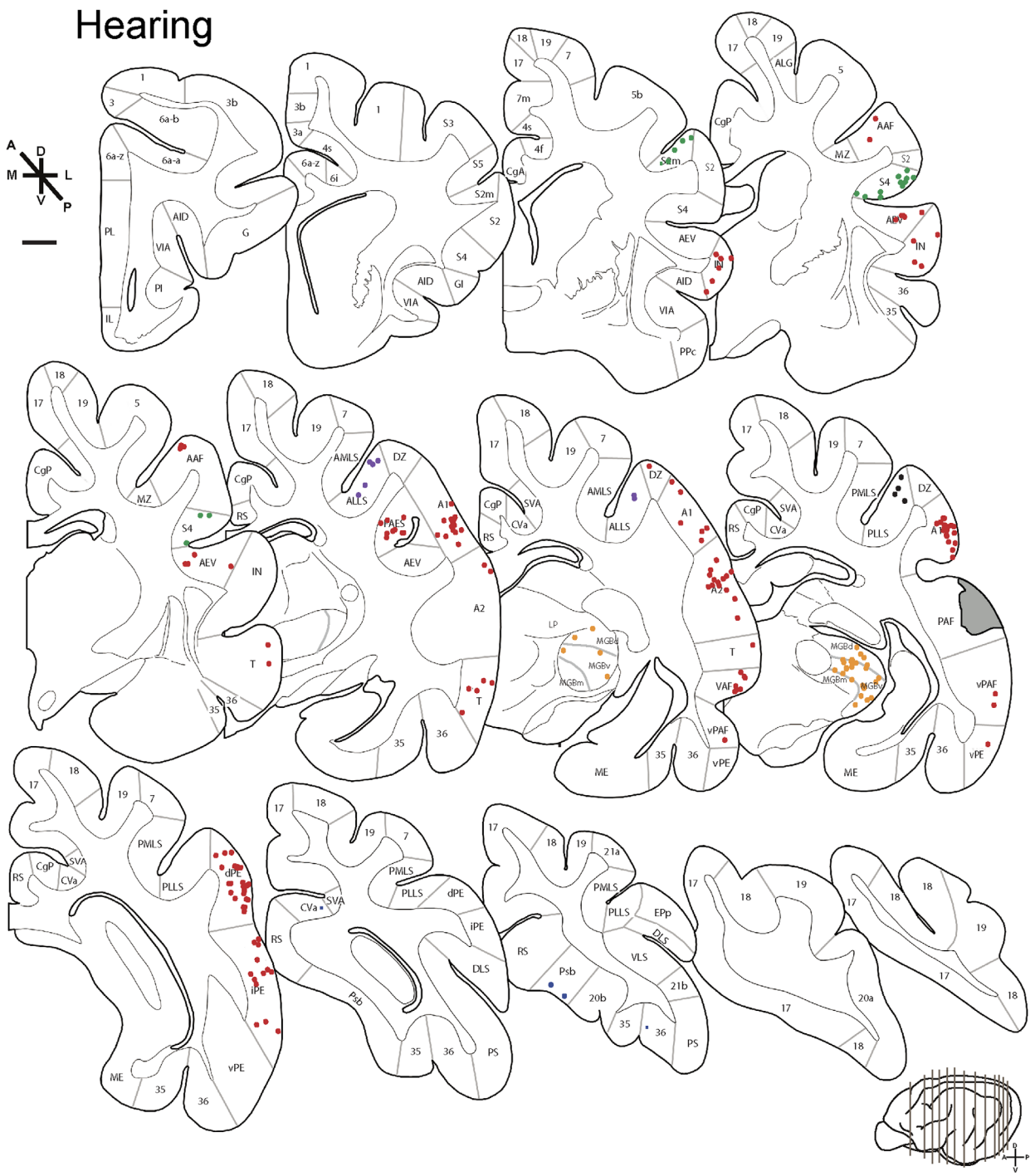

Figure 7. Representative distribution of labeled neurons projecting to the posterior auditory field of a hearing cat (H4). Color-coded dots represent labeled neurons from auditory (red), visual (purple), somatomotor (green), and other (blue) cortical areas, as well as projections from the auditory thalamus (orange). Injection spread in the PAF is shown in gray. Bottom right: a lateral brain view showing the selected levels from which the mapped coronal sections were taken. For abbreviations, see list. Scale bar = 2 mm.

with BDA has been shown to be stable with age (Rajakumar et al., 1993).

Cytoarchitectural, sulcal, and gyral landmarks that define areal borders were used to assign labeled neurons to cortical areas on an individual-animal basis. Patterns of SMI-32 labeling differ by area in auditory and visual cortices, allowing for demarcation of areal borders (van der Gucht et al., 2001; Mellott et al., 2010), and these patterns are conserved following hearing loss (Wong et al., 2014). Borders between auditory

TABLE 3.

Ipsilateral Cortical Projections to the PAF by Area for Individual Animals (percent of the total number of ipsilateral projections) for Auditory (red), Visual (purple), Somatosensory (green), and Other Cortical Areas (blue).

	A1	A2	AAF	dPE	DZ	fAES	IN	iPE	T	VAF	VPAF	vPE
H1	17.3	8.7	1.3	7.5	0.9	0.3	0.8	3.9	1.2	3.9	5.1	1.1
H2	25.7	6.7	0.0	1.3	4.9	4.9	0.3	6.6	0.5	1.9	5.2	3.5
H3	43.2	8.2	1.4	0.8	3.0	1.0	1.5	1.1	0.8	7.4	10.4	0.8
H4	19.3	4.4	1.7	12.5	4.7	2.8	3.4	4.5	2.0	3.5	4.2	2.9
E1	31.3	0.0	2.4	7.1	4.7	0.0	0.5	27.5	1.9	0.0	4.3	1.9
E2	21.6	5.4	1.4	5.8	0.0	2.5	0.8	3.5	2.9	6.7	5.5	3.5
E3	11.0	6.5	3.0	6.9	1.2	0.2	2.2	4.6	0.3	0.4	9.7	2.5
E4	11.6	3.4	5.2	5.1	13.1	0.8	0.7	3.9	1.8	0.7	10.8	1.8
L1	20.6	6.6	2.3	4.6	6.4	0.5	0.4	0.0	0.6	3.1	9.5	0.5
L2	12.8	8.7	3.0	2.7	1.4	4.4	0.4	4.2	1.8	4.1	7.3	2.1
L3	9.2	8.5	0.0	2.5	6.3	0.9	0.1	1.4	0.2	0.7	6.8	0.6
L4	20.1	5.8	2.2	8.0	6.2	1.6	1.2	1.6	1.4	3.5	6.0	0.9

	19	20a	20b	21b	AEV	ALLS	CVA	EPp	PLLS	PS
H1	0.0	0.0	0.0	0.0	0.5	0.6	0.0	0.1	0.3	0.0
H2	0.0	0.0	0.0	0.0	2.4	0.0	0.0	0.0	1.4	0.0
H3	0.0	0.0	0.0	0.0	0.4	1.0	0.0	0.0	2.6	0.0
H4	0.0	0.0	0.0	0.0	2.0	0.9	0.1	0.0	1.6	0.1
E1	2.4	0.0	0.0	0.0	0.0	5.2	0.0	1.0	3.8	1.4
E2	0.0	0.0	0.0	0.0	0.0	0.4	0.0	2.5	0.2	0.0
E3	0.0	0.0	0.0	0.0	0.0	0.1	0.1	1.7	2.2	0.1
E4	0.0	0.0	0.0	0.0	2.6	0.0	0.0	0.0	0.3	0.9
L1	0.1	0.2	0.2	0.6	0.2	1.6	0.4	4.8	0.5	0.5
L2	0.0	0.0	0.0	0.1	1.0	1.4	0.0	2.4	0.5	0.1
L3	0.0	0.0	0.0	0.0	0.9	0.1	0.0	0.5	2.5	0.0
L4	0.0	0.0	0.0	0.0	1.0	4.2	0.0	3.1	5.8	0.0

	S2	S2m	S4
H1	1.7	1.4	0.1
H2	0.0	1.3	0.5
H3	0.3	0.3	0.6
H4	0.0	0.9	1.6
E1	0.0	0.0	1.0
E2	1.0	0.9	0.1
E3	1.4	0.8	3.3
E4	3.2	3.8	0.8
L1	0.0	0.2	0.4
L2	1.4	0.9	1.7
L3	0.6	10.5	0.2
L4	0.1	0.4	0.3

	35	36	CgA	CGP	Psb	RS	MZ
H1	0.2	0.5	0.0	0.0	0.0	0.0	0.0
H2	0.0	0.2	0.0	0.0	0.0	0.0	0.0
H3	0.0	0.4	0.0	0.0	0.0	0.0	0.0
H4	0.3	0.8	0.1	0.0	0.1	0.1	0.0
E1	0.0	0.0	0.0	1.0	0.0	0.5	0.0
E2	0.1	2.4	0.0	0.2	0.2	0.1	0.0
E3	0.3	1.2	0.0	0.3	0.1	0.0	0.0
E4	0.1	0.2	0.0	0.0	0.1	0.2	0.0
L1	0.7	1.1	0.1	0.4	0.9	0.8	0.6
L2	0.1	0.6	0.0	0.0	0.0	0.2	1.0
L3	0.1	0.1	0.0	0.2	0.0	0.0	0.0
L4	0.0	0.6	0.0	0.2	0.0	0.1	0.2

For abbreviations, see list.

and somatosensory areas can be distinguished by a marked increase in SMI-32 reactivity (van der Gucht et al., 2001), while borders between somatosensory areas are primarily delineated using Nissl labeling profiles (Clascá et al., 1997). Borders between the posterior lateral suprasylvian areas (PLLS and PMLS), and the dorsal and ventral lateral suprasylvian areas (DLS and VLS, respectively) of the visual cortex were placed on the lateral bank of the middle suprasylvian sulcus and the dorsal bank of the posterior limb of the suprasylvian sulcus, respectively (as per Palmer et al., 1978; Updyke, 1986; Rauschecker et al., 1987). This convention is supported by cytoarchitectonic methods in the visual system (van der Gucht et al., 2001). Labeled neurons lying on the border between cortical areas, or within the transitional zone between two areas, were distributed equally to each of the two areas. Complete labeling profiles were constructed for each of the three groups examined, and these groups were contrasted to determine whether any significant connectivity differences existed. In one hearing animal (H3), the contralateral cortex was unavailable for cell quantification due to electrophysiological examination in that hemisphere. However, the variability within the hearing group did not differ from either deaf group. To simplify visual comparisons between groups, labeled neurons from one animal in each group were plotted on standardized

TABLE 4.

Ipsilateral Thalamic Projections to the PAF (orange) by Area for Individual Animals (percent of the total number of ipsilateral projections) and Contralateral Cortical Projections to the PAF (gray) by Area for Individual Animals (percent of the total number of contralateral projections)[1]

	Claustrum	LP	MGBd	MGBm	MGBv	Pulvinar	Putamen
H1	0.0	0.7	12.0	9.2	20.3	0.0	0.4
H2	0.0	0.0	3.3	5.3	15.5	0.0	0.0
H3	0.3	2.5	1.9	1.6	8.6	0.0	0.0
H4	0.1	1.6	7.9	4.4	10.7	0.0	0.9
E1	0.0	0.5	0.0	1.9	0.0	0.0	0.0
E2	0.0	0.2	7.9	3.2	19.7	0.0	1.9
E3	0.0	0.8	9.2	6.7	20.3	0.1	3.0
E4	0.0	0.9	9.5	7.6	11.0	0.0	0.1
L1	0.0	0.2	4.5	6.5	15.6	0.1	3.4
L2	0.0	0.5	8.1	8.2	19.1	0.0	0.2
L3	0.2	0.6	29.4	4.3	11.4	0.0	1.3
L4	0.0	2.1	1.7	6.3	13.9	0.0	1.4

	A1	A2	AAF	IN	dPE	DZ	iPE	PAF	T	VAF	VPAF	vPE	AEV	CGp	ALLS
H1	5.6	2.8	5.6	0.0	0.0	0.0	4.2	73.6	0.0	8.3	0.0	0.0	0.0	0.0	0.0
H2	0.0	9.9	0.0	0.0	0.0	0.0	0.0	70.3	0.0	1.1	15.4	3.3	0.0	0.0	0.0
H4	13.6	0.0	0.0	0.0	0.0	0.0	4.6	68.2	0.0	4.6	0.0	0.0	0.0	9.1	0.0
E1	17.6	0.0	17.7	11.8	0.0	52.9	0.0	0.0	0.0	0.0	0.0	0.0	0.0	0.0	0.0
E2	28.2	7.7	2.6	2.6	0.0	2.6	0.0	2.6	2.6	2.6	48.7	0.0	0.0	0.0	0.0
E3	10.0	0.0	0.0	0.0	8.3	0.0	5.0	68.3	1.7	0.0	5.0	1.7	0.0	0.0	0.0
E4	5.9	0.0	0.0	0.0	14.7	8.8	17.7	23.5	0.0	0.0	20.6	8.8	0.0	0.0	0.0
L1	3.1	0.0	0.0	0.0	4.7	0.0	0.0	82.8	0.0	9.4	0.0	0.0	0.0	0.0	0.0
L2	9.8	4.9	0.0	0.0	0.0	2.4	0.0	63.4	0.0	0.0	17.1	0.0	0.0	0.0	2.4
L3	0.0	4.4	0.0	0.0	0.0	0.0	0.0	92.8	0.0	0.0	2.9	0.0	0.0	0.0	0.0
L4	0.0	2.1	2.1	0.0	29.5	7.4	9.5	42.1	0.0	1.1	1.1	0.0	2.1	1.1	2.1

[1]The contralateral hemisphere of animal H3 was not available for quantification due to electrophysiological examination.
For abbreviations, see list.

slices with labeled neurons repositioned to lie within the correct cortical areas. Separate univariate analyses of variance were conducted for ipsilateral and contralateral inputs to the PAF, and corrections for multiple comparisons were applied where necessary to allow comparisons between groups at individual cortical regions.

RESULTS

Injection sites and tracer spread

A total of 12 cats received injections of the retrograde tracer BDA throughout all six cortical layers of the right PAF to ensure uptake at axon terminals. The three injection tracks were placed in a line along the posterior bank of the posterior ectosylvian sulcus. In all cases, the tracer spread throughout all six cortical layers, with no evidence of tracer deposits in any other cortical area. Despite holding constant the amount of tracer injected, and with similar spread across animals, it remains possible that the injections in the current study did not permeate the PAF equally in every group due to a small but significant increase in the fractional volume of the PAF in deaf animals compared with normal hearing controls (Wong et al., 2014).

Summary of the projections to the PAF in the hearing cat

A representative labeling profile is presented in Figure 7. Following a tracer injection in the PAF, labeled neurons throughout the brain were assigned to cortical and thalamic areas of origin, counted, and converted to a proportion of the total number of labeled cells on an individual basis (Tables 3, 4). Proportions of labeled cells were used in place of raw numbers to allow meaningful comparisons to be made despite variability in the uptake of BDA or the immunohistochemical process used to visualize labeled cells. Projections were observed to arise from each of the areas of the auditory cortex, with a dominant projection arising from A1. Smaller numbers of labeled cells were observed in the second auditory cortex (A2), AAF, dorsoposterior ectosylvian gyrus (dPE), dorsal zone of the auditory cortex (DZ), auditory field of the anterior ectosylvian sulcus (fAES), insular and temporal cortices (IN and T, respectively), ventral and ventral posterior auditory fields (VAF and VPAF, respectively), and the intermediate and ventral divisions of the posterior ectosylvian auditory cortex (iPE and vPE, respectively). In the visual cortex, a significant number of labeled cells were observed in the anterior ectosylvian visual area (AEV), the anterolateral and

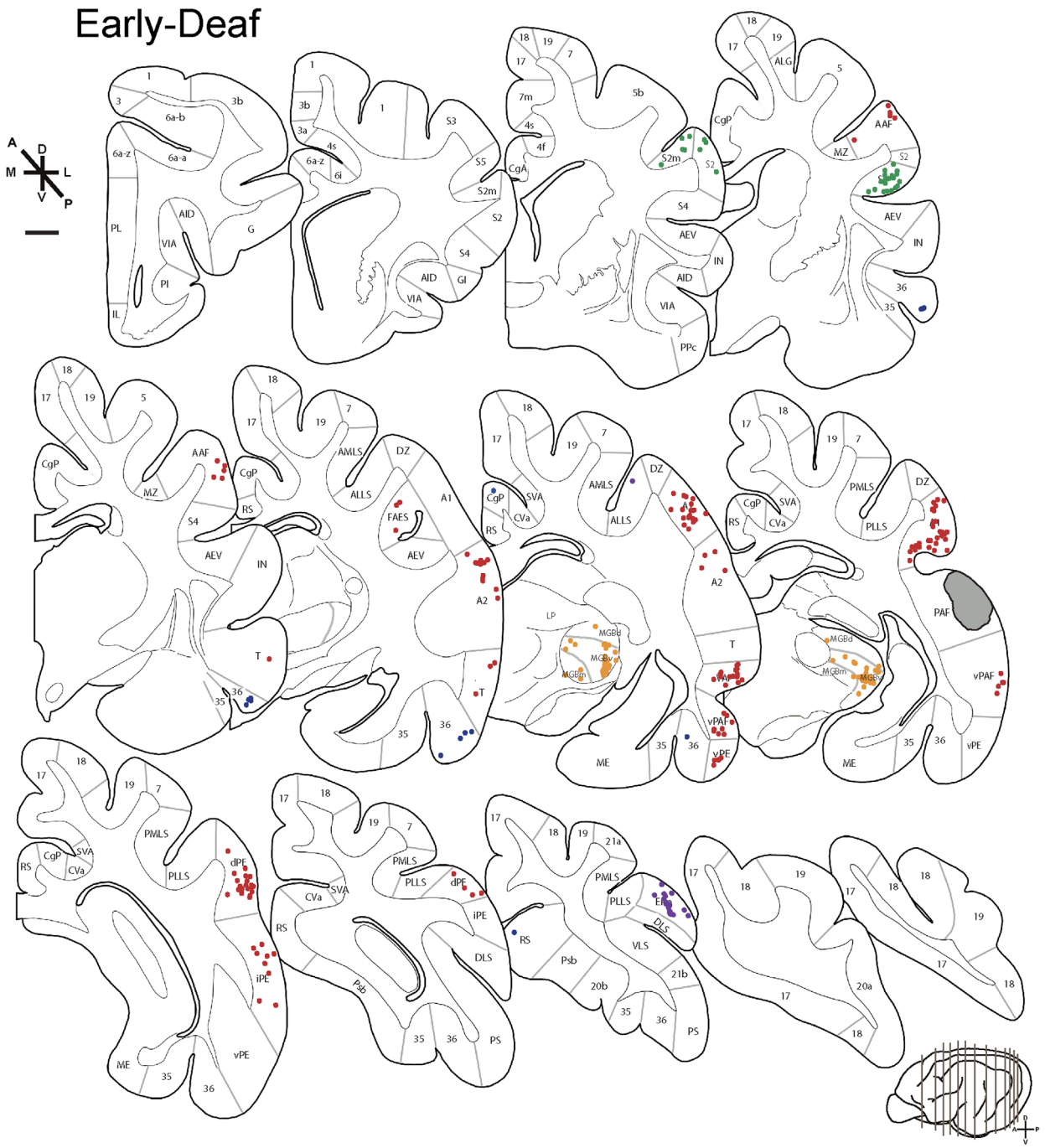

Figure 8. Representative distribution of labeled neurons projecting to the posterior auditory field of an early-deaf cat (E2). Color-coded dots represent labeled neurons from auditory (red), visual (purple), somatomotor (green), and other (blue) cortical areas, as well as projections from the auditory thalamus (orange). Injection spread in the PAF is shown in gray. Bottom right: a lateral brain view showing the selected levels from which the mapped coronal sections were taken. For abbreviations, see list. Scale bar = 2 mm.

posterolateral lateral suprasylvian areas (ALLS and PLLS, respectively), and the posterior ectosylvian field (EPp). Somatosensory projections originated in secondary areas (S2, S2m) and the fourth somatosensory cortex (S4), and significant numbers of neurons were counted in perirhinal areas 35 and 36. Thalamic labeling was exclusively ipsilateral, and was dominated by projections from the medial geniculate body (MGB), with a smaller projection from the lateral posterior nucleus (LP). Within the MGB, the number of labeled cells was greatest in the ventral division (MGBv), with smaller but significant projections from the dorsal (MGBd) and medial (MGBm) divisions.

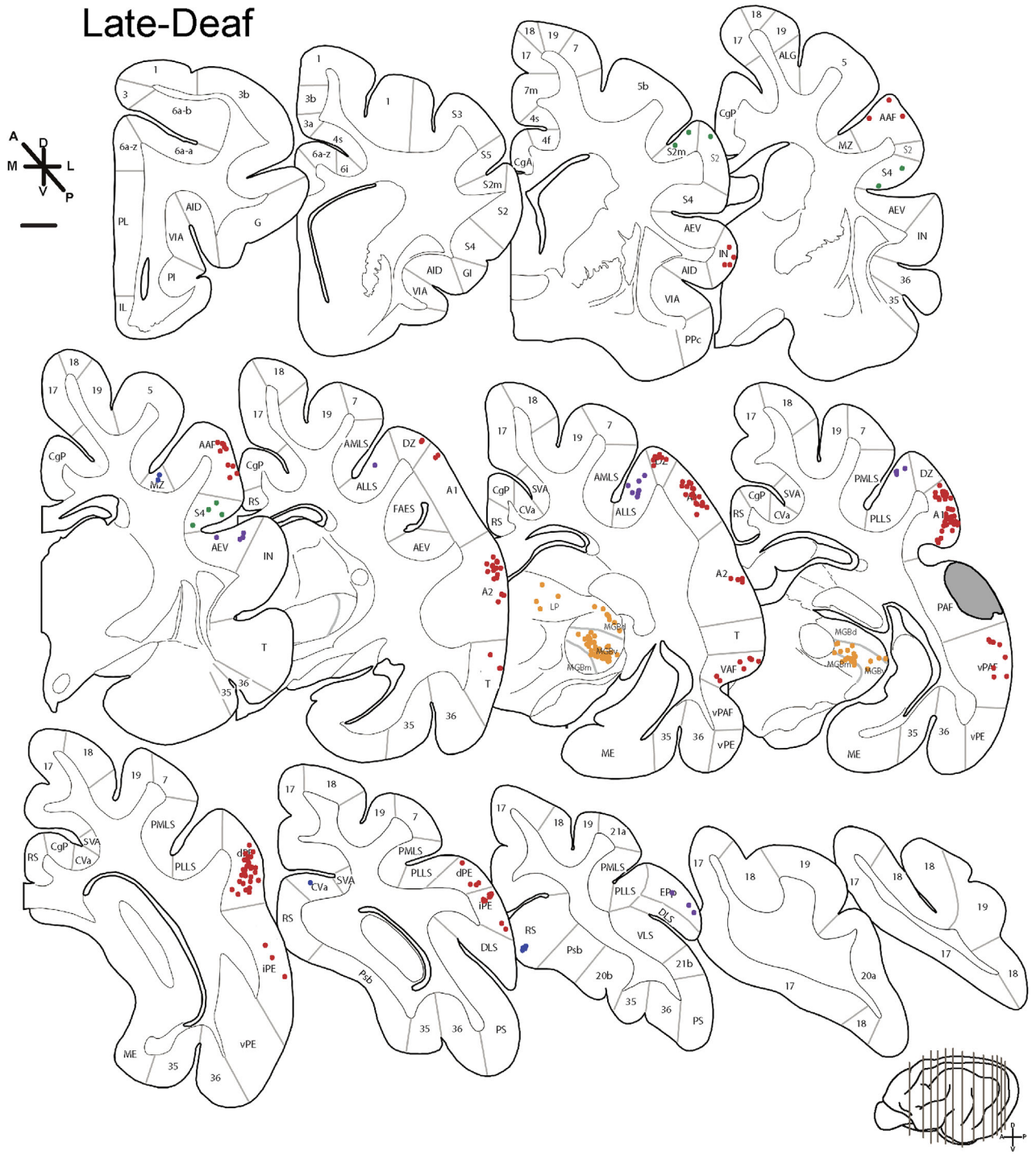

Figure 9. Representative distribution of labeled neurons projecting to the posterior auditory field of a late-deaf cat (H4). Color-coded dots represent labeled neurons from auditory (red), visual (purple), somatomotor (green), and other (blue) cortical areas, as well as projections from the auditory thalamus (orange). Injection spread in the PAF is shown in gray. Bottom right: a lateral brain view showing the selected levels from which the mapped coronal sections were taken. For abbreviations, see list. Scale bar = 2 mm.

Changes in the pattern of projections following hearing loss

To examine the changes in connectivity resulting from hearing loss, and to measure the impact of age at the onset of deafness, the extent of auditory, visual, somatosensory, and other cortical and thalamic projections to the PAF were examined. Representative labeling profiles for early-deaf and late-deaf animals are presented in Figures 8 and 9, respectively. In general, the number of cells projecting to the PAF by area was

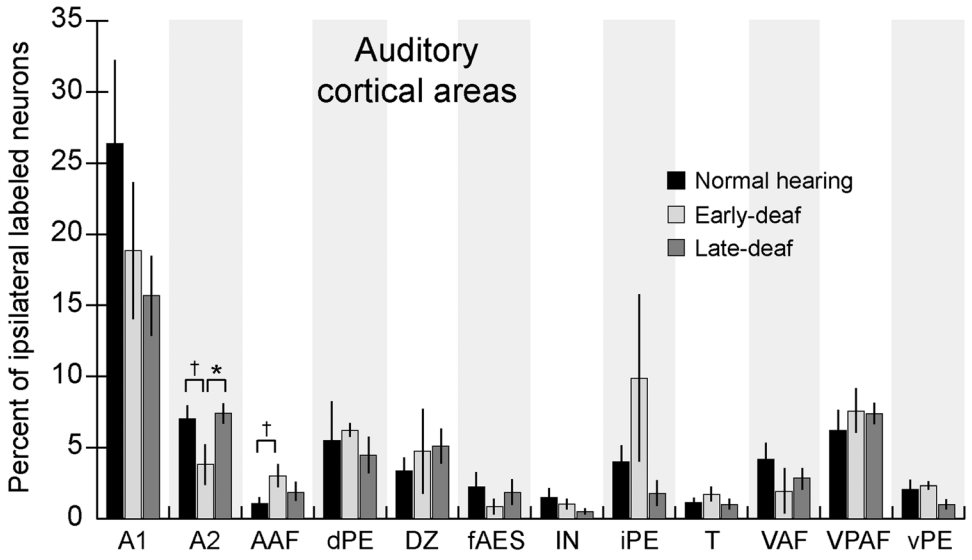

Figure 10. Histogram illustrating the mean proportion of labeled neurons projecting from areas in the ipsilateral auditory cortex. The y-axis represents the percent of all labeled neurons in the ipsilateral hemisphere. Ipsilateral auditory areas projecting to the PAF are listed along the x-axis. Error bars show the standard error of the mean. For abbreviations, see list. *, $P < 0.05$; †, $P = 0.06$.

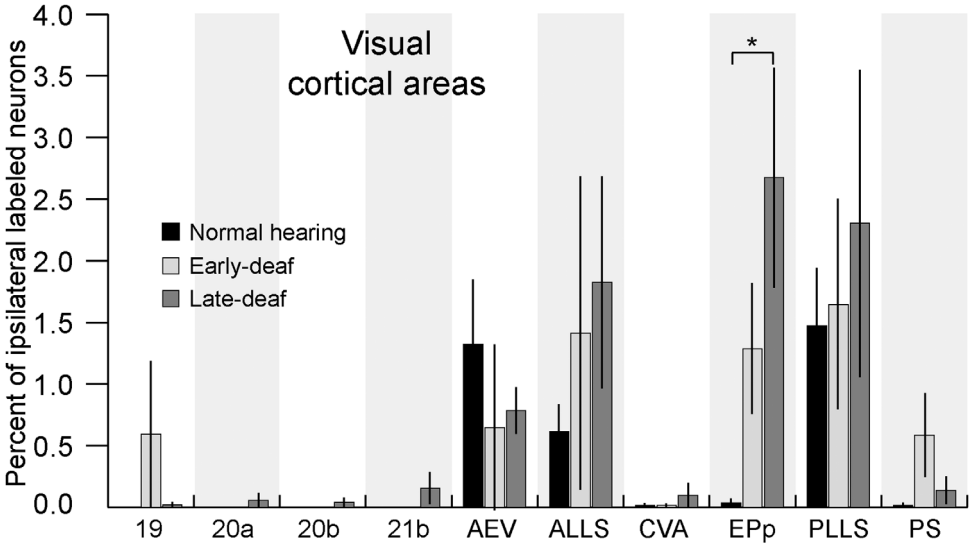

Figure 11. Histogram illustrating the mean proportion of labeled neurons projecting from areas in the ipsilateral visual cortex. The y-axis represents the percent of all labeled neurons in the ipsilateral hemisphere. Ipsilateral visual areas projecting to the PAF are listed along the x-axis. Error bars show the standard error of the mean. For abbreviations, see list. *, $P < 0.05$.

quite similar across groups. For ease of illustration, these areas have been grouped by modality as follows: auditory cortical areas (Fig. 10), visual cortical areas (Fig. 11), somatosensory cortical areas (Fig. 12), other ipsilateral cortical areas (Fig. 13), thalamic areas (Fig. 14), and contralateral cortical areas (Fig. 15). Within the auditory cortex, a smaller proportion of labeled cells was observed in A2 following early-onset hearing loss than in late-deaf animals ($P = 0.04$; hearing: 7.0%, early-deaf: 3.8%, late-deaf: 7.4%). However, late-deaf animals had significant increases in the proportion of labeled cells in visual cortical area EPp ($P = 0.01$; hearing: 0.04%, early-deaf: 1.3%, late-deaf: 2.7%) and the multisensory zone (MZ; $P = 0.03$; hearing: 0.0%, early-deaf: 0.0%, late-deaf: 0.5%). In both hearing and late-deaf animals, contralateral labeling was dominated by cells originating in the PAF; however, this callosal input (hearing: 70.7%, early-deaf: 23.6%, late-deaf: 70.3%)

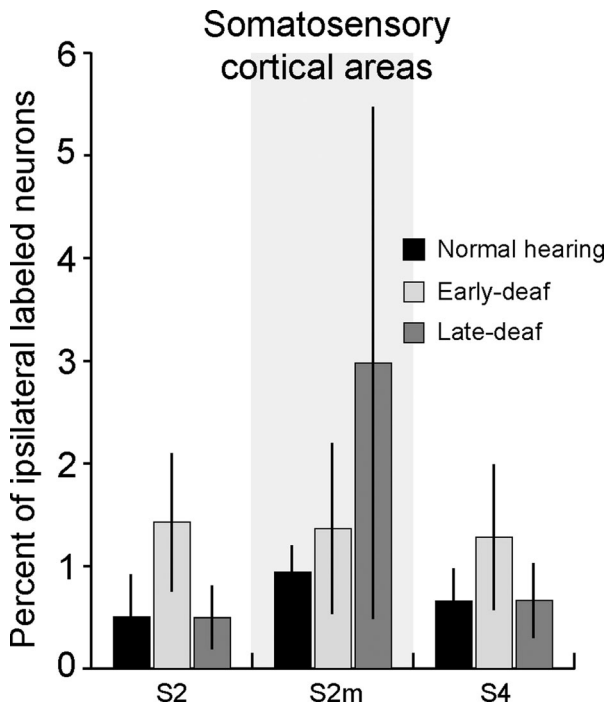

Figure 12. Histogram illustrating the mean proportion of labeled neurons projecting from areas in the ipsilateral somatosensory cortex. The y-axis represents the percent of all labeled neurons in the ipsilateral hemisphere. Ipsilateral somatosensory areas projecting to the PAF are listed along the x-axis. Error bars show the standard error of the mean.

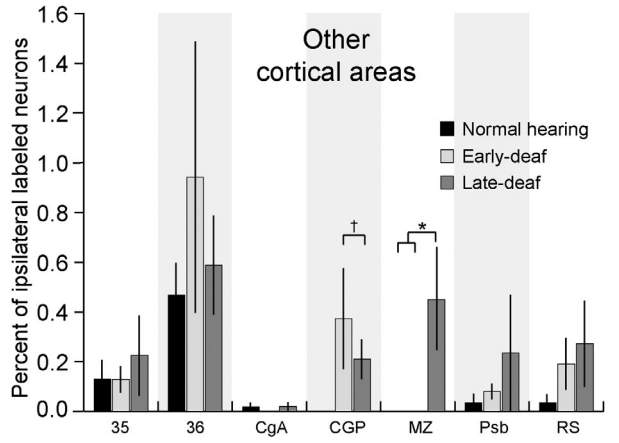

Figure 13. Histogram illustrating the mean proportion of labeled neurons projecting from other ipsilateral cortical areas (those not regarded as visual-, auditory-, or somatosensory-dominant in nature). The y-axis represents the percent of all labeled neurons in the ipsilateral hemisphere. Ipsilateral cortical areas projecting to the PAF are listed along the x-axis. Error bars show the standard error of the mean. For abbreviations, see list. †, $P = 0.06$.

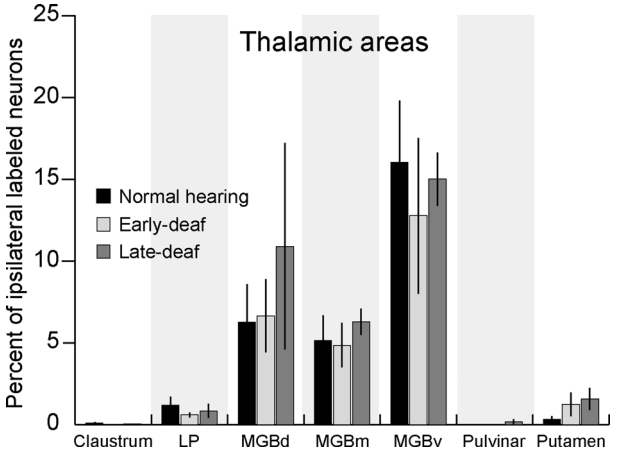

Figure 14. Histogram illustrating the mean proportion of labeled neurons projecting from thalamic nuclei. The y-axis represents the percent of all labeled neurons in the ipsilateral hemisphere. Thalamic nuclei projecting to the PAF are listed along the x-axis. Error bars show the standard error of the mean. For abbreviations, see list.

was significantly reduced in early-deaf animals relative to both hearing ($P = 0.03$) and late-deaf ($P = 0.02$) animals. The proportions of labeled cells projecting from somatosensory, thalamic, or other cortical areas did not differ significantly with age of deafness onset.

Projections to the PAF by modality

To generate modality-level estimates of the projections to the PAF, labeled cells were classified as either thalamic in origin, or as arising from auditory, visual, somatosensory, or other cortical areas (as outlined in Fig. 1). These summary values were divided by the total number of labeled cells in the entire brain for each individual to determine the proportion of labeled cells arising from each modality. Figure 16 illustrates trends toward modality-level changes in crossmodal connections to the PAF that appear to depend upon age at the onset of deafness. While the proportion of auditory projections is similar between normal hearing and early-deaf animals (66.0% and 62.6%, respectively), this value is diminished in late-deaf animals (51.7%). This change is partially accounted for by an increase in the proportion of labeled cells in thalamic areas (34.8% in late-deaf compared with 29.1% in hearing and 26.1% in early-deaf animals). However, both early- and late-deaf animals show small-scale increases in the strength of projections from visual (hearing: 2.2%, early-deaf: 5.5%, late-deaf: 7.8%), somatosensory (hearing: 2.1%, early-deaf: 4.1%, late-deaf: 4.1%), and other cortical areas (hearing: 0.7%, early-deaf: 1.7%, late-deaf: 1.6%) when compared with normal hearing controls.

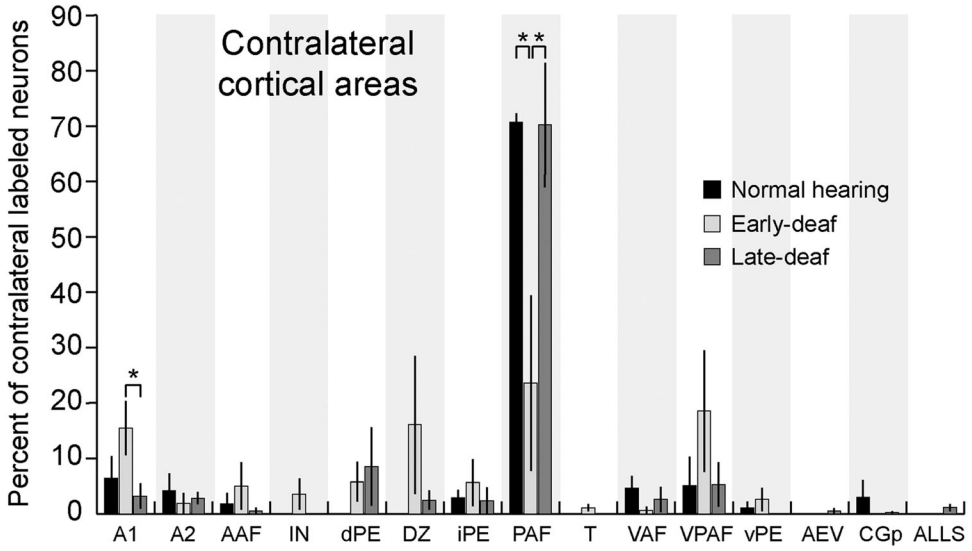

Figure 15. Histogram illustrating the mean proportion of labeled neurons projecting from areas in the contralateral cortex. The y-axis represents the percent of all labeled neurons in the contralateral hemisphere. Contralateral areas projecting to the PAF are listed along the x-axis. Error bars show the standard error of the mean. For abbreviations, see list. *, $P < 0.05$.

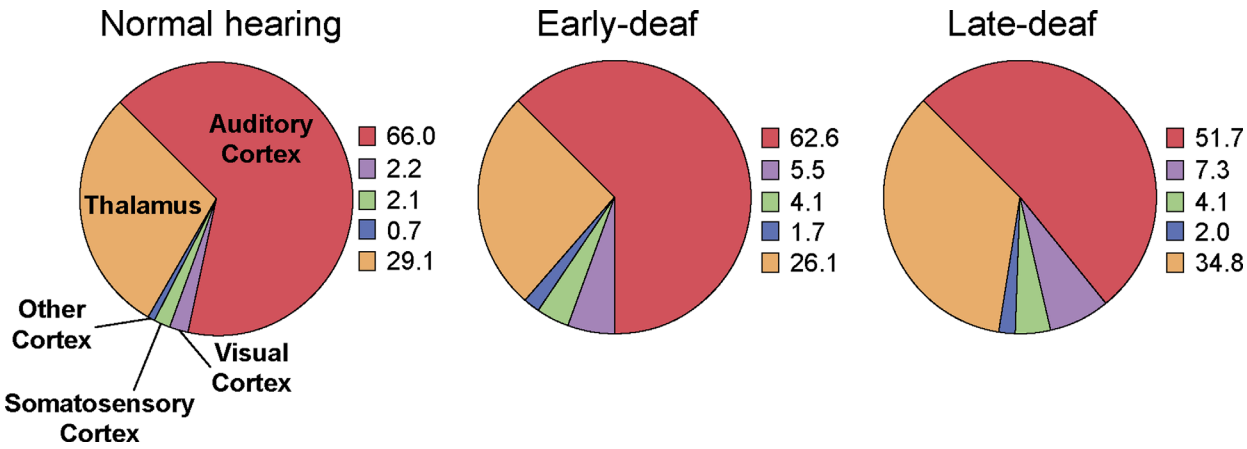

Figure 16. Pie charts displaying the relative percentage of labeled neurons projecting to the PAF arising from each sensory area of the brain. The percentages of labeled neurons in each region are indicated to the right of each graph.

DISCUSSION

Overview

This study illustrates small-scale changes in connectivity to the PAF that occur following hearing loss, suggesting that the specific areas that undergo reorganization are dependent on age at the onset of deafness. At the modality level, small increases in non-auditory inputs to the PAF were observed following both early- and late-onset hearing loss. Still, the vast majority of cortical and thalamic areas projecting to the PAF showed no significant change in the proportion of labeled cells following deafness. Exceptions include decreased projections from A2 and the contralateral PAF in early-deaf animals, and increased projections from visual area EPp and the MZ in the late-deaf. While failing to reach significance, deaf animals showed small projections from a number of visual cortical fields (areas 19, 20, 20b, and 21b), the multisensory cortical area MZ, and contralateral auditory areas (IN, dPE, DZ, and T) that show no labeling in hearing animals.

Comparison with existing literature

The current study quantifies the thalamocortical and corticocortical projections to the PAF, and is generally

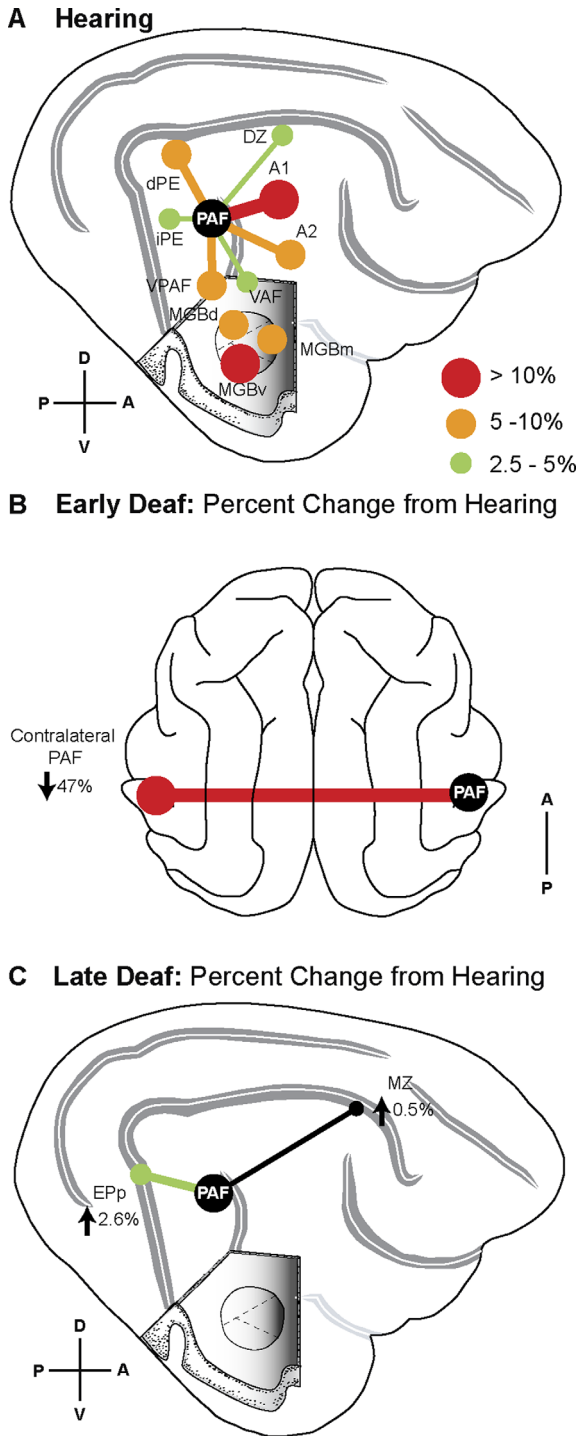

Figure 17. Corticocortical and thalamocortical neurons projecting to the PAF that are affected by deafness. **A:** In hearing animals, the number of labeled cells is represented by the size and color of the circles, with the largest circle representing an area that accounts for 10% or more of the total labeled cells projecting to the PAF. In the ventral region of the brain, the cortex has been "removed" to allow for visualization of the location of the medial geniculate body. **B,C:** In deaf animals, the changes in the number of labeled cells relative to control animals are represented by the size and color of the circles, with the mean change indicated next to each area. For abbreviations, see list.

in agreement with the existing literature on projections in hearing animals. Lee and Winer (2008a) also describe the primary contribution from the thalamus as arising from the ventral division of the medial geniculate body. While a previous examination of cortical inputs also determined that the principle auditory input to the PAF arises from A1 (Lee and Winer, 2008c), the current study found a smaller proportion of labeled cells in the ipsilateral VPAF and VAF. Additionally, contralateral cortical inputs were in strong accordance with previously published results (Lee and Winer, 2008b), except that the current study found a smaller projection from the contralateral VAF.

Interestingly, a previous neuroanatomical study found that neurons in the PAF project to peripheral visual field representations of the primary visual cortex (V1; Hall and Lomber, 2008). However, the current study provides no evidence of a reciprocal connection from V1 to the PAF (Fig. 11). This unidirectional connectivity likely arises from the disparity in the response latencies of PAF and V1 neurons. Auditory signals are represented in the PAF following latencies ranging from ~8 ms for broadband noise stimuli to ~25 ms for frequency-modulated sweeps (Carrasco and Lomber, 2011). By comparison, the response latencies of neurons in V1 to a simple light bar have been estimated to be between 45 and 55 ms (Ikeda and Wright, 1975). Thus, the comparatively late arrival of stimulus-evoked activity in V1 would make modulation of neural responses in the PAF moot.

While Lee and Winer provided a comprehensive examination of auditory inputs to the PAF in hearing animals, the current study extends this work to include nonauditory projections, and provides a description of how connectivity is altered by hearing loss both during and following auditory system maturation.

A number of recent studies have used retrograde tracers to quantify the effects of hearing loss on other areas of the cat auditory cortex. As in the PAF, the primary auditory cortex also shows no change in the pattern of labeled cells in nonauditory cortical fields (Chabot et al., 2015) following early-onset deafness. However, the projections to the AAF from a small number of visual and somatosensory areas were shown to be altered by hearing loss (Wong et al., 2015). Two of the 18 visual cortical fields projecting to the dorsal zone of the auditory cortex were shown to be affected by deafness (Kok et al., 2014), and behavioral evidence demonstrates that this field is reorganized to subserve visual motion processing in the deaf (Lomber et al., 2010). Perhaps most striking is the similarity between the results of the current study of PAF connectivity and what has been observed in the fAES, where no

significant change is observed in connectivity between sensory cortices (Meredith et al., 2016), despite behavioral and electrophysiological evidence of crossmodal reorganization (Meredith et al., 2011). Taken together, these studies suggest that changes in the patterns of nonauditory projections to auditory cortical areas are limited (AAF, DZ) or absent (A1, fAES, PAF) following early-onset hearing loss, but that this absence of change does not preclude functional reorganization.

Intramodal changes following deafness

The DZ represents one of the principle targets of PAF neurons (Lee and Winer, 2011), but reciprocal connections from DZ to PAF account for only a small proportion of labeled cells (<5% in the current study). Interestingly, the presumptive feed-forward connections from the PAF to the DZ undergo only a very small decrease in number in the deaf animal (Kok et al., 2014), whereas feedback connections from the DZ to the PAF are unchanged.

Previous anatomical studies have demonstrated strong reciprocal connectivity between the PAF and VAF, and a significant presumptive feedback projection from the VPAF to the PAF (Lee and Winer 2009c, 2011). As noted above, the current study revealed much smaller projections originating in the VAF and VPAF, but demonstrated that the proportion of labeled cells is not significantly altered following early- and late-onset hearing loss in either area. Feed-forward projections from core areas of auditory cortex were dominated by those arising in A1, with a much smaller proportion of labeled cells in the AAF. Both early- and late-deaf animals showed fewer labeled cells in A1 compared with normal hearing controls; however, this difference failed to reach significance. There was a significant difference in the proportion of labeled cells in A2, with fewer cells in early-deaf than in late-deaf animals, suggesting that the reorganization in connectivity between these two structures depends upon the age at which hearing loss occurs. This sort of age-dependent effect is likely the result of Hebbian-type reorganization, whereby neural connections that do not undergo coincident stimulus-evoked activity are pruned away over time (Hebb, 1949). Moreover, this change is in accordance with the suggestion that top-down modulation of auditory activity is decreased following hearing loss during the sensitive period for auditory development (see Kral and Sharma, 2012 for review). This highlights a possible hierarchy of neuroplastic potential, in which even the limited auditory experience of early-deaf animals may be sufficient to solidify connections from core auditory areas to the PAF, while neurons projecting from secondary fields (such as A2) remain susceptible to reorganization for a longer period. Indeed, there is evidence in the visual system that while the refinement of ascending connectivity is largely complete prenatally (Price et al., 2006), the refinement of feedback pathways occurs over a longer time period (Batardiere et al., 2002).

In accordance with previously published data (Lee and Winer, 2008a), the current study found that the principle thalamocortical projection to the PAF arises from the tonotopically organized, ventral division of the medial geniculate body. In contrast to results following BDA injection into A1 (the primary source of ascending cortical inputs to the PAF; Chabot et al., 2015), the relative proportion of labeled cells in thalamic nuclei projecting to the PAF did not show evidence of significant reorganization following hearing loss.

Nonauditory changes following hearing loss

As noted above, the changes in nonauditory projections to the PAF following hearing loss were limited to those arising from the visual cortical area EPp and the multisensory zone. Area EPp saw sharp increases in the proportion of labeled cells for both hearing loss groups compared with normal hearing controls, but this difference only reached significance for the late-deaf animals. One possible explanation for increased labeling following the onset of deafness is the formation of novel projections; however, our current understanding of the changes in neuronal guidance mechanisms that occur with aging suggest that this is improbable. For example, age-related changes in molecules that direct the growth of novel projections suggest that, with the exception of brain structures that undergo routine remodeling (e.g., the hippocampus), the concentration gradient required to guide new connections could not be established in the adult brain (Liebl et al., 2003). Instead, increases in EPp labeling are likely the result of synaptogenesis, which has been shown to occur largely in the absence of stimulus-evoked activity (Wilson, 1988), and which would provide more potential for the uptake of BDA in the current study. Faced with the absence of stimulation, the number of synapses on existing projections from the EPp to the PAF may be upregulated to strengthen the relative input to this area from visually responsive regions of the cortex. This same principle holds as an explanation for the increased proportion of labeled cells in the MZ following PAF injection in late-deaf animals. The multisensory zone is an area of the cortex that, as its name would suggest, is involved with the integration of information from multiple sensory modalities, with neurons predominantly responding to somatosensory, auditory, or somatosensory–auditory stimulation (Clemo et al., 2007).

The current study suggests that projections from the MZ may be increased in number following deafness in an effort to functionally reorganize the PAF to subserve the remaining sensory systems.

Change in callosal connectivity following early-onset deafness

When hearing and early-deaf animals are considered in isolation, the only significant difference in connectivity is a sharp change in the number of neurons projecting from the PAF in the contralateral hemisphere (Fig. 17B). Given the absence of thalamocortical or ipsilateral corticocortical differences between these groups, the most straightforward interpretation of this callosal change involves the timing of hearing loss relative to developmental trends across these different types of neural connections. A similar explanation has been offered by Meredith and colleagues (2016) to explain the absence of thalamocortical reorganization observed following injections across fields of the auditory cortex of the cat (A1, AAF, fAES, and now PAF). Thalamic sensory projections are among the first to arrive in the cerebral cortex during embryonic development (Molnàr et al., 2003) and are considered to be well established in utero (Johnson and Casagrande, 1993; Hermann et al., 1994), well before the onset of hearing loss for the early-deaf animals in the current study. Accordingly, previous anatomical studies by our group (Chabot et al., 2015; Wong et al., 2015; Meredith et al., 2016) as well as others (Stanton and Harrison, 2000; Meredith and Allman, 2012) have repeatedly demonstrated that patterns of thalamocortical innervation are largely preserved following hearing loss across a number of auditory cortical areas and species.

In contrast, corticocortical projections undergo a more prolonged period of refinement that spans the sensitive period for normal development of auditory function. Despite this relative delay, the pattern of projections to the PAF from ipsilateral cortical fields was no different between hearing and early-deaf animals in the current study. This pattern of stability, despite large-scale alteration in sensory input, has been demonstrated previously for projections to the primary auditory cortex (A1, the principle cortical input to the PAF; Chabot et al., 2015). However, both the dorsal zone (Kok et al., 2014) and the anterior auditory field (Wong et al., 2015) *do* undergo significant changes in ipsilateral cortical inputs following deafness, suggesting that this pattern of change is field-specific.

The elongated timeframe of development appears particularly pronounced for callosal projections; auditory projections to the contralateral hemisphere are present at postnatal day 1 in the cat, but assume a distribution that does not resemble that of an adult animal (forming a uniform band across the presumptive layer III as opposed to a pattern of aggregated clusters typical of developed cortex; Feng and Brugge, 1983). While the pattern of afferent projections from these neurons appears well established by postnatal day 18, the pattern of somatic distribution does not reach an adult-like state until postnatal week 14 (Feng and Brugge, 1983). Moreover, assuming a similar timeline to the development of callosal connectivity in the visual system, the onset of deafness in our early-deaf animals occurs during a period of substantial axonal loss (a decrease of ~21% between postnatal days 4 and 26) and near the onset of myelination of callosal neurons (Berbel and Innocenti, 1988). The pattern of change observed in the current study (a decrease in homotopic contralateral connectivity and concurrent increase in heterotopic connectivity) mirrors that observed early in normal development, wherein the cortical areas targeted by callosal projections are much more diffuse than in older, mature animals (Innocenti, 1981). Thus, the change observed here may reflect the arresting of callosal development, resulting from the absence of stimulus-evoked activity during a period of substantial change in the number, distribution, and myelination of auditory callosal projections. Indeed, a similar shift toward more dispersed contralateral projections has been demonstrated following disturbances to visual input, including strabismus (Lund et al., 1978) or genetic abnormalities of the optic pathway (Shatz, 1977).

Absence of large-scale reorganization

Across modalities, it has been proposed that neuroplastic potential is lowest at core cortical areas, and increases as one proceeds upward through the functional hierarchy. In the auditory cortex, the capacity for crossmodal plasticity in the primary field has been the subject of debate, with electrophysiological studies in the mouse (Hunt et al., 2006) and ferret (Bizley et al., 2007; Bizley and King, 2008, 2009; Meredith and Allman, 2015) showing significant crossmodal activation of A1 neurons, while studies in the cat find little (Rebillard et al., 1977) or no response (Stewart and Starr, 1970; Kral et al., 2003) to nonauditory stimulation. Indeed, a recent anatomical study found that cortical and thalamic inputs to A1 of the cat arise predominantly from auditory structures; however, approximately 12% of labeled cells were located in nonauditory areas following similar tracer injections to those used in the current study (Chabot et al., 2015).

Following hearing loss, Chabot and colleagues (2015) observe only small-scale changes in the relative proportion of cells projecting to A1 from nonauditory areas. Conversely, more substantial crossmodal anatomical reorganization occurs in the AAF, another core area of the auditory cortex, following early hearing loss in the cat (Wong et al., 2015). Unlike in A1, robust crossmodal responses are also observed in the AAF following early hearing loss in both in the cat (Meredith and Lomber, 2011) and other carnivores (Meredith and Allman, 2012). Given some evidence of core-level reorganization, and the placement of the PAF above A1 and AAF in the auditory processing hierarchy (Lee and Winer, 2011), it was anticipated that the PAF may undergo a measurable change in the pattern of connectivity with nonauditory cortical areas following auditory deprivation. However, the results of the current study would suggest otherwise.

The absence of evidence of a substantial change in the proportion of projections to the PAF arising from nonauditory cortical areas following early-onset hearing loss is particularly interesting given the growing body of literature suggesting that the PAF is functionally reorganized to contribute to visual processing in these animals. For example, while deaf cats demonstrate superior peripheral acuity for visual localization, this benefit is eliminated by the reversible deactivation of the PAF (Lomber et al., 2010). Moreover, our group has demonstrated that moving high-contrast gratings modulate blood oxygen-level–dependent (BOLD) activity in the PAF of early-deaf cats, but have no measurable effect on activity across the auditory cortex of hearing animals (Brown and Lomber, 2012). This disparity underscores the fact that functional crossmodal reorganization is not necessarily dependent on large-scale changes in projections between sensory cortices. In fact, a number of mechanisms have been proposed that might contribute to crossmodal plasticity (Rauschecker, 1995), including: the growth of novel projections; the enhancement of the synaptic efficacy of existing projections; or the unmasking of projections that do not provide suprathreshold inputs under normal circumstances (Théoret et al., 2004). In reality, functional plasticity likely results from some combination of these mechanisms (as well as some not listed); however, the contributions of changes in synaptic strength and sensory unmasking in the PAF cannot be captured by the methodology used in the current study. An additional limitation that warrants some consideration is that even early-deaf animals were exposed to sound in the days between the opening of the ear canals and deafening; whether this brief period of auditory exposure is sufficient to drive normal development of connections to the PAF remains unknown.

Implications of connectional preservation

The onset of hearing loss does not appear to initiate large-scale changes in the patterns of labeled cells projecting to the PAF, nor does it elicit significant changes in the patterns of cells projecting to A1 of the cat, the principle input to the PAF (Chabot et al., 2015). As described above, this connectional preservation has implications for our understanding of the nature of the change that underlies visual recruitment of the PAF in deaf animals. Importantly, the absence of change in the patterns of labeled cells implies that neurons projecting from auditory cortical areas to A1 and the PAF survive extended periods of hearing loss, and may support the resumption of auditory-evoked activity following hearing restoration. Even in early-deaf animals, the thalamic input to the PAF continues to arise almost exclusively from auditory nuclei (Fig. 14). Moreover, while there are small changes in the balance of inputs at a modality level, the principle corticocortical inputs arise overwhelmingly from ipsilateral auditory cortical fields (Fig. 16). Thus, as one might expect behavioral crossmodal activity to depend upon the existence of functionally relevant projections between sensory modalities, the similarity between the patterns of labeled cells projecting to the PAF from auditory cortical and thalamic areas in normal hearing and deaf animals suggests that if hearing was restored, such as following a cochlear implant, the anatomy would be in place to allow for the resumption of sound processing in the PAF. This is particularly important as the PAF has been shown to contribute widely to sound processing, playing a demonstrable role in both sound localization (Malhotra et al., 2004; Malhotra and Lomber, 2007) and pitch processing (Butler et al., 2015).

CONCLUSIONS

The current study demonstrates that, whereas the majority of projections to the PAF are unchanged following early- or late-onset deafness, a small number of visual and multisensory cortical areas show differences in the pattern of projection that depend upon the age of the animal at the onset of deafness. As a nonprimary field of auditory cortex, the PAF was considered to be a strong candidate for crossmodal reorganization, having previously been shown to subserve enhanced visual peripheral localization in the deaf. However, the current study suggests that this functional enhancement is not the result of a significant shift in the proportion of projections from visual cortical or thalamic fields. In the

absence of such a shift, hypotheses based on changes in synaptic strength (Clemo et al., 2016) or alterations to the relative weighting of existing projections provide the most likely alternatives. Additional studies designed to quantify changes in synaptic endings on existing visual cortical projections will help to clarify this hypothesis.

ACKNOWLEDGMENTS

The authors thank Pam Nixon for technical and surgical assistance, and Brittany Chow for assistance with tissue processing.

CONFLICT OF INTEREST STATEMENT

The authors declare they have no conflicts of interest.

ROLE OF AUTHORS

All authors had full access to all of the data in the study and take responsibility for the integrity of the data and the accuracy of the data analysis. Study concept and design: BEB, NC, and SGL. Acquisition of data: BEB and NC. Analysis and interpretation of data: BEB. Drafting of the manuscript: BEB. Critical revision of the manuscript for important intellectual content: BEB, NC, and SGL. Statistical analysis: BEB. Obtained funding: SGL.

LITERATURE CITED

Allman BL, Keniston LP, Meredith MA. 2009. Adult deafness induces somatosensory conversion of ferret auditory cortex. Proc Natl Acad Sci U S A 106:5925–5930.

Antonini A, Fagiolini M, Stryker MP. 1999. Anatomical correlates of functional plasticity in mouse visual cortex. J Neurosci 19:4388–4406.

Batardière A, Barone P, Knoblauch K, Giroud P, Berland M, Dumas A-M, Kennedy H. 2002. Early specification of the hierarchical organization of visual cortical areas in the macaque monkey. Cereb Cortex 12:453–465.

Berbel P, Innocenti GM. 1988. The development of the corpus callosum in cats: a light- and electron-microscope study. J Comp Neurol 276:132–156.

Bhattacharjee A, Ye AJ, Lisak JA, Vargas MG, Goldreich D. 2010. Vibrotactile masking experiments reveal accelerated somatosensory processing in congenitally blind braille readers. J Neurosci 30:14288–14298.

Bickford MA, Guido W, Godwin DW. 1998. Neurofilament proteins in Y-cells of the cat lateral geniculate nucleus: normal expression and alteration with visual deprivation. J Neurosci 18:6549–6557.

Bizley JK, King AJ. 2008. Visual-auditory spatial processing in auditory cortical neurons. Brain Res 1242:24–36.

Bizley JK, King AJ. 2009. Visual influences on ferret auditory cortex. Hear Res 258:55–63.

Bizley JK, Nodal FR, Bajo VM, Nelken I, King AJ. 2007. Physiological and anatomical evidence for multisensory interactions in auditory cortex. Cereb Cortex 17:2172–2189.

Brown TA, Lomber SG. 2012. Hemodynamic activity in auditory cortex of deaf cats during visual stimulation. Proceedings of the 2012 International Conference on Auditory Cortex. August 31–September 3, 2012. Lausanne, Switzerland.

Brugge JF, Javel E, Kitzes LM. 1978. Signs of functional maturation of peripheral auditory system discharge patterns of neurons in anteroventral nucleus of kitten. J Neurophysiol 41:1557–1579.

Budinger E, Heil P, Scheich H. 2000. Functional organization of auditory cortex in the Mongolian gerbil (*Meriones unguiculatus*). III. Anatomical subdivisions and corticocortical connections. Eur J Neurosci 12:2425–2451.

Butler BE, Hall AJ, Lomber SG. 2015. High-field functional imaging of pitch processing in auditory cortex of the cat. PLoS One. doi:10.1371/journal.pone.0134362.

Carrasco A, Lomber SG. 2009. Evidence for hierarchical processing in cat auditory cortex: nonreciprocal influence of primary auditory cortex on the posterior auditory field. J Neurosci 29:14323–14333.

Carrasco A, Lomber SG. 2013. Influence of inter-field communication on neuronal response synchrony across auditory cortex. Hear Res 304:57–69.

Carrasco A, Lomber SG. 2011. Neuronal activation times to simple, complex, and natural sounds in cat primary and nonprimary auditory cortex. J Neurophysiol 106:1166–1178.

Chabot N, Robert S, Tremblay R, Miceli D, Boire D, Bronchti G. 2007. Audition activates differently the visual system in neonatally enucleated mice compared to anophthalmic mutant. Eur J Neurosci 26:2334–2348.

Chabot N, Butler BE, Lomber SG. 2015. Differential modification of cortical and thalamic projections to cat primary auditory cortex following early- and late-onset deafness. J Comp Neurol 523:2297–2320.

Clascá F, Llamas A, Reinoso-Suárez F. 1997. Insular cortex and neighboring fields in the cat: a redefinition based on cortical microarchitecture and connections with the thalamus. J Comp Neurol 384:456–482.

Clemo HR, Allman BL, Donlan MA, Meredith MA. 2007. Sensory and multisensory representations within the cat rostral suprasylvian cortex. J Comp Neurol 503:110–127.

Clemo HR, Lomber SG, Meredith MA. 2016. Synaptic basis for cross-modal plasticity: enhanced supragranular dendritic spine density in anterior ectosylvian auditory cortex of the early deaf cat. Cereb Cortex 26:1365–1376.

Cohen LG, Weeks RA, Sadato N, Celnik P, Ishii K, Hallett M. 1999. Period of susceptibility for cross-modal plasticity in the blind. Ann Neurol 45:451–460.

Concannon PW. 1991. Reproduction in the dog and cat. In: Cupps PT, editor. Reproduction in domestic animals, 4th ed. San Diego, CA: Academic Press. p 517–554.

Erwin RJ, Buchwald JS. Midlatency auditory evoked responses in the human and the cat model. EEG Cl N Su 40:461–467.

Feng JZ, Brugge JF. 1983. Postnatal development of auditory callosal connections in the kitten. J Comp Neurol 214: 416–426.

Finney EM, Fine I, Dobkins KR. 2001. Visual stimuli activate auditory cortex in the deaf. Nat Neurosci 4:1171–1173.

Finney EM, Clementz BA, Hickok G, Dobkins KR. 2003. Visual stimuli activate auditory cortex in deaf subjects: evidence from MEG. Neuroreport 14:1425–1427.

Hall AJ, Lomber SG. 2008. Auditory cortex projections target the peripheral field representation of primary visual cortex. Exp Brain Res 190:413–440.

Hebb DO. 1949. *The organization of behaviour: A neuropsychological approach*. John Wiley & Sons.

Hensch TK. 2004. Critical period regulation. Annu Rev Neurosci 27:549–579.

Hermann K, Antonini A, Shatz CJ. 1994. Ultrastructural evidence for synaptic interactions between thalamocortical axons and subplate neurons. Eur J Neurosci 6:1729–1742.

Horsley V, Clarke RH. 1908. The structure and function of the cerebellum examined by a new method. Brain Behav Evol 31:45–124.

Hunt DL, Yamoah EN, Krubitzer L. 2006. Multisensory plasticity in congenitally deaf mice: how are cortical areas functionally specified. Neuroscience 139:1507–1524.

Ikeda H, Wright MJ. 1975. Retinotopic distribution, visual latency and orientation tuning of 'sustained' and 'transient' cortical neurones in area 17 of the cat. Exp Brain Res 22:385–398.

Innocenti GM. 1981. Growth and reshaping of axons in the establishment of visual callosal connections. Science 212:824–827.

Johnson JK, Casagrande VA. 1993. Prenatal development of axon outgrowth and connectivity in the ferret visual system. Vis Neurosci 10:117–103.

Karns CM, Dow MW, Neville HJ. 2012. Altered cross-modal processing in the primary auditory cortex of congenitally deaf adults: a visual-somatosensory fMRI study with a double-flash illusion. J Neurosci 32:9626–9638.

Kok MA, Chabot N, Lomber SG. 2014. Cross-modal reorganization of cortical afferents to dorsal auditory cortex following early- and late-onset deafness. J Comp Neurol 522:654–675.

Kral A, Sharma A. 2012. Developmental neuroplasticity after cochlear implantation. Trends Neurosci 35:111–122.

Kral A, Schröder J-H, Klinke R, Engel AK. 2003. Absence of cross-modal reorganization in the primary auditory cortex of congenitally deaf cats. Exp Brain Res 153:605–613.

Kral A, Tillein J, Heid S, Hartmann R, Klinke R. 2005. Postnatal cortical development in congenital auditory deprivation. Cereb Cortex 15:552–562.

Lambertz N, Gizewski ER, de Greiff A, Forsting M. 2005. Cross-modal plasticity in deaf subjects dependent on the extent of hearing loss. Brain Res Cogn Brain Res 25: 884–890.

Lapper SR, Bolam JP. 1991. The anterograde and retrograde transport of neurobiotin in the central nervous system of the rat: comparison with biocytin. J Neurosci Methods 39:173–174.

Lee CC, Winer JA. 2008a. Connections of cat auditory cortex: I. Thalamocortical system. J Comp Neurol 507:1879–1900.

Lee CC, Winer JA. 2008b. Connections of cat auditory cortex: II. Commissural system. J Comp Neurol 507:1901–1919.

Lee CC, Winer JA. 2008c. Connections of cat auditory cortex: III. Corticocortical system. J Comp Neurol 507:1920–1943.

Lee CC, Winer JA. 2011. Convergence of thalamic and cortical pathways in cat auditory cortex. Hear Res 274:85–94.

Lee DS, Lee JS, Oh SH, Kim SK, Kim JW, Chung JK, Lee MC, Kim CS. 2001. Cross-modal plasticity and cochlear implants. Nature 409:149–150.

Levänen S, Hamdorf D. 2001. Feeling vibrations: enhanced tactile sensitivity in congenitally deaf humans. Neurosci Lett 301:75–77.

Levänen S, Jousmäki V, Hari R. 1998. Vibration-induced auditory-cortex activation in a congenitally deaf adult. Curr Biol 8:869–872.

Lewis TL, Maurer D. 2009. Effects of early pattern deprivation on visual development. Optom Vis Sci 86:640–646.

Liebl DJ, Morris CJ, Henkemeyer M, Parada LF. 2003. mRNA expression of ephrins and Eph receptor tyrosine kinases in the neonatal and adult mouse central nervous system. J Neurosci Res 71:7–22.

Lomber SG, Malhotra S. 2008. Double dissociation of 'what' and 'where' processing in auditory cortex. Nat Neurosci 11:609–616.

Lomber SG, Meredith MA, Kral A. 2010. Cross-modal plasticity in specific auditory cortices underlies visual compensations in the deaf. Nat Neurosci 13:1421–1427.

Lund RD, Mitchell DE, Henry GH. 1978. Squint-induced modification of callosal connections in cats. Brain Res 144: 169–172.

Malhotra S, Lomber SG. 2007. Sound localization during homotopic and heterotopic bilateral cooling deactivation of primary and nonprimary auditory cortical areas in the cat. J Neurophysiol 97:26–43.

Malhotra S, Hall AJ, Lomber SG. 2004. Cortical control of sound localization in the cat: unilateral cooling deactivation of 19 cerebral areas. J Neurophysiol 92:1625–1643.

Mellott JG, van der Gucht E, Lee CC, Carrasco A, Winer JA, Lomber SG. 2010. Areas of the cat auditory cortex as defined by neurofilament proteins expressing SMI-32. Hear Res 267:119–136.

Meredith MA, Allman BL. 2012. Early hearing-impairment results in crossmodal reorganization of ferret auditory cortex. Neural Plast 2012:601591

Meredith MA, Allman BL. 2015. Single-unit analysis of somatosensory processing in the core auditory cortex of hearing ferrets. Eur J Neurosci 41:686–698.

Meredith MA, Lomber SG. 2011. Somatosensory and visual crossmodal plasticity in the anterior auditory field of early-deaf cats. Hear Res 280:38–47.

Meredith MA, Kryklywy J, McMillan AJ, Malhotra S, Lum-Tai R, Lomber SG. 2011. Crossmodal reorganization in the early deaf switches sensory, but not behavioral roles of auditory cortex. Proc Natl Acad Sci U S A 108:8856–8861.

Meredith MA, Clemo HR, Corley SB, Chabot N, Lomber SG. 2016. Cortical and thalamic connectivity of the auditory anterior ectosylvian cortex of early-deaf cats: implications for neural mechanisms of crossmodal plasticity. Hear Res 333:25–36.

Molnar Z, Higashi S, Lopez-Bendito G. 2003. Choreography of early thalamocortical development. Cereb Cortex 13: 661–669.

Munnerley GM, Greville KA, Purdy SC, Keith WJ. 1991. Frequency-specific auditory brainstem responses relationship to behavioural thresholds in cochlear-impaired adults. Audiology 30:25–32.

Neville HJ, Schmidt A, Kutas M. 1983. Altered visual-evoked potentials in congenitally deaf adults. Brain Res 266: 127–132.

Olfert ED, Cross BM, McWilliam AA. 1993. Guide to the Care and Use of Experimental Animals: Canadian Council on Animal Care.

Palmer LA, Rosenquist AC, Tusa RJ. 1978. The retinotopic organization of lateral suprasylvian visual areas in the cat. J Comp Neurol 177:237–256.

Payne BR, Lomber SG. 1996. Age dependent modification of cytochrome oxidase activity in the cat dorsal lateral geniculate nucleus following removal of primary visual cortex. Vis Neurosci 13:805–816.

Pekkola J, Ojanen V, Autti T, Jaaskelainen IP, Mottonen R, Tarkiainen A, Sams M. 2005. Primary auditory cortex activation by visual speech: an fMRI study at 3 T. Neuroreport 16:125–128.

Picton TW, Woods DL, Baribeau-Braun J, Healey TMG. 1977. Evoked potential audiometry. J Otolarygnol 6:90–119.

Price DJ, Kennedy H, Dehay C, Zhou L, Mercier M, Jossin Y, Goffinet AM, Tissir F, Blakey D, Molnar Z. 2006. The

development of cortical connections. Eur J Neurosci 23: 910–920.
Rajakumar N, Elisevice K, Flumerfelt BA. 1993. Biotinylated dextran: a versatile anterograde and retrograde neuronal tracer. Brain Res 607:47–53.
Rauschecker JP. 1995. Compensatory plasticity and sensory substitution in the cerebral cortex. Trends Neurosci 18:36–43.
Rauschecker JP, Grunau M, Poulin C. 1987. Centrifugal organization of direction preferences in the cat's lateral suprasylvian visual cortex and its relation to flow field processing. J Neurosci 7:943–958.
Rebillard G, Carlier E, Rebillard M, Pujol R. 1977. Enhancement of visual responses on the primary auditory cortex of the cat after an early destruction of cochlear receptors. Brain Res 1290:1620–1640.
Reiner A, Veenman CL, Medina L, Jiao Y, Del Mar N, Honig MG. 2000. Pathway tracing using biotinylated dextran amines. J Neurosci Methods 103:23–37.
Sadato N. 2006. Cross-modal plasticity in the blind revealed by functional neuroimaging. Suppl Clin Neurophysiol 59: 75–79.
Sadato N, Okada T, Honda M, Yonekura Y. 2002. Critical period for cross-modal plasticity in blind humans: a functional MRI study. Neuroimage 16:389–400.
Sharma A, Dorman MF, Kral A. 2005. The influence of a sensitive period on central auditory development in children with unilateral and bilateral cochlear implants. Hear Res 203:134–143.
Sharma A, Nash AA, Dorman M. 2009. Cortical development, plasticity and re-organization in children with cochlear implants. J Commun Disord 42:272–279.
Shatz CJ. 1977. Anatomy of interhemispheric connections in the visual system of Boston Siamese and ordinary cats. J Comp Neurol 173:497–518.
Shepherd RK, Martin RL. 1995. Onset of ototoxicity in the cat is related to onset of auditory function. Hear Res 92: 131–142.
Stanton SG, Harrison RV. 2000. Projections from the medial geniculate body to primary auditory cortex in neonatally deafened cats. J Comp Neurol 426:117–129.
Sternberger LA, Sternberger NH. 1983. Monoclonal antibodies distinguish phosphorylated and nonphosphorylated forms of neurofilaments in situ. Proc Natl Acad Sci U S A 80: 6126–6130.
Stevens C, Neville H. 2006. Neuroplasticity as a double-edged sword: deaf enhancements and dyslexic deficits in motion processing. J Cogn Neurosci 18:701–714.
Stewart DL, Starr A. 1970. Absence of visually influenced cells in auditory cortex of normal and congenitally deaf cats. Exp Neurol 28:525–528.
Théoret H, Merabet L, Pascual-Leone A. 2004. Behavioral and neuroplastic changes in the blind: evidence for functionally relevant cross-modal interactions. J Physiol Paris 98: 221–233.
Updyke BV. 2004. Retinitopic organization within the cat's posterior suprasylvian sulcus and gyrus. J Comp Neurol 246:265–280.
van der Gucht E, Vandesande F, Arckens L. 2001. Neurofilament protein: a selective marker for the architectonic parcellation of the visual cortex in audlt cat brain. J Comp Neurol 441:345–368.
Veenman CL, Reiner A, Honig MG. 1992. Biotinylated dextran amine as an anterograde tracer for single- and double-labeling studies. J Neurosci Methods 41:239–254.
Walsh EJ, McGee J, Javel E. 1985. Development of auditory-evoked potentials in the cat. II. Wave latencies. J Acoust Soc Am 79:725–744.
Webster WR, Martin RL. 1991. The development of frequency representation in the inferior colliculus of the kitten. Hear Res 55:70–80.
Wilson HR. 1988. Development of spatiotemporal mechanisms in infant vision. Vision Res 28:611–628.
Wong C, Chabot N, Kok MA, Lomber SG. 2014. Modified areal cartography in auditory cortex following early- and late-onset deafness. Cereb Cortex 24:1778–1792.
Wong C, Chabot N, Kok MA, Lomber SG. 2015. Amplified somatosensory and visual cortical projections to a core auditory area, the anterior auditory field, following early- and late-onset deafness. J Comp Neurol 523: 1925–1947.
Xu SA, Shepherd RK, Chen Y, Clark GM. 1993. Profound hearing loss in the cat following the single co-administration of kanamycin and ethacrynic acid. Hear Res 70:205–215.

A Quantitative Comparison of the Hemispheric, Areal, and Laminar Origins of Sensory and Motor Cortical Projections to the Superior Colliculus of the Cat

Blake E. Butler,[1,2,4] Nicole Chabot,[1,2,4] and Stephen G. Lomber[1,2,3,4,5]*

[1]Cerebral Systems Laboratory, University of Western Ontario, London, Ontario, Canada N6A 5C2
[2]Department of Physiology and Pharmacology, University of Western Ontario, London, Ontario, Canada N6A 5C1
[3]Department of Psychology, University of Western Ontario, London, Ontario, Canada N6A 5C2
[4]Brain and Mind Institute, University of Western Ontario, London, Ontario, Canada N6A 5B7
[5]National Centre for Audiology, University of Western Ontario, London, Ontario, Canada N6G 1H1

ABSTRACT

The superior colliculus (SC) is a midbrain structure central to orienting behaviors. The organization of descending projections from sensory cortices to the SC has garnered much attention; however, rarely have projections from multiple modalities been quantified and contrasted, allowing for meaningful conclusions within a single species. Here, we examine corticotectal projections from visual, auditory, somatosensory, motor, and limbic cortices via retrograde pathway tracers injected throughout the superficial and deep layers of the cat SC. As anticipated, the majority of cortical inputs to the SC originate in the visual cortex. In fact, each field implicated in visual orienting behavior makes a substantial projection. Conversely, only one area of the auditory orienting system, the auditory field of the anterior ectosylvian sulcus (fAES), and no area involved in somatosensory orienting, shows significant corticotectal inputs. Although small relative to visual inputs, the projection from the fAES is of particular interest, as it represents the only bilateral cortical input to the SC. This detailed, quantitative study allows for comparison across modalities in an animal that serves as a useful model for both auditory and visual perception. Moreover, the differences in patterns of corticotectal projections between modalities inform the ways in which orienting systems are modulated by cortical feedback. J. Comp. Neurol. 524:2623–2642, 2016.

INDEXING TERMS: auditory cortex; corticotectal projections; somatosensory cortex; visual cortex; RRID:SciRes_000161; RRID:nif-0000-1029

Across modalities, the principle function of sensory systems is to form an accurate representation of the world around us through the sensation and perception of environmental stimuli. To ensure that potentially relevant stimuli are attended to, a system exists that reorients sensory organs and directs behavioral responses toward appetitive stimuli, such as potential prey, and away from aversive stimuli. Central to this orienting system is the superior colliculus (SC), a midbrain structure composed of multiple layers (Kanaseki and Sprague, 1974). The SC is capable of integrating information from diverse sensory systems (Stein, 1998; King, 2004) with maps of visual and auditory space, and somatosensation across the body surface that are in register across the structure (Stein, 1984; see May, 2006 for a review of SC structure and gross connectivity). Moreover, the intermediate and deep laminae of the SC in the cat have been shown to contain maps of pinna and eye movements that are in register with sensory topographies, suggesting an efficient mechanism for sensorimotor integration (Stein and Clamann, 1981). Indeed, a model of integration that involves the remapping of sensory inputs to motor coordinates, to direct overt

The first two authors contributed equally to this work.

Grant sponsor: the Canadian Institutes of Health Research; Grant sponsor: the Natural Science and Engineering Research Council of Canada; Grant sponsor: the Canada Foundation for Innovation.

*CORRESPONDENCE TO: Stephen G. Lomber, The University of Western Ontario, Medical Sciences Building, Room 216, 1151 Richmond Street North, London, Ontario, N6A 5C1, Canada. E-mail: steve.lomber@uwo.ca

Received September 28, 2015; Revised February 3, 2016;
Accepted February 3, 2016.
DOI 10.1002/cne.23980
Published online March 5, 2016 in Wiley Online Library (wileyonlinelibrary.com)

behavior via a common pathway, appears to hold across species (Sparks, 1988; Stein et al., 1995). Such a pathway has been demonstrated electrophysiologically in monkeys, in which retinal and auditory signals, although initially encoded in different coordinate systems, share a common efferent pathway via the SC for the generation of saccadic eye movements (Jay and Sparks, 1987).

Signal processing in the SC can be modulated by corticotectal projections from the sensory cortex (Diamond et al., 1969; Wallace et al., 1993). Early studies suggested that top-down regulation of SC function was particularly critical for visual orienting relative to other sensory systems (Stein, 1978). However, subsequent studies have reinforced the critical influence of both somatosensory (Clemo and Stein, 1986) and auditory (Meredith and Clemo, 1989) cortices on SC-mediated orienting behaviors. In some species, a differential pattern of innervation has been observed between the medial and lateral poles of the SC. For example, the upper half of the rat's visual field is involved in predator recognition and avoidance and projects to the medial SC, whereas the lower half of the field is involved in prey recognition and projects laterally. These field representations are consequently involved in defensive and approach behaviors, respectively, and have been shown to have largely non-overlapping cortical projections (Comoli et al., 2012). Although this pattern of differential projection would not be expected to hold for larger species, in which the division between behavioral outputs of the visual field representations is much less clear, it nevertheless underscores the importance of the SC for sensorimotor integration and the control of relevant behavior.

A number of studies have attempted to identify or quantify the sources of top-down projections to the SC, typically within a particular sensory modality. Within the visual system, a number of cortical areas have been implicated in regulating orienting behavior. Early studies revealed that deactivation of lower-level striate (area 17) and extrastriate (areas 18 and 19) cortices results in drastic decreases in SC activity in the cat (Wickelgren and Sterling, 1969; Stein, 1978). Similar deficits are observed following deactivation of areas along the banks of the posterior middle suprasylvian sulcus, including the posteromedial and posterolateral lateral suprasylvian areas (PMLS and PLLS, respectively; Lomber et al., 1994b). Indeed, anatomical evidence of direct corticotectal projections between each of these areas and the SC has been demonstrated (Harting et al., 1992).

As in the visual system, deactivation of at least one of the core areas of the cat auditory cortex (the primary auditory cortex; A1) results in a deficit in spatial orienting behavior (Lomber et al., 2007a; Malhotra et al., 2008). Moreover, similar deficits are observed following deactivation of the dorsal zone (DZ), posterior auditory field (PAF), and auditory field of the anterior ectosylvian sulcus (fAES; Lomber et al., 2007a; Malhotra et al., 2008). Anatomical examinations of corticotectal projections from auditory areas have been limited in scope, or have provided contradictory results. A robust projection from the fAES to the SC has been described (Meredith and Clemo, 1989; Chabot et al., 2013), and it was noted that stimulation of the fAES drove auditory neurons of the SC, whereas this was not the case for any other field of the auditory cortex (Meredith and Clemo, 1989). However, some studies note sizeable projections to the SC from other nonprimary auditory fields, including the second auditory cortex (A2; Winer et al., 1998).

The cortical areas implicated in somatosensory orienting behavior include both primary (Burton and Sinclair, 2000) and secondary areas (Burton et al., 1997). Early electrophysiological studies demonstrated that stimulation of somatosensory cortex elicits field potentials (Tamai, 1973) and unit responses (Kassel, 1982) in the ipsilateral SC (but see Stein, 1978). Previous anatomical examinations of somatosensory projections to the SC of the cat found only weak projections from primary (S1) and secondary (S2) somatosensory cortices (Stein et al., 1983). Instead, input has been shown to be dominated by the fourth somatosensory area (S4; Stein et al., 1983; McHaffie et al., 1988), and areas located along the rostral suprasylvian sulcus (rSS), including parts of the medial division of the second (S2m), and the fifth somatosensory (S5) areas (Clemo et al., 2007). Somatosensory representations within the S4 and along the rSS show a topographical relationship to somatosensory receptive fields in the SC, and these cortical areas have been shown to modulate the responses of SC neurons (Clemo and Stein, 1984, 1986), including descending output neurons of the SC that are directly involved in initiating orienting behaviors (Wallace et al., 1993). Indeed, electrical stimulation in and around area S4 in the unrestrained cat appears to elicit gaze shifts, reaching movements of the contralateral limb, and adjustments in body posture (Jiang and Guitton, 1995). Although a number of the studies described above have addressed the top-down connectivity between sensory cortices and the SC, it remains difficult to interpret these projections in a holistic manner, as these studies have typically been undertaken within a single modality, and across a number of species (Table 1). The few studies that have looked across visual, auditory, and somatosensory modalities were limited to descriptive discussions. Moreover, those

studies that have attempted to provide more quantitative analyses often fail to describe the source of corticotectal projections with respect to sensory system (Manger et al., 2010), or provide a comparison across hemispheres (Powell, 1976; Tortelly et al., 1980; Galetti et al., 1981; Berman and Payne, 1982; Wallace et al., 1993). Thus, the current study aims to compare the bilateral patterns of corticotectal projections arising from auditory, visual, somatosensory, motor, and limbic cortices of the cat. The retrograde tracer wheat-germ agglutinin conjugated to horseradish peroxidase (WGA-HRP) is employed to allow for ease of comparison with previous studies. Although it is anticipated that the visual cortex will dominate the corticotectal projections to the SC, the current approach will reveal the principal auditory and somatosensory inputs and, importantly, allow for within-animal comparison across modality and cortex of origin.

MATERIALS AND METHODS

Five adult (>6 months old) female domestic cats were examined. All the cats were obtained from a US Department of Agriculture (USDA)-licensed commercial animal breeding facility (Liberty Laboratories, Waverly, NY). All surgical and experimental procedures were conducted in accordance with the US National Research Council's *Guidelines for the Care and Use of Mammals in Neuroscience and Behavioral Research* and the Canadian Council on Animal Care's *Guide to the Care and Use of Experimental Animals* and were approved by the Western University Animal Use Subcommittee of the University Council on Animal Care.

Surgical procedures

The afternoon prior to each surgical procedure, cats were fasted, lightly anesthetized with ketamine (4 mg/kg, i.m.) and Domitor (Zoetis, Florham Park, NJ; 0.05 mg/kg, i.m.), and an indwelling catheter was inserted into the cephalic vein to deliver antiinflammatory medication (dexamethasone, 0.05mg/kg, i.v.). On the day of surgery, each cat was given atropine (0.02 mg/kg, s.c.) to minimize respiratory and alimentary secretions, acepromazine (0.02 mg/kg, s.c.), an additional dose of dexamethasone (0.5 mg/kg, i.v.), and buprenorphine (0.01 mg/kg, s.c.). Sodium pentobarbital (25 mg/kg to effect, i.v.) was administered through the catheter to induce general anesthesia. The cat was positioned in a stereotaxic apparatus and prepared for surgery using aseptic procedures. Body temperature, respiration rate, and heart rate were monitored throughout the procedure. Temperature was maintained at 37°C using a water-filled heating pad (Gaymar, Orchard Park, NY).

A midline incision was made and the temporalis muscle was reflected laterally. A large craniotomy was made over the marginal, posterolateral, and middle suprasylvian gyri of the left hemisphere. The bone piece was removed and stored in sterile saline for later replacement, and the dura was reflected laterally. Mannitol (25 mg/kg, i.v.) was infused to make the cerebrum more malleable and to permit lateral displacement. This approach has been repeatedly shown to permit direct visualization of the dorsal surface of the SC, just anterior to the bony tentorium (Lomber et al., 2001, 2002, 2007b; Chabot et al., 2013). To better visualize the dorsal surface of the SC, the posterior half of the splenium of the corpus callosum was ablated by aspiration.

Abbreviations

A1	Primary auditory cortex
A2	Second auditory cortex
AAF	Anterior auditory field
AEV	Anterior ectosylvian area
ALLS	Anterolateral lateral suprasylvian area
AMLS	Anteromedial lateral suprasylvian area
ca	Anterior commissure
CgA	Anterior cingulate area
CgP	Posterior cingulate area
CVa	Cingulate visual area
DLS	Dorsal lateral suprasylvian area
dPE	Dorsal posterior ectosylvian gyrus
DZ	Dorsal zone of auditory cortex
EPp	Posterior posterior ectosylvian field
fAES	Auditory field of the anterior ectosylvian sulcus
FRS	Multisensory–auditory field of the rostral suprasylvian sulcus
IC	Inferior colliculus
Ipe	Intermediate posterior ectosylvian gyrus
IN	Insular auditory cortex
MGB	Medial geniculate body
mSS	Middle suprasylvian sulcus
PAF	Posterior auditory field
Pag	Periaqueductal gray
PLLS	Posterolateral lateral suprasylvian area
PMLS	Posteromedial lateral suprasylvian area
PS	Posterior suprasylvian area
Psb	Postsubiculum
Rsp	Retrosplenial area
S1	Primary somatosensory cortex
S2	Second somatosensory area
S3	Third somatosensory area
S4	Fourth somatosensory area
S5	Fifth somatosensory area
S*	Somatosensory representation on the lateral bank of the anterior ectosylvian sulcus
SC	Superior colliculus
SGI	Stratum griseum intermediale
SGP	Stratum griseum profundum
SGS	Stratum griseum superficiale
SVA	Splenial visual area
T	Temporal auditory cortex
V1	Primary visual cortex
VAF	Ventral auditory field
VLS	Ventral lateral suprasylvian area
VPAF	Ventral posterior auditory field
vPE	Ventral posterior ectosylvian gyrus
WGA-HRP	Wheat-germ agglutinin conjugated to horseradish peroxidise
wm	White matter

TABLE 1.
Summary of Corticotectal Connectional Studies

Species	Authors	Modality			Antero from cortex	Retro from SC	Quantified	Compared
		Visual	Auditory	Somatosensory				
Cat	Holländer, 1974	X				X	No	No
Cat	Magalhães-Castro et al., 1975	X				X	No	No
Cat	Updyke, 1977	X			X		No	No
Rat	Wise and Jones, 1977			X	X	X	No	No
Cat	Kawamura et al., 1978	X				X	No	No
NWM	Graham et al., 1979	X			X		No	No
Rat	Sefton et al., 1981	X				X	No	No
OWM	Leichnetz et al., 1981	X			X	X	No	No
NWM	Tigges and Tigges, 1981	X			X		No	No
Cat	Baleydier et al., 1983	X			X	X	No	No
Cat	Stein et al., 1983			X	X	X	No	No
Cat	Segal and Beckstead, 1984	X			X	X	No	No
NWM	Cusick, 1988	X			X		No	No
Rat	Harvey and Worthington, 1990	X			X		No	No
Cat	Norita et al., 1991	X			X	X	No	No
Cat	Harting et al., 1992	X			X		No	No
OWM	Lui et al., 1995	X			X		No	No
Opossum	Martinich et al., 2000	X				X	No	No
Cat	McHaffie et al., 2001	X			X	X	No	No
Cat	Baleydier, 1977	X	X			X	No	No
Cat	Kawamura and Konno, 1979	X	X	X		X	No	No
Cat	Tortelly et al., 1980		X	X		X	No	No
Rat	Thong and Dreher, 1986	X	X	X		X	No	No
OWM	Lock et al., 2003	X	X	X		X	No	No
Tree shrew	Baldwin et al., 2013	X	X	X		X	No	No
Cat	Meredith and Clemo, 1989		X		X	X	Yes (Retro)	No
NWM	Collins et al., 2005	X				X	Yes	No
Rat	Hoffer et al., 2005			X	X		Yes	No
Ferret	Bajo et al., 2010		X		X	X	Yes (Antero)	No
Cat	Chabot et al., 2013		X			X	Yes	No
OWM	Fries, 1984	X	X	X		X	Yes	No
Tree shrew	Casseday et al., 1979	X	X	X		X	No	Yes
Hedgehog	Künzle, 1995	X	X	X		X	No	Yes
Tree shrew	Baldwin et al., 2013	X	X	X		X	No	Yes
NWM	Baldwin and Kaas, 2012	X	X	X		X	No	Yes
Ferret	Manger et al., 2010	X	X	X		X	Yes	Yes

Abbreviations: SC, superior colliculus; OWM, Old World monkey; NWM, New World monkey.

Severing the posterior end of the corpus callosum permitted the injection pipette to enter the SC orthogonal to its dorsal surface.

Tracer deposits

WGA-HRP was deposited into the left SC of five cats. WGA-HRP has previously been demonstrated to be a highly sensitive retrograde neuronal tracer (particularly when used in conjunction with a tetramethyl benzidine [TMB] protocol); it has been used previously to successfully quantify corticotectal inputs in the cat (Chabot et al., 2013), and allows for direct comparison with the majority of anatomical examinations of the cortical projections to the SC. Each animal received three penetrations, and two separate injections were made at each penetration between 1,000 and 2,000 μm below the surface of the SC to optimally inject both the superficial and deeper layers (Fig. 1). Each of the six total injections was made with a microliter syringe (Hamilton, Reno, NV), and consisted of 0.025–0.050 μl of 5% WGA-HRP pressure injected through a 30–35 μm-diameter pipette tip. Any leakage of WGA-HRP tracer over the surface of the SC during the injections was removed with sterile saline flushes to prevent tracer contamination of surrounding brain tissue. Following each deposit, the pipette remained stationary for 5 minutes. As is true of any protocol involving penetrations into neural tissue, there was likely some uptake of tracer by damaged fibers of passage in the current study; however, our protocol aims to minimize this uptake through the combination of multiple, small-volume injections and by allowing sufficient time

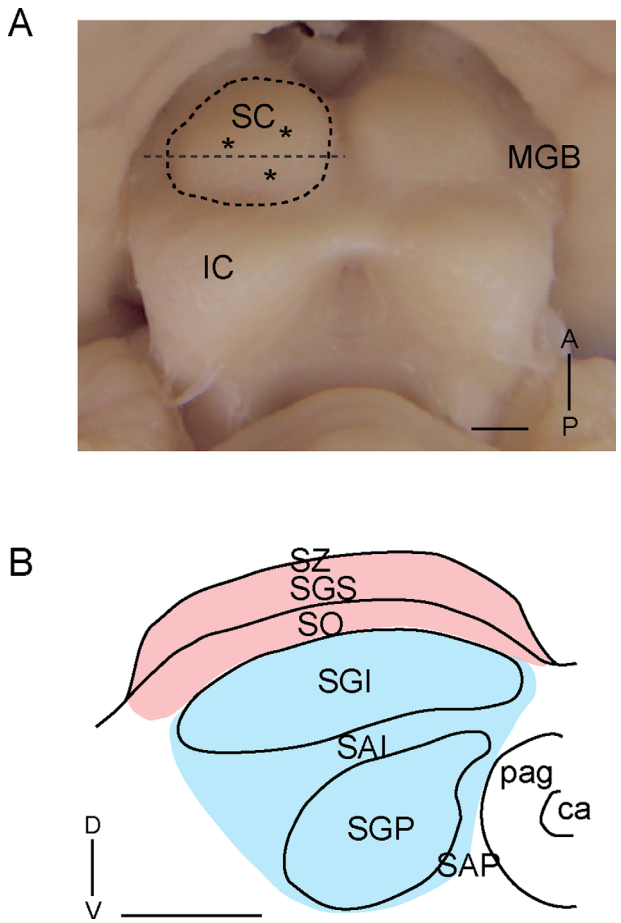

Figure 1. Injection locations and layers of the superior colliculus. **A**: Dorsal view of the mesencephalon: superior colliculus (SC) and inferior colliculus (IC). The anteroposterior axis is indicated at the bottom right. The dashed line bisecting the SC represents the level at which the SC is presented in B. The three asterisks indicate locations of the penetrations. **B**: The superior colliculus contains alternating gray and white layers. From dorsal to ventral, these layers are: the stratum zonale (SZ), superficial gray layer (SGS), stratum opticum (SO), intermediate gray layer (SGI), intermediate white layer (SAI), deep gray layer (SGP), and stratum album profundum (SAP). The superficial zone (pink shading; SZ, SG, and SO) receives the visual inputs, whereas the deep zone (blue shading; SGI, SAI, SGP, and SGP) receives multisensory inputs. For abbreviations, see list. Scale bar = 500 μm in A,B.

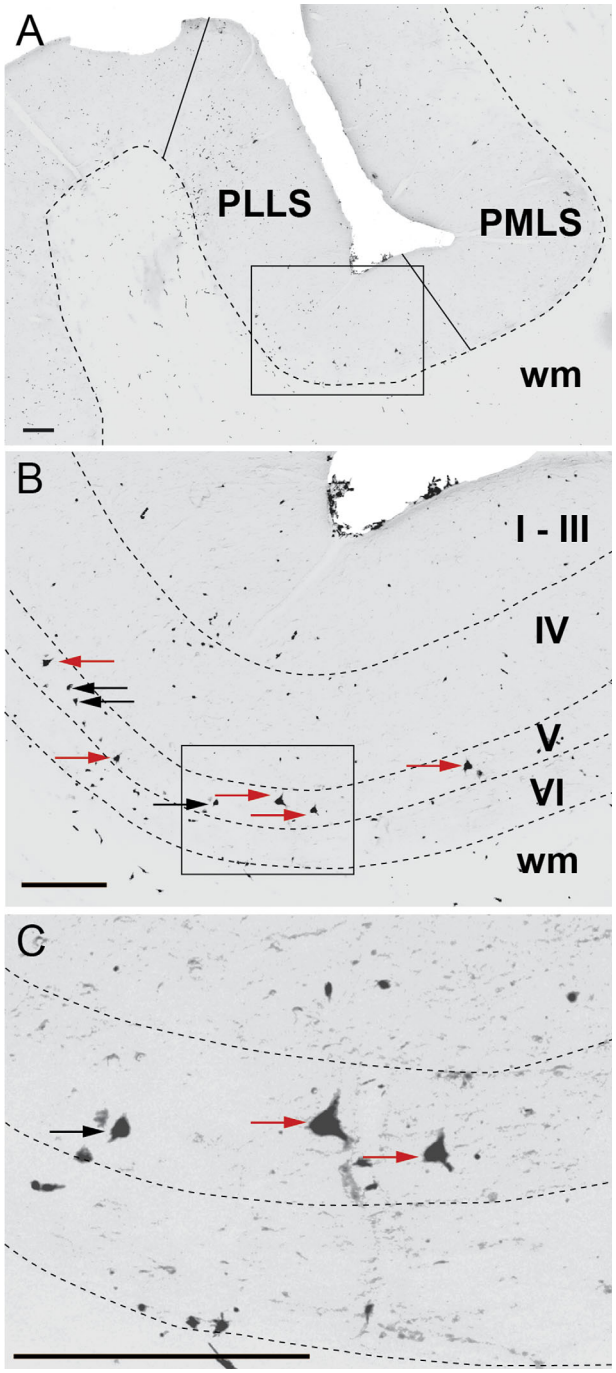

Figure 2. Labeled neurons in the posterolateral lateral suprasylvian (PLLS) area. The dashed lines indicate the boundaries between gray and white matter (**A**) or between cortical layers (**B,C**). The red arrows indicate labeled neurons. To be considered a labeled neuron, the nucleus and the entirety of the somatic membrane had to be present. The black arrows point to neurons that are too faintly labeled, and were not included in the count. For abbreviations, see list. Scale bar = 50 μm in A–C.

between injections. When all three penetrations were complete, the bone piece was replaced and secured with dental acrylic and stainless steel skull screws. Dermal incisions were sutured with 3-0 silk.

Postsurgical procedures

The indwelling catheter was removed, and half-strength lactated Ringer's solution (20 ml/kg, s.c.) was administered as needed during the first 4 hours following surgery. Heart rate, respiratory rate, and temperature were continually monitored until the animal was sternally recumbent. The analgesic buprenorphine (0.01 m/kg, s.c.) was administered every 6 hours for

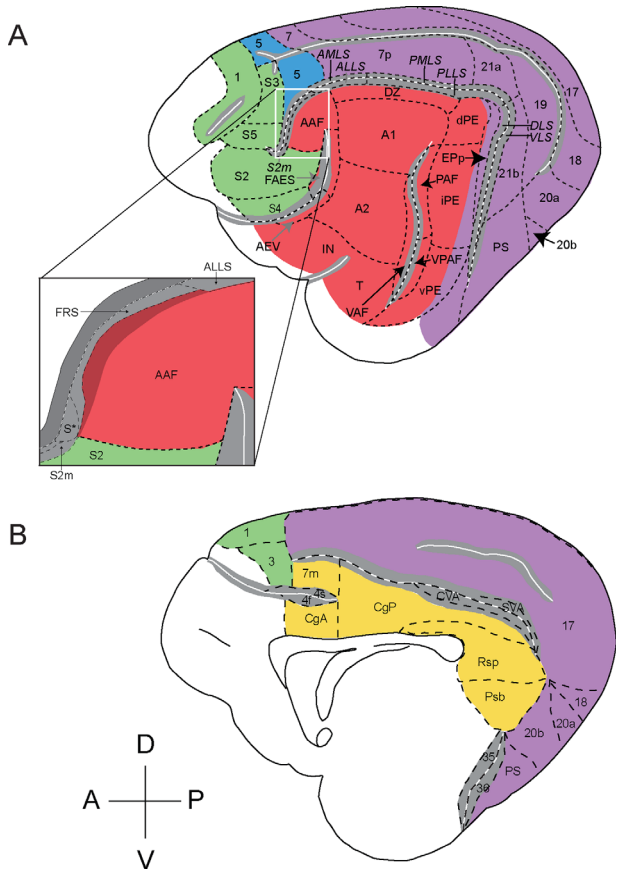

Figure 3. Schematic views of the cat cerebrum showing the visual, auditory, somatosensory, motor, and limbic cortical areas. **A**: Lateral view of the cat brain showing visual (purple), auditory (red), somatosensory (green), and motor areas (blue). Sulci (gray) are open to represent the sulcal cortex. Inset provides detailed structure of the anterior ectosylvian sulcus, and is adapted from Clemo et al. (2007). Dashed lines indicate cortical area borders. Dorsoventral and anteroposterior axes are indicated at bottom left. **B**: Medial view of the cat brain with the same general organization as in A. Limbic areas are presented in yellow. For abbreviations, see list.

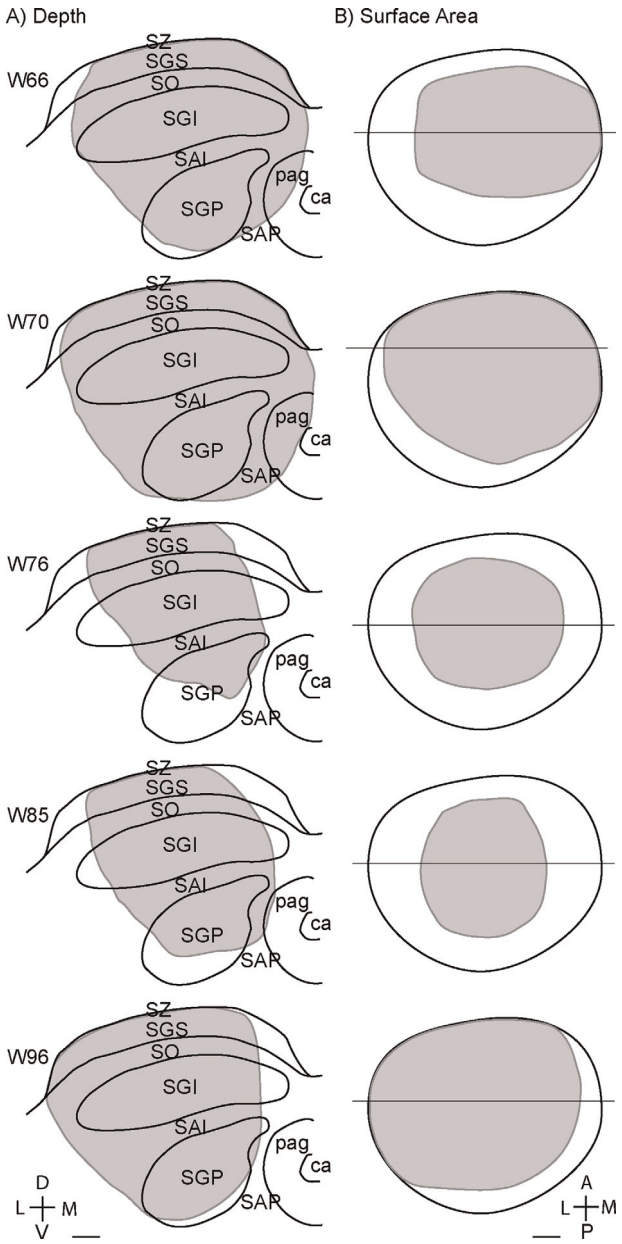

Figure 4. Schematic representations of the five cases in the present study, presented on a standardized superior colliculus. **A**: The tracer spread across the coronal plane of the SC for each animal. **B**: The tracer spread along a dorsal view in the same animals. Note that the tracer spread throughout the superficial and deep layers of the superior colliculus. Tracer spread ventromedially into the periaqueductal gray (pag) in two cases, but there is no evidence of spread into the contralateral SC or ipsilateral pretectum in any case. For abbreviations, see list. Scale bar = 500 μm in A,B.

the first 24 hours, and every 12 hours for the subsequent 24 hours. Animals also received the systemic antibiotic Convenia (Zoetis; 8 mg/kg, s.c.) to guard against possible infection. Cats received dexamethasone (0.05 mg/kg, s.c.) every 24 hours for 2 days after surgery. In all cases, recovery was uneventful.

Perfusion and tissue processing

Forty-eight hours following tracer injections, the cephalic vein was cannulated, and the cat was deeply anesthetized (sodium pentobarbital, 25 mg/kg i.v). The anticoagulant heparin (10,000 U; 1 ml), and the vasodilator 1% sodium nitrite (1 ml) were administered. The cat was then perfused through the ascending aorta with physiological saline for 5 minutes. Next, aldehyde fixatives (1% paraformaldehyde/1.5% gluteraldehyde) were perfused for 20 minutes, followed by 10% sucrose for 5 minutes. All solutions were buffered to a pH of 7.4 with 0.1 M Sorenson's buffer and infused at a rate of 100 ml/min. Immediately following the perfusion, the head was mounted in a stereotaxic frame. The brain

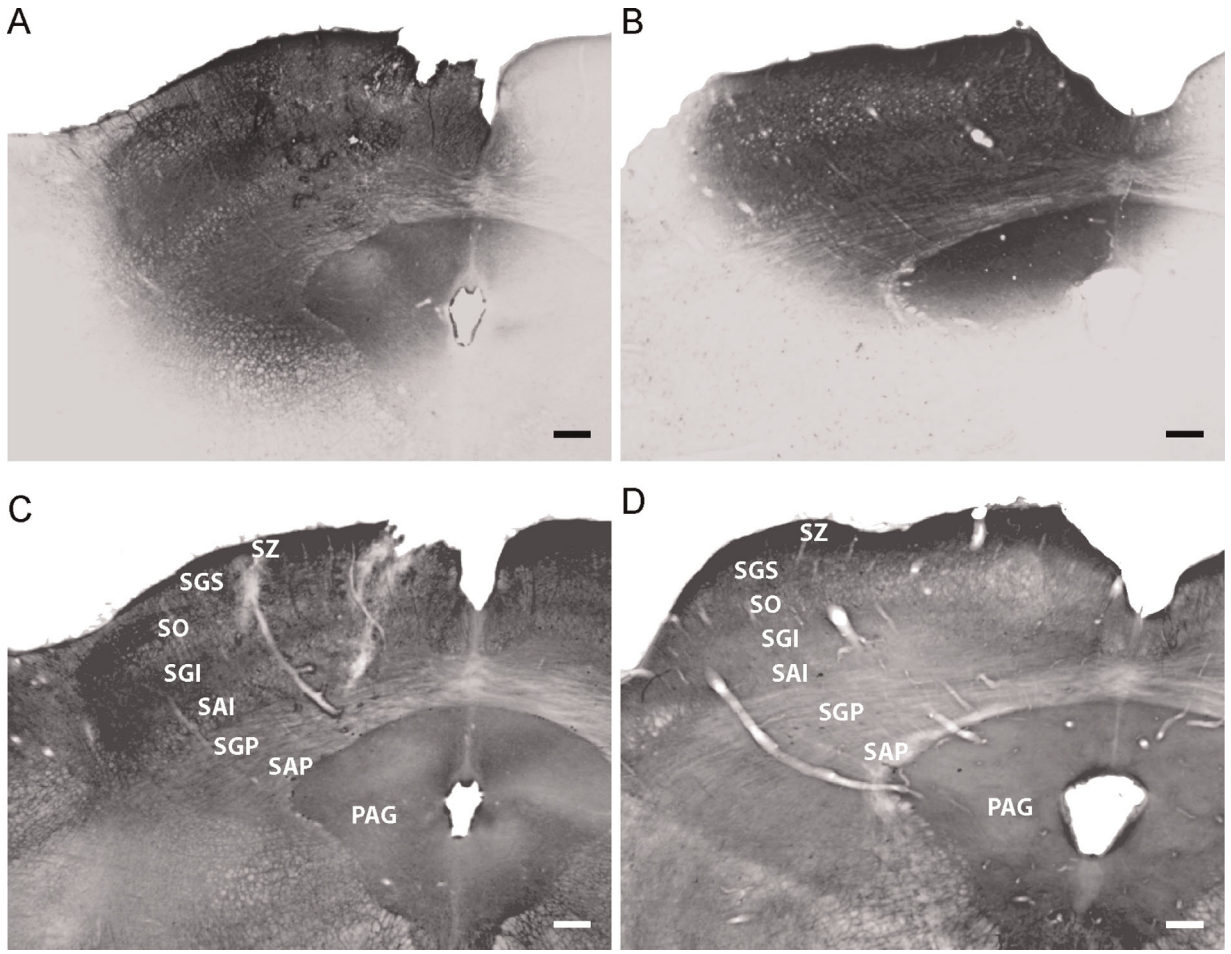

Figure 5. Photomicrographs of coronal sections passing through the superior colliculus of cases W70 (**A,C**) and W66 (**B,D**). A and B depict the injection sites, and C and D present photomicrographs from the cytochrome oxidase series with layers of the superior colliculus indicated. A track left by the Hamilton syringe is visible in C. Note that the WGA-HRP tracer spread into all the layers of the superior colliculus, with some spread into the periaqueductal gray in these two cases only. For abbreviations, see list. Scale bar is 500 μm in A–D.

was then exposed, blocked in the coronal plane at Horsley–Clarke level A25 (for review, see Schurr and Merrington, 1978), and removed from the cranium. Each brain was photographed to provide a permanent record, and immersed in 30% sucrose in 0.1 M Sorenson's buffer until it sank, to cryoprotect it for histological processing.

Brains were frozen, and sections were cut in the coronal plane at 60 μm using a freezing microtome, and collected serially through the entire brain. Six series of sections at 360 μm intervals were created. Individual series were processed for: 1) HRP–diaminobenzidine (HRP-DAB) intensified with cobalt-nickel (Adams, 1981); 2) HRP–tetramethyl benzidine (HRP-TMB) histochemistry (Mesulam, 1978; as modified by Olucha et al., 1985); 3) cytochrome oxidase (Payne and Lomber, 1976); and 4) cresyl violet (Nissl stain). The remaining series were extras and were discarded after all tissue was successfully mounted onto gelatin-coated slides, air-dried, cleared, and coverslipped.

Data analysis

Tissue was analyzed using standard light/darkfield microscopy with a Nikon E600 microscope mounted with a DXM 1200 digital camera. The contours of sections and the injection sites were traced, and labeled cells were examined, quantified, and plotted using Neurolucida software (MicroBrightfield, Williston, VT; RRID:nif-0000-10294). The quantification was performed using the tissue series processed for HRP-TMB due to the sensitivity of this approach, and used an exhaustive search paradigm that ensured all tissue was examined and labeled cells were identified. An additional series from each animal was reacted using the HRP–DAB procedure as a backup (the DAB reaction is more stable over time than TMB); however, in all cases the series processed using

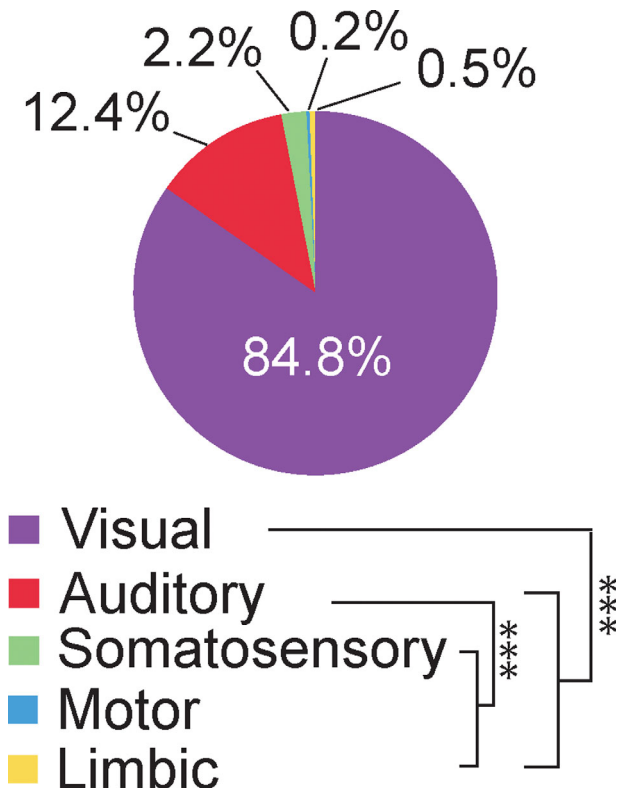

Figure 6. Pie graph illustrating the distribution of corticotectal projections by modality in the cortex. The percentages of labeled cells arising from each modality are presented on the graph. The magnitude of corticotectal projection differed significantly by modality ($F(4,16) = 344.53$, $P < 0.001$). The results of corrected pairwise comparisons are indicated (*** denotes $P < 0.001$).

the HRP–TMB protocol were reacted and quantified successfully, and thus the HRP–DAB series were ultimately redundant. Photomicrographs presented in this manuscript were adjusted for brightness and contrast using Adobe (San Jose, CA) Photoshop 12.1 (RRID:SciRes_000161), but were not otherwise altered.

For a neuron to be considered HRP-positively labeled and not merely an artifact of the reaction process, the nucleus had to be visible and the entirety of the somatic membrane had to be present (Fig. 2). Portions of a cell or remnants of membrane were not counted. When labeled cells were determined to lie on the border of two cortical areas, or within a transitional zone between areas, the cells were equally distributed between the two areas. The focus of the microscope lens was adjusted throughout the z-plane to ensure that the full thickness of each section was examined.

Labeled neurons were assigned to cortical areas on an individual-animal basis based on cytoarchitecture and sulcal and gyral landmarks defining areal borders. The cortical area and layer in which each labeled cell was located were determined from superimposed images of adjacent sections stained for the presence of Nissl or cytochrome oxidase. Borders between the posterior lateral suprasylvian areas (PLLS and PMLS), and the dorsal and ventral lateral suprasylvian areas (DLS and VLS) of the visual cortex were placed on the lateral bank of the middle suprasylvian sulcus and the dorsal bank of the posterior limb of the suprasylvian sulcus, respectively (as per Palmer et al., 1978, Updyke, 1986, Rauschecker et al., 1987). This convention is supported by cytoarchitectonic methods in the visual system (van der Gucht et al., 2001). Overall, previously published cytoarchitectonic descriptions were utilized to determine boundaries between auditory, visual, somatosensory, motor, and limbic areas (Sanides, 1969; Meredith and Clemo, 1989; Clascá et al., 1997, 2000; Winer and Prieto, 2001). Figure 3 presents lateral and medial views of the cat cerebrum showing these delimitations with abbreviations based on the wide body of literature examining different sensory and motor fields of the cat cortex. A univariate analysis of variance (ANOVA) was performed with each cortical field projecting to the SC included, and a Tukey's HSD test was performed to compute all pairwise comparisons between fields. The same tests were also applied to compute the relative strength of projections at a modality level.

RESULTS

Tracer injections site and tracer spread

Five cats received deposits of WGA–HRP that spread throughout the superficial and deep layers of the left SC. The injection sizes were very similar to those of Meredith and Clemo (1989) and Chabot and colleagues (2013). The extents of injections in all five animals are illustrated on the coronal plane (Fig. 4A) and on a dorsal view of the SC (Fig. 4B). In all cases, the tracer was exposed to axon terminals in the stratum griseum superficiale (SGS), stratum griseum intermediale (SGI), and stratum griseum profundum (SGP; Fig. 5) and covered the majority of the SC (Fig. 4B). In two cases, the tracer spread into the periaqueductal gray (Fig. 4A, W66 and W70), whereas there was no evidence of spread into any portion of the pretectal nuclei or the inferior colliculus in any case. There was also no evidence of tracer spread to the contralateral SC.

Profile of labeling by modality, hemisphere, and layer

All neurons in the cerebral cortex showing positive labeling were counted. On an individual-animal basis, the number of labeled neurons in each cortical area was expressed as a percentage of the total number of

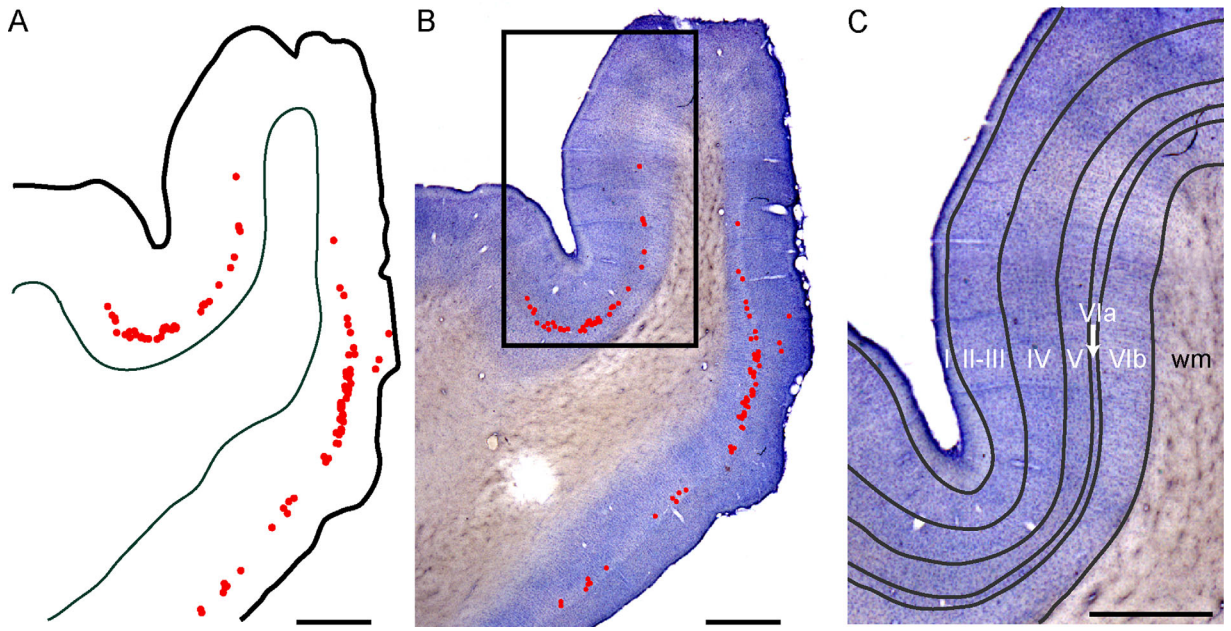

Figure 7. Determining layer-specific origins of corticotectal projections. **A**: Location of all labeled neurons in a partial cortical section. The outline of the section is shown as a thick black line, and the gray/white matter border is shown as a thin gray line. Labeled neurons are plotted as red dots. **B**: An adjacent Nissl-stained section. The labeled cells from A have been superimposed to identify their laminar location. **C**: A detailed view of the region outlined by the black box; laminar borders are denoted with gray lines. wm = white matter, scale bar = 1 mm.

labeled cells in the entire cortex to allow for meaningful conclusions despite variability in tracer uptake and spread, as well as in the tissue processing used to visualize labeled neurons.

As expected, the greatest direct projection to the SC emerged from the visual cortex (84.8%), with much smaller inputs from the auditory (12.4%), somatosensory (2.2%), motor (0.2%), and limbic cortices (0.5%; Fig. 6). The limbic projections arose from the anterior and posterior cingulate areas and accounted for 0.5% of all labeled cells (areal data not plotted). Labeled cells originated overwhelmingly from the infragranular layers (99.6%) of the ipsilateral cortex (93.4%). Infragranular projections arose almost entirely from layer V with few labeled cells present in layer VI. Although no further subdivision of cortical layers was explicitly made in the current study, labeled cells in layer VI appeared to be predominantly located in the VIa, suggesting an association with corticocortical projections. An example of this pattern of labeling and laminar delineation is provided in Figure 7. The sparse supragranular labeling observed was confined to layer II, and presented no discernable areal pattern of distribution. Thus a specific layer-wise comparison was not undertaken due to the lack of statistical power resulting from layers with few (layers II and VI) or no (layers I, III, and IV) labeled cells. Instead, cells were considered to be either supragranular or infragranular in nature to allow for a gross comparison of the laminar origin of cortical projections.

Profiles of labeling across cortical fields

A representative plot of labeled cells in one animal (W76) is presented in Figure 8. Labeling in the visual cortex covered the entirety of the visual field, from the representation of the fovea at the occipital pole to the most peripheral point of the visual field at the anterior portion of the visual cortex. Interestingly, the areas involved in visual orienting behavior, namely, areas 17, 18, 19, and the PMLS and PLLS, showed the strongest projections to the SC. The primary visual cortex (area 17) was the predominant source of projections to the SC, making up 36% of labeled cells across animals. Labeling was heaviest at the posterior aspect (upper visual field), with fewer labeled cells toward the anterior end (lower visual field). The next largest projections arose from the PLLS (13%), area 18 (9%), area 19 (7%), and the PMLS (7%; Fig. 9). Labeling in areas 18 and 19 was heaviest anteriorly, whereas the PMLS, PLLS, and the anterolateral and anteromedial lateral suprasylvian areas (ALLS and AMLS, respectively) were labeled uniformly along the anteroposterior axis. The remaining areas of the visual cortex are not involved in orienting behavior, and each made up less than 3% of the total labeled cells.

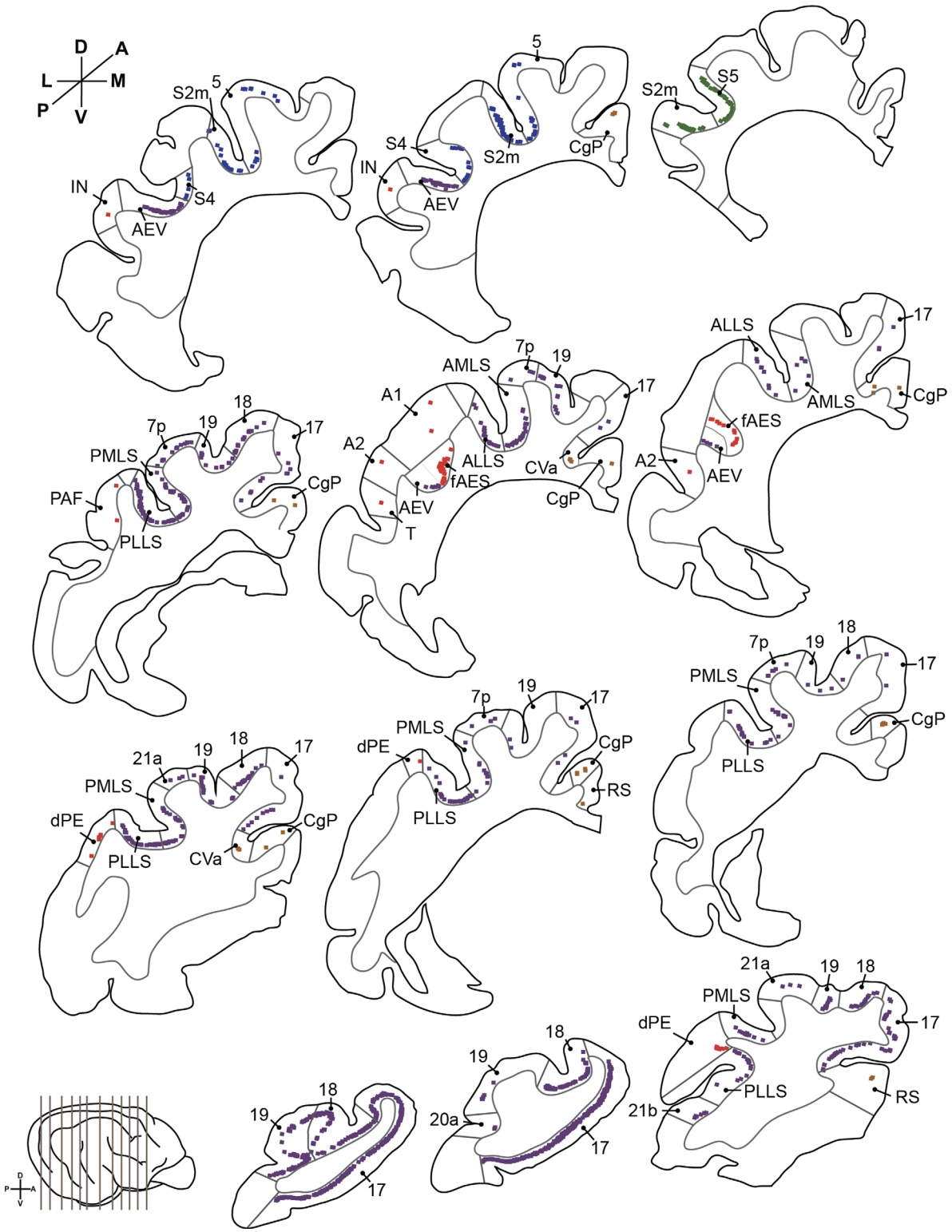

Figure 8. Representative distribution of visual (purple), auditory (red), somatosensory (green), motor (blue), and limbic (brown) corticotectal projections. The lateral schematic of the brain (lower left) shows the levels from which these mapped coronal sections through the cortex were taken. Note that visual areas 17, 18, 19, 20, 21, PLLS, PMLS, ALLS, AMLS, and area 7 are all labeled, with the most substantial labeling in the primary visual cortex (area 17). Labeled cells cover the entirety of area 17 from posterior to anterior. Contrary to the primary visual cortex, the primary auditory cortex is poorly labeled, as are the PAF and DZ. Labeled cells in the AI and PAF are found primarily in their posterior extent, adjacent to the dPE and iPE. Conversely, the fAES is heavily labeled following a superior colliculus injection. Similar to the auditory system, the S1 (areas 1 and 3) is devoid of labeling, with somatosensory cells projecting to SC confined to S2. For abbreviations, see list.

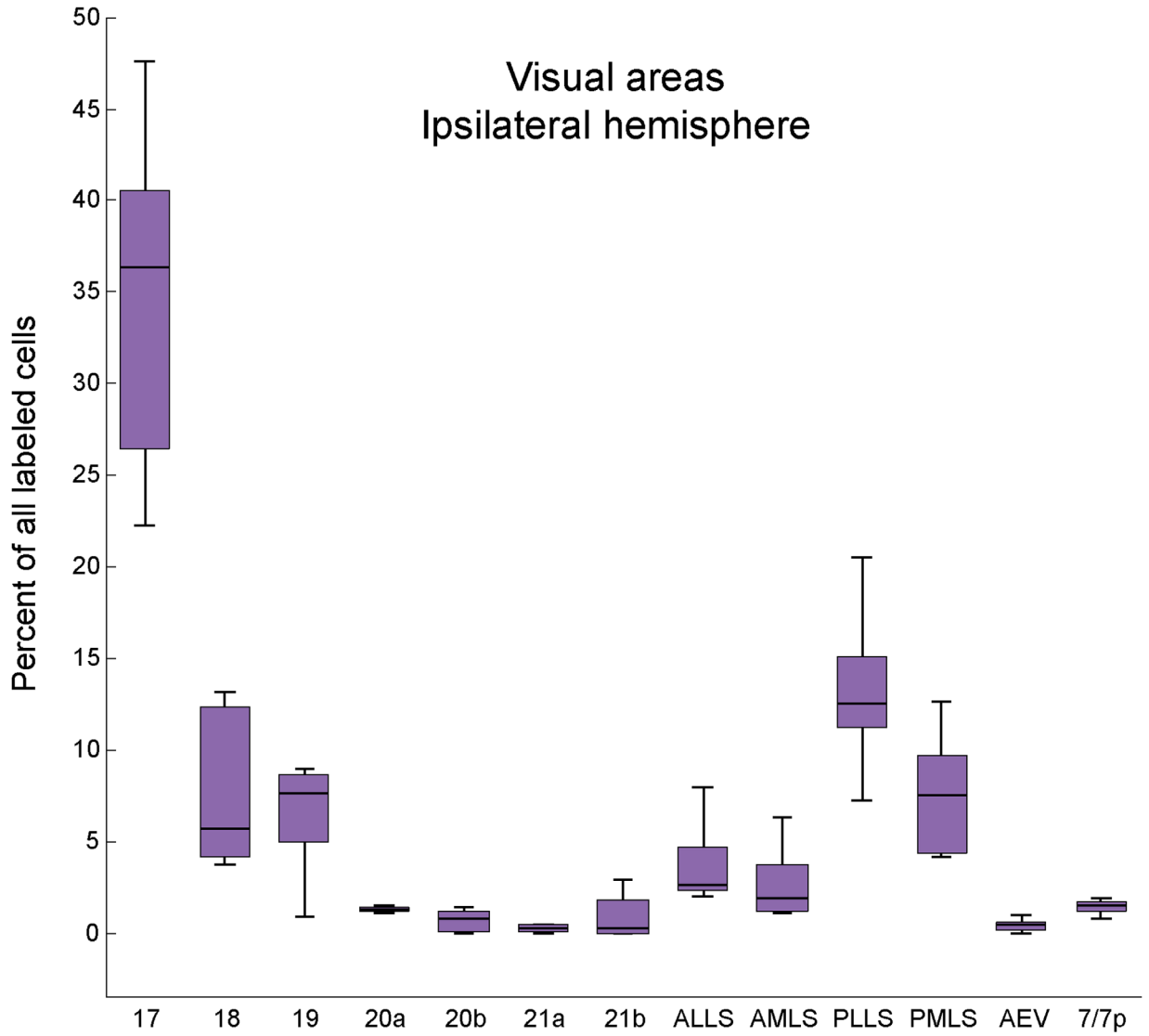

Figure 9. Box-and-whisker plot illustrating the distribution of visual corticotectal projections by cortical area. The y-axis indicates the percentage of labeled neurons, and whiskers extend a maximum of 1.5 times the interquartile range. The two major connections from the visual cortex originate from the primary area 17 (median = 36.4%) and PLLS (median = 12.6%). The other visual areas involved in visual orienting behavior (18, 19, PMLS) show weaker connections with the superior colliculus (median of 5.7%, 7.6%, and 7.5%, respectively). For abbreviations, see list.

Although labeling in the auditory cortex was sparse relative to visual areas, projections arose from 9 of the 13 auditory fields. Neuronal labeling was particularly abundant in the auditory field of the anterior ectosylvian sulcus (fAES; 4.7%) relative to other auditory fields (all $<$ 1%; Fig. 10). The remaining labeled cells were located in dorsoposterior areas, with more ventral fields showing little to no labeling. Interestingly, the primary auditory cortex (A1), the posterior auditory field (PAF), and the dorsal zone (DZ) showed very weak projections to the SC, with labeled cells confined to their posterior limits, adjacent to the dorsal and intermediate portions of the posterior ectosylvian sulcus (fields dPE and iPE, respectively).

In somatosensory and motor cortices, labeled neurons were observed in a small number of fields. These fields included the second (0.6%), fourth (0.5%), and fifth (0.5%) somatosensory areas (S2, S4, and S5, respectively), area 4 (0.2%), and area 5 (0.6%; Fig. 11). As in the auditory cortex, the primary somatosensory cortex has been implicated in orienting behavior, but does not have a substantial direct projection to the SC. The remaining fields involved with orienting, S2 and area 5, showed weak projections to the SC. It should be noted that blocking the brain at Horsley–Clarke level A25 prior to sectioning, as described above, precluded the quantification of labeled cells in the most anterior

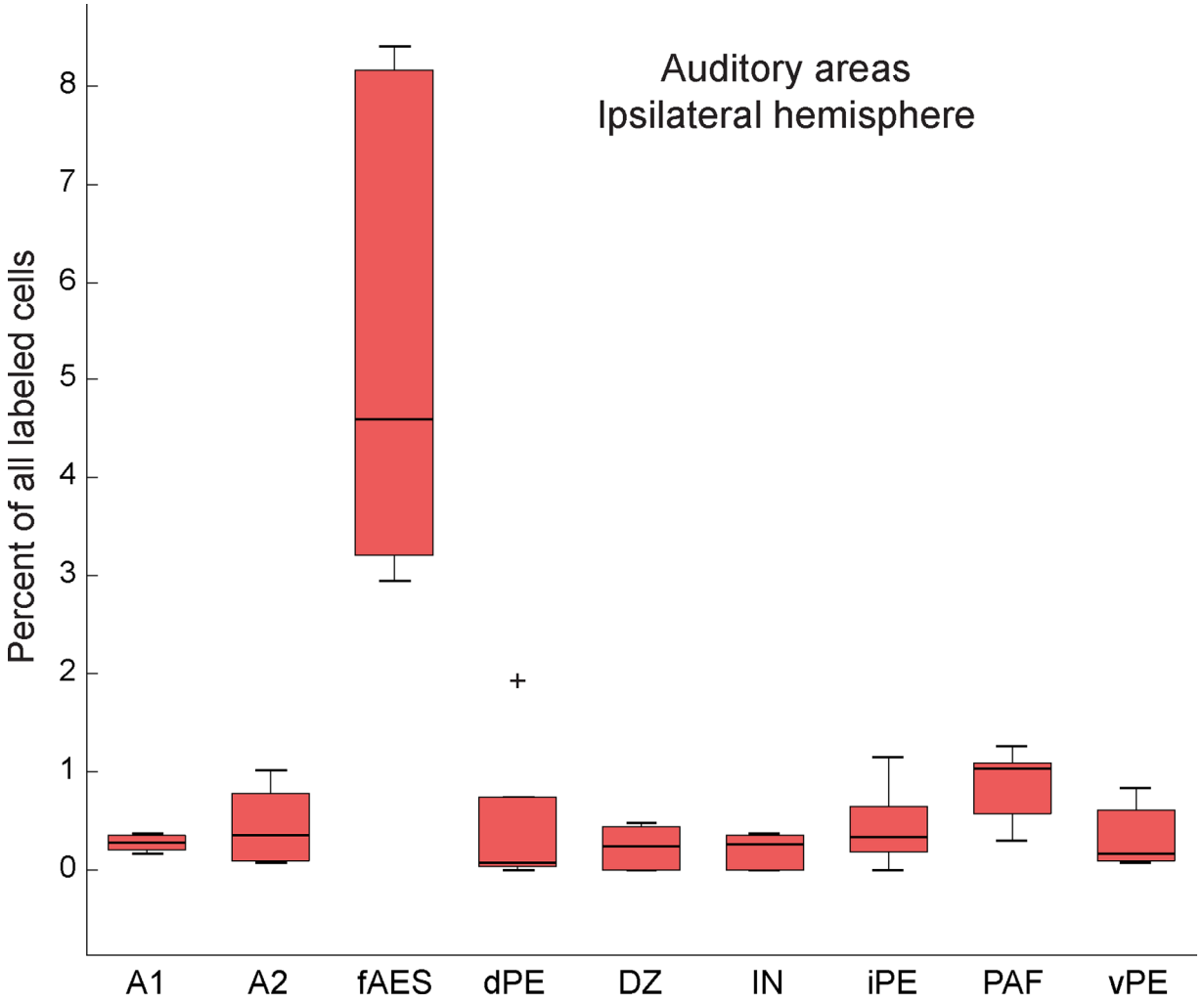

Figure 10. Box-and-whisker plot illustrating the distribution of auditory corticotectal projections by cortical area. The y-axis indicates the percentage of labeled neurons, whiskers extend a maximum of 1.5 times the interquartile range, and outliers are denoted by a black cross. The majority of the auditory cortical areas involved in the acoustic orienting behavior (A1, DZ, and PAF) do not show substantial direct axonal projections to the superior colliculus. However, the fAES is a significant source of projections to the superior colliculus (median = 4.6%). For abbreviations, see list.

fields of cat cortex. This includes areas that would be expected to have substantial inputs to the SC, including the medial portion of area 6, which has been shown to contribute to visually guided head orienting behavior in cats (Lomber and Payne, 2004) and which projects to the ipsilateral SC in the cat (Harting et al., 1992) and bilaterally to the SC in the macaque (Distel and Fries, 1982).

Considerably fewer labeled cells were identified in the contralateral than in the ipsilateral hemisphere (6.6% vs. 93.4%), and a somewhat different labeling profile was observed. Unlike in the ipsilateral hemisphere, labeling was very sparse in the visual cortex, and almost absent in the somatosensory cortical areas following an injection in the SC (Figs. 12 and 13). Within the auditory modality, the fAES remained the primary source of projections to the SC (4.24% of labeled cells compared with less than 1% in all other auditory areas; Fig. 13).

DISCUSSION

The current study presents the first quantitative analysis of corticotectal projections originating from the visual, auditory, somatosensory, motor, and limbic cortices of the cat (see Fig. 14 for a summary). This within-animal study provides the unique opportunity to compare the strength of projections across modalities and hemispheres, and is of particular importance given that stimuli that elicit an orienting response from the SC are often multisensory in nature.

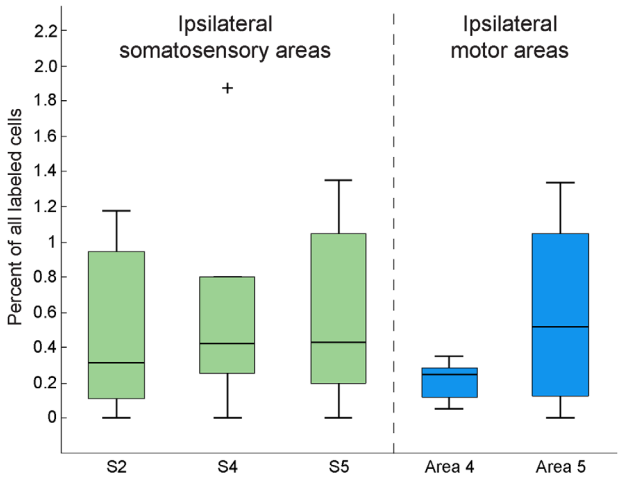

Figure 11. Box-and-whisker plot illustrating the distribution of somatosensory and motor corticotectal projections by cortical area. The y-axis indicates the percentage of labeled neurons, whiskers extend a maximum of 1.5 times the interquartile range, and outliers are denoted by a black cross. Note that the primary somatosensory area does not have a direct projection to the superior colliculus. For abbreviations, see list.

Ipsilateral projections by modality and cortical area

Retrograde pathway tracing with WGA–HRP confirms that corticotectal projections arise almost entirely from infragranular layers of cortex. This conforms to the laminar pattern observed across a number of other mammalian species (Kawamura et al., 1978; Tortelly et al., 1980; Baleydier et al., 1983; Fries, 1984; Segal and Beckstead, 1984; Kunzle, 1995; Martinich et al., 2000; Lock et al., 2003; Bajo et al. 2010; Manger et al., 2010). At the modality level, the principal source of projections is the visual cortex, with smaller projections originating from the auditory, somatosensory, motor, and limbic cortices. Although the absolute strengths differ, this relative pattern echoes that observed in the ferret (Manger et al., 2010).

The tracer injections made in the current study ensured that all layers of the SC were exposed to WGA–HRP. This is critical to quantifying visual corticotectal projections, as two systems have been identified in the cat: one that projects from the primary and secondary visual cortices to the superficial layers of the SC, and one that projects from fields along the middle suprasylvian sulcus (mSS) to both superficial (Segal and Beckstead, 1984) and deeper layers of the SC (Segal and Beckstead, 1984; Ogasawara et al., 1984). In ensuring that all layers of the SC were exposed to WGA–HRP, some tracer spread occurred into the periaqueductal gray (PAG) in two of five animals. Patterns of cortical projections to the PAG in the cat have been reported previously, and are dominated by fields of the frontal cortex including areas 6, 4, and 32 (Bandler et al., 19895). Although these oculomotor and motor areas are likely involved in defense-based reactions in response to sensory stimuli, they were not included in the analyses presented here due to the technical constraints outlined above. Smaller projections to the PAG have also been noted from sensory areas, including the primary and secondary somatosensory cortices (Bragin et al., 1984), auditory insular cortex (Winer et al., 1998), and fields surrounding the ventral extent of the anterior ectosylvian sulcus (Bandler et al., 1985; although that study is, itself, confounded by tracer spread from the PAG into adjacent tegmental and superior collicular divisions). The absence of projections from these fields in the current study suggests that the data presented here are not unduly confounded by tracer spread into the PAG. Moreover, animals with tracer spread into PAG (W66 and W70) showed no significant differences in the patterns of labeling across cortical fields when compared with those in which the injection was entirely confined within the SC (W76, W85, and W96).

Each of the areas previously demonstrated to be involved in visual orienting behavior in the cat—17, 18, 19, PLLS, and PMLS—show direct projections to the SC. This supports previous studies undertaken within the visual modality that involved either ablation techniques (Altman and Carpenter, 1961; Sprague et al., 1963, Kawamura et al., 1974; Baleydier, 1977; Kawamura and Konno, 1979; Berson and McIlwain, 1983) or retrograde axonal transport of HRP (Kelly and Gilbert, 1975; Magalhães-Castro et al., 1975). Contrary to previous studies that have noted labeling of visual cortical areas that was limited to caudal fields (Baleydier, 1977; Baleydier et al., 1983), the current study reveals projections arising from the caudal to rostral extents of the visual cortex. The wider distribution in our results is likely the result of injections that exposed the entirety of the SC, rather than being confined to its central portion. The pattern of visual corticotectal projections observed here is in accordance with qualitative patterns observed in *Didelphis aurita* (South American opossum; Martinich et al., 2000) and in monkeys (Tigges and Tigges, 1981; Lock et al., 2003; Baldwin and Kaas, 2012). It fits well with the few quantitative analyses that have been undertaken (Fries, 1984; Collins et al., 2005). However, despite sharing similar organizational principles (Innocenti et al., 2002; Manger et al., 2005), the current results are discordant with those of the ferret, in which the principal visual corticotectal projections arise from areas 18 and 21 (Manger et al., 2010). Moreover, Berson and McIlwain

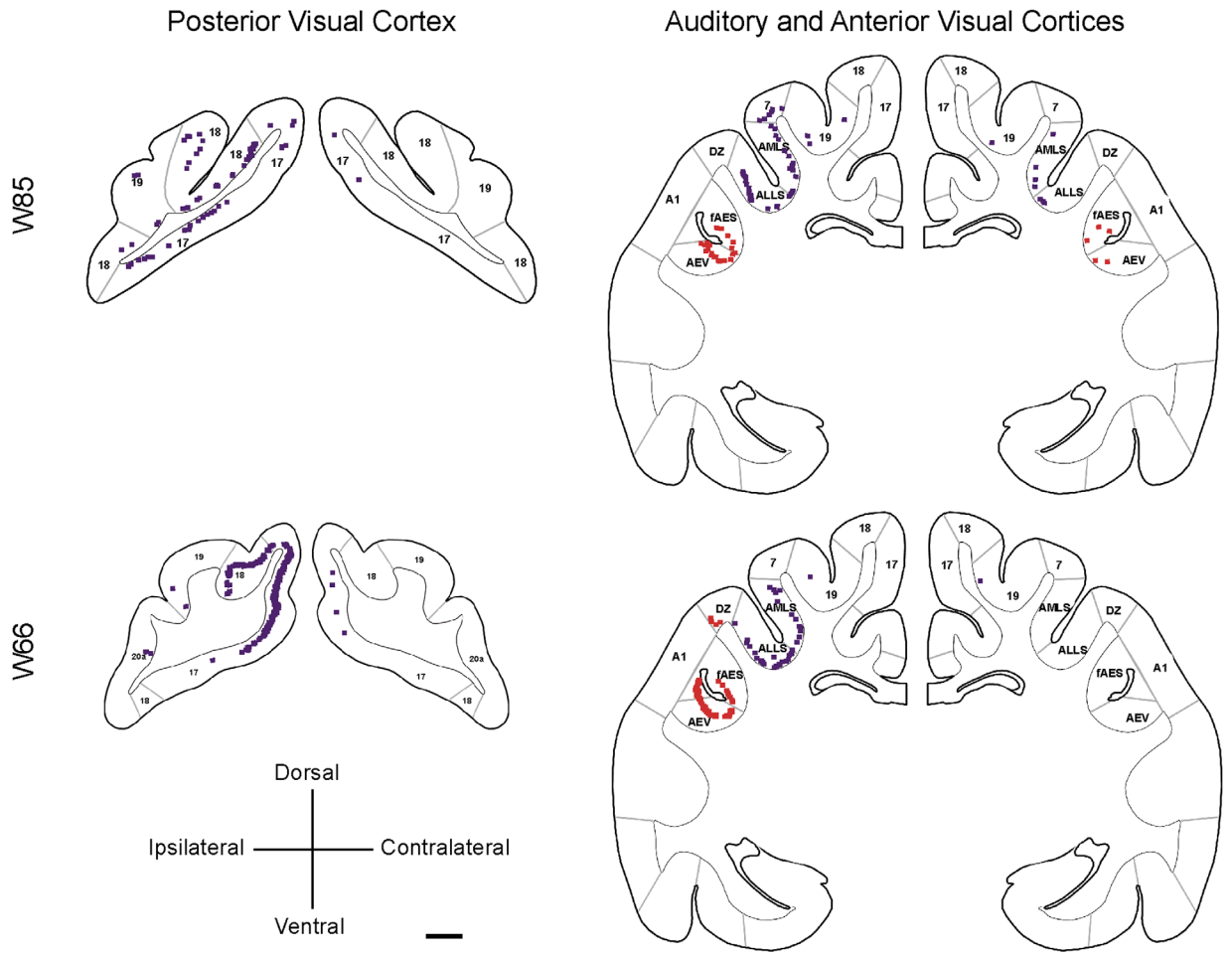

Figure 12. Profiles of HRP labeling in ipsilateral and contralateral hemispheres for two representative animals. In each case, individual animal data have been plotted on standardized coronal sections for ease of comparison. The left column shows plots of sections passing through the posterior visual cortices of the two animals. Plots of sections passing through the auditory and anterior visual cortices are presented on the right. Note that across modalities (visual in purple, auditory in red), the HRP-positive labeling in the contralateral hemisphere is quite sparse in comparison with that in the ipsilateral hemisphere. For abbreviations, see list. Scale bar = 2 mm.

(1983) observed that similar numbers of visual cells in the SC were driven by electrical stimulation of areas 17, 18, and 19, and the banks of the mSS, whereas the current study reveals that the projection from area 17 to the SC is 3 to 4 times larger than the projections from each of these other visual cortical areas. This may reflect the fact that, whereas the effects of cortical inputs are undoubtedly dependent on the number of neurons projecting from a given cortical area, there are other factors (including the number of terminals expressed on these projections, the cell types targeted, and the arrangement of synaptic terminals on target cell dendrites) that also contribute to synaptic strength. These additional factors are not measured using the current methodology. Contrary to what is observed in the visual system, only one of the areas considered to be involved in auditory orienting behavior—the fAES—shows a significant projection to the SC, confirming the results of Meredith and Clemo (1989). Although the ferret does not have an fAES, the region surrounding the pseudosylvian sulcus is considered to be the functional analogue (Ramsay and Meredith, 2004; Bajo et al., 2010) and contains a robust projection to the SC. The absence of a substantive direct projection from the A1 to the SC is in accordance with previous anatomical data. For example, auditory cortical lesions do not result in the degeneration of fibers in the SC when these lesions are confined within the borders of the A1 (Diamond et al., 1969). Moreover, Lomber and colleagues (2007a) demonstrated that reversible deactivation of the superficial layers of the A1, DZ, and PAF was sufficient to impair auditory localization, suggesting a mechanism for these areas that does not necessitate a direct projection to the SC. However, these findings are at odds with neuroanatomical studies in the Mongolian gerbil (Budinger et al.,

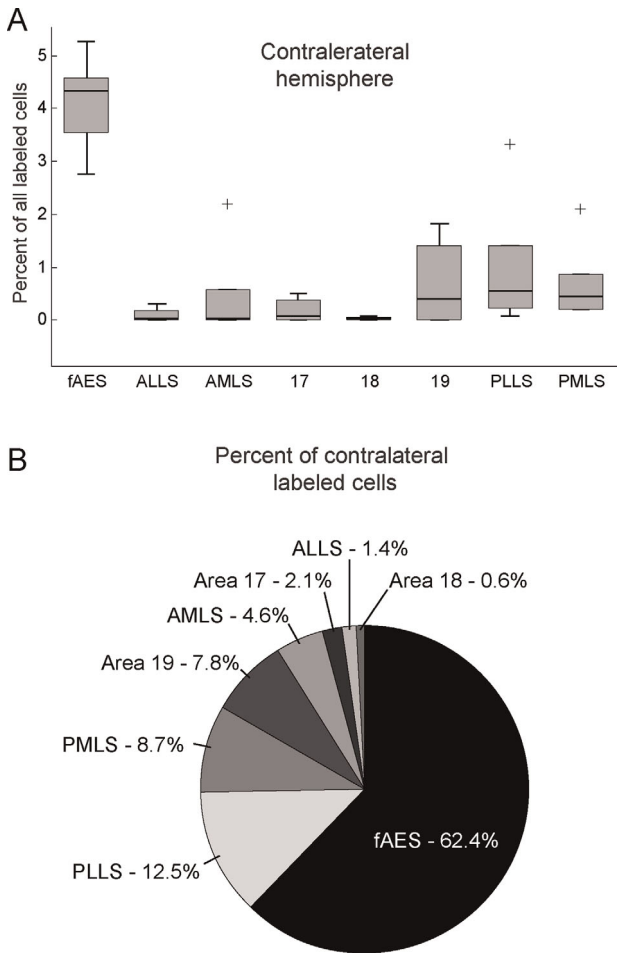

Figure 13. **A**: Box-and-whisker plot illustrating the distribution of contralateral corticotectal projections by cortical area. The y-axis indicates the percentage of labeled neurons, whiskers extend a maximum of 1.5 times the interquartile range, and outliers are denoted by a black cross. The majority of the contralateral cortical areas have a projection accounting for less than 1% of total labeled neurons. However, the fAES is a significant source of contralateral projections to the superior colliculus (median = 4.3%). **B**: Contralateral projections by cortical area expressed as the mean proportion of total contralateral projections. For abbreviations, see list.

2006, 2008; Budinger and Scheich, 2009) and the ferret (Manger et al., 2010), which describe projections from primary auditory fields to the SC. Also somewhat discordant with the current study, Winer and colleagues (1998) demonstrated corticotectal projections originating in the second auditory cortex (A2) and multisensory areas that are designated as auditory cortical fields in cats. Moreover, using an anterograde degenerative technique, Paula-Barbosa and Sousa-Pinto (1973) described significant projections from the A2 and DZ, in addition to the fAES. However, the thermocoagulation method is more invasive and less precise than the retrograde labeling technique employed here, and this may account for the differences.

Contrary to previous anatomical evidence (Stein et al., 1983; McHaffie et al., 1988), the current study does not characterize projections from somatosensory areas to the SC as substantial. Similar to these previous studies, we demonstrate no projection from the primary (0%) and small projections from the secondary (0.5%) somatosensory cortex. However, although the projection from the S4 has been described as dominating somatosensory input to the SC, the current study demonstrates balanced, small projections from the S2, S4, and S5 (all contributing ~0.5%). The cause of this discrepancy is not immediately apparent. Clemo and Stein (1984) have noted that the subset of somatosensory neurons of the SC influenced by corticotectal inputs from the S4 are not distributed in a laminar pattern that distinguishes them from the total population of somatosensory cells; thus, the injections in the current study, which ensured that tracer spread throughout the SC, would be expected to successfully label these projections. It is worth noting again that, although the absence of a substantial projection from the S4 in the current study appears discordant with electrophysiological evidence showing that this cortical field is capable of modulating response properties of SC neurons (Clemo and Stein, 1984, 1986), the strength of electrophysiological responses is determined by more than the number of neurons projecting between areas of the brain.

Contralateral projections to the SC

Previous evidence for contralateral visual projections to the SC is mixed; some studies have suggested that areas involved in orienting behavior send sizable projections to the contralateral SC (Powell, 1976; Galletti et al., 1981; Berman and Payne, 1982). However, the current study supports the opposite finding that the contralateral visual cortex contains a small number of labeled cells (Baleydier, 1977; Baleydier et al., 1983). Instead, the only substantial contralateral projection arises from the fAES, a field of the auditory cortex that has been previously shown to project bilaterally to the SC (Fuentes-Santamaria et al. 2008, 2009; Chabot et al., 2013). Although they did not quantify labeled cells, Tortelly and colleagues (1980) also demonstrated bilateral corticotectal projections from the fAES, as well as from the banks of the suprasylvian sulcus. In the current study, the number of labeled cells in the areas of the cortex surrounding the contralateral suprasylvian sulcus (the ALLS, AMLS, PLLS, PMLS) are negligible when considered as a proportion of total labeled cells across hemispheres (Fig. 13A). However, if these

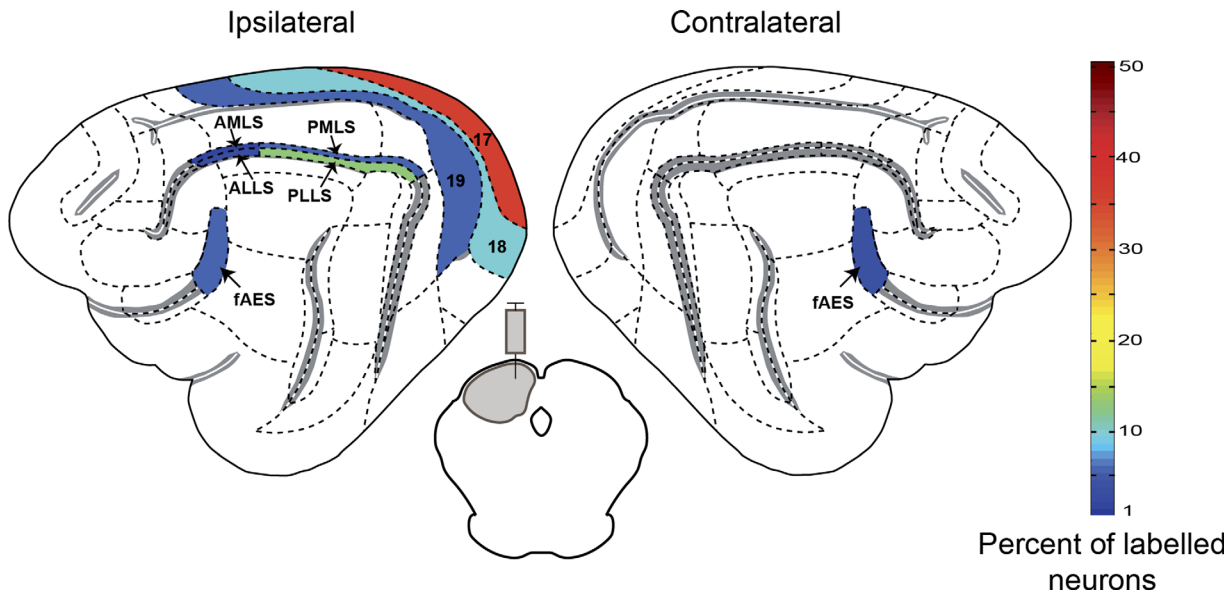

Figure 14. Summary of the visual, auditory, and somatosensory cortical projections to the SC. Areas containing greater than 1% of the total labeled cells are shown, with projecting strength color coded according to the color bar on the right. Each of the visual areas involved in orienting (17, 18, 19, PLLS, and PMLS) has a direct connection with the SC. Conversely, that majority of the auditory areas implicated in orienting behavior (A1, DZ, and PAF) shows no substantial projection to the SC. Only the fAES has a direct connection, which is of approximately equal strength bilaterally. Finally, only somatosensory area S2 and motor area 5 have direct connections to the SC. For abbreviations, see list.

projections are considered as a proportion of total contralateral labeling (Fig. 13B), the size of each is similar to its corresponding ipsilateral field. This alternate representation also serves to underscore the magnitude of the projection from the contralateral fAES. Indeed, a link between the fAES and acoustic orienting behavior is in accordance with findings that inactivation of the fAES by local anesthetic injection (Wilkinson et al., 1996) or by reversible cooling (Malhotra et al., 2004) results in profound deficits in acoustic localization. Interestingly, however, these deficits were shown to be robust for stimuli in the contralateral field, but negligible for ipsilaterally presented stimuli.

It is important to note that resection of the caudal splenium of the corpus callosum is not expected to have a substantial effect on the labeling of contralateral cortical neurons following injection into the SC. Previous research suggests that crossed corticotectal projections originating in visual (Powell, 1976; Galletti et al., 1981; Baleydier et al. 1983; Harting et al, 1992) and auditory (Paula-Barbosa and Sousa-Pinto, 1973) cortical areas travel via the intercollicular commissure, rather than passing through the corpus callosum. Additionally, callosal resection does not selectively target interhemispheric connections of the posterior visual cortex as, unlike in some species (Pandya et al., 1971; Gould and Ebner, 1978; Dursteler et al., 1979; de Lacoste et al., 1985), visual fibers in the cat are not confined to the caudal splenium. Instead, they pass through the entirety of the splenium and much of the body of the corpus collosum (Payne and Siwek, 1991; Lomber et al., 1994a). Thus, the patterns of contralateral labeling in the current study are unlikely to be biased by the surgical approach.

Unilateral visual, but bilateral auditory inputs

The current study demonstrates that whereas overall corticotectal input to the SC is dominated by visual cortical projections, the auditory field fAES makes the largest bilateral projection. Contralateral visual cortical fields located on the banks of the suprasylvian sulcus show projections to the SC that are comparable to ipsilateral fields when only contralaterally originating cells are considered. However, these projections appear much smaller when placed in the context of whole-brain projections, whereas the projection originating in the fAES remains compelling in either context. There are a number of ways that this differential pattern of projections might be interpreted. It is possible that the disparity between sensory cortices reflects differences in their intrinsic architecture. For example, thalamic afferents selectively target spiny stellate cells in layer

IV of the primary visual cortex (V1), whereas layer IV pyramidal cells are the preferential target in the A1 (Smith and Populin, 2001). Moreover, layer III cells in V1 make corticocortical connections that are almost exclusively ipsilateral (Fisken et al., 1975), whereas layer III cells in the A1 are commissural (Code and Winer, 1985). Such modality-specific architectures are established as early as the primary sensory cortex, persist throughout higher level sensory cortices (such as the fAES), and may underlie differences in corticotectal projections.

It may also be the case that modality-level differences in contralateral connectivity to the SC may reflect a contrast in the way that stimulus features, specifically those related to spatial representations and orienting behavior, are represented in these two modalities. In stark contrast to the retinotopic representations present in the primary visual cortex, there appears to be no topographic representation of acoustic space in the A1 (Middlebrooks and Pettigrew, 1981; Imig et al., 1990; Rajan et al., 1990a,b; Recanzone and Cohen, 2010). Moreover, although it is accepted that binaural cues to localization are established subcortically at the level of the superior olivary complex, the exact role of the auditory cortex in sound localization remains somewhat ambiguous. However, both electrophysiological (Stecker et al., 2005) and behavioral studies (Malhotra et al., 2004) suggest that interhemispheric connectivity plays a critical role. Based on these findings, Lee and Winer (2011) have suggested that commissural projections might serve to unify lateralized representations of stimulus features from the auditory cortices to improve the fidelity of the perceived auditory object. Thus, contralateral projections to the SC may arise from the auditory modality due to the functional necessity of bilateral cues for the perception of, and orientation toward, auditory stimuli. In addition, this projection may function cooperatively with smaller bilateral visual projections to establish a multisensory representation of stimulus location in the SC. Finally, it should be noted that injections in the current study sought to avoid tracer spread into the pretectal area, and as a consequence may have also limited spread into the anterior pole of the colliculus, where activity related to the ipsilateral visual field is represented (Feldon et al., 1970).

CONCLUSIONS

The present study quantifies and compares the patterns of corticotectal projections from visual, auditory, somatosensory, motor, and limbic cortices in the cat. Importantly, although all of the areas thought to contribute to visual localization have substantial inputs to the SC, only one area involved with auditory orienting (the fAES), and no areas thought to contribute to somatosensory orienting, showed inputs of similar size. Additionally, we demonstrate that whereas ipsilateral visual cortical fields dominate the input to the SC, the only extensive contralateral input arises from a high-level field of the auditory cortex. We propose that this differential pattern of projections from visual and auditory cortices to the SC is due to the specific physiology and connectivity of these cortical structures. Further studies into the connectivity between these structures and electrophysiological examinations of function will be critical to an improved understanding of how multisensory environmental stimuli elicit orienting responses.

ACKNOWLEDGMENTS

The authors thank Pam Nixon for assistance with animal care, and Amee J. Hall for help with various phases of the project.

CONFLICT OF INTEREST STATEMENT

The authors declare they have no conflicts of interest.

ROLE OF AUTHORS

All authors had full access to all the data in the study and take responsibility for the integrity of the data and the accuracy of the data analysis. Study concept and design: BEB, NC, andSGL. Acquisition of data: BEB and NC. Analysis and interpretation of data: BEB and NC. Drafting of the manuscript: BEB. Critical revision of the manuscript for important intellectual content: BEB, NC, and SGL. Statistical analysis: BEB and NC. Obtained funding: SGL.

LITERATURE CITED

Adams JC. 1981. Heavy metal intensification of DAB-based HRP reaction product. J Histochem Cytochem 29:775.

Altman J, Carpenter MB. 1961. Fiber projections of the superior colliculus in the cat. J Comp Neurol 116:157–177.

Bajo VM, Nodal FR, Bizley JK, King AJ. 2010. The non-lemniscal auditory cortex in ferrets: convergence of corticotectal inputs in the superior colliculus. Front Neuroanat 4:18.

Baldwin MK, Kaas JH. 2012. Cortical projections to the superior colliculus in prosimian galagos (*Otolemur garnetti*). J Comp Neurol 520:2002–2020.

Baldwin MK, Wei H, Reed JL, Bickford ME, Petry HM, Kaas JH. 2013. Cortical projections to the superior colliculus in tree shrews (*Tupaia belangeri*). J Comp Neurol 521: 1614–1632.

Baleydier C. 1977. A bilateral cortical projection to the superior colliculus in the cat. Neurosci Lett 4:9–14.

Baleydier C, Kahungu M, Mauguiere F. 1983. A crossed corticotectal projection from the lateral suprasylvian area in the cat. J Comp Neurol 214:344–351.

Bandler R, McCulloch T, Dreher B. 1985. Afferents to a midbrain periaqueductal gray region involved in the 'defense reaction' in the cat as revealed by horseradish peroxidase. I. The telencephalon. Brain Res 330:109–119.

Berman N, Payne BR. 1982. Contralateral corticofugal projections from the lateral, suprasylvian and ectosylvian gyri in the cat. Exp Brain Res 47:234–238.

Berson DM, McIlwain JT. 1983. Visual cortical inputs to deep layers of cat's superior colliculus. J Neurophysiol 50: 1143–1155.

Bragin EO, Yeliseeva ZV, Vasilenko GF, Meizerov EE, Chuvin BT, Durinyan RA. 1984. Cortical projections to the periaqueductal grey in the cat: A retrograde horseradish peroxidase study. Neurosci Lett 51:271–275.

Budinger E, Scheich H. 2009. Anatomical connections suitable for the direct processing of neuronal information of different modalities via the rodent primary auditory cortex. Hear Res 258:16–27.

Budinger E, Heil P, Hess A, Scheich H. 2006. Multisensory processing via early cortical stages: connections of the primary auditory cortical field with other sensory systems. Neuroscience 143:1065–1083.

Budinger E, Laszcz A, Lison H, Scheich H, Ohl FW. 2008. Non-sensory cortical and subcortical connections of the primary auditory cortex in Mongolian gerbils: bottom-up and top-down processing of neuronal information via field AI. Brain Res 1220:2–32.

Burton H, Sinclair RJ. 2000. Tactile-spatial and cross-modal attention effects in the primary somatosensory cortical areas 3b and 1-2 of rhesus monkeys. Somatosens Mot Res 17:213–228.

Burton H, Sinclair RJ, Hong S-Y, Pruett JR, Whang KC. 1997. Tactile-spatial and cross-modal attention effects in the second somatosensory and 7b cortical areas of rhesus mokeys. Somatosens Mot Res 14:237–267.

Casseday JH, Jones DR, Diamond IT. 1979. Projections from cortex to tectum in the tree shrew, *Tupaia glis*. J Comp Neurol 185:253–291.

Chabot N, Mellott JG, Hall AJ, Tichenoff EL, Lomber SG. 2013. Cerebral origins of the auditory projection to the superior colliculus of the cat. Hear Res 300:33–45.

Clascá F, Llamas A, Reinoso-Suarez F. 1997. Insular cortex and neighboring fields in the cat: a redefinition based on cortical microarchitecture and connections with the thalamus. J Comp Neurol 384:456–482.

Clascá F, Llamas A, Reinoso-Suarez F. 2000. Cortical connections of the insular and adjacent parieto-temporal fields in the cat. Cereb Cortex 10:371–399.

Clemo HR, Stein BE. 1984. Topographic organization of somatosensory corticotectal influences in cat. J Neurophysiol 51:843–858.

Clemo HR, Stein BE. 1986. Effects of cooling somatosensory cortex on response properties of tactile cells in the superior colliculus. J Neurophysiol 55:1352–1368.

Clemo HR, Allman BL, Donlan MA, Meredith MA. 2007. Sensory and multisensory representations within the cat rostral suprasylvian cortex. J Comp Neurol 503:110–127.

Code RA, Winer JA. 1985. Commissural neurons in layer III of cat primary auditory cortex (AI): pyramidal and nonpyramidal cell input. J Comp Neurol 242:485–510.

Collins CE, Lyon DC, Kaas JH. 2005. Distribution across cortical areas of neurons projecting to the superior colliculus in new world monkeys. Anat Rec A Discov Mol Cell Evol Biol 285:619–627.

Comoli E, Favaro PD, Vautrelle N, Leriche M, Overton PG, Redgrave P. 2012. Segregated anatomical input to subregions of the rodent superior colliculus associated with approach and defense. Front Neuroanat 6(9).

Cusick CG. 1988. Anatomical organization of the superior colliculus in monkeys: corticotectal pathways for visual and visuomotor functions. Prog Brain Res 75:1–15.

de Lacoste MC, Kirkpatrick JB, Ross ED. 1985. Topography of the human corpus callosum. J Neuropathol Exp Neurol 44:578–591.

Diamond IT, Jones EG, Powell TPS. 1969. The projection of the auditory cortex upon the diencephalon and brain stem of the cat. Brain Res 15:305–340.

Distel H, Fries W. 1982. Contralateral cortical projections to the superior colliculus in the macaque monkey. Exp Brain Res 48:157–162.

Dursteler MR, Blakemore C, Garey LJ. 1979. Projections to the visual cortex in the golden hamster. J Comp Neurol 183:185–204.

Feldon S, Feldon P, Kruger L. 1970. Topography of the retinal projection upon the superior colliculus of the cat. Vision Res 10:135–143.

Fisken RA, Garey LJ, Powell TP. 1975. The intrinsic, association and commissural connections of area 17 on the visual cortex. Philos Trans R Soc Lond B Biol Sci 272:487–536.

Fries W. 1984. Cortical projections to the superior colliculus in the macaque monkey: a retrograde study using horseradish peroxidase. J Comp Neurol 230:55–76.

Fuentes-Santamaria V, Alvarado JC, Stein BE, McHaffie JG. 2008. Cortex contacts both output neurons and nitrergic interneurons in the superior colliculus: direct and indirect routes for multisensory integration. Cereb Cortex 18:1640–1652.

Fuentes-Santamaria V, Alvarado JC, McHaffie JG, Stein BE. 2009. Axon morphologies and convergence patterns of projections from different sensory-specific cortices of the anterior ectosylvian sulcus onto multisensory neurons in the cat superior colliculus. Cereb Cortex 19:2902–2915.

Galletti C, Squatrito S, Battaglini PP, Maioli MG. 1981. Contralateral tectal projections from single areas of the visual cortex in the cat. Arch Ital Biol 119:43–51.

Gould HJ, Ebner FF. 1978. Connections of the visual cortex in the hedgehog (*Paraechinus hypomelas*). II. Corticocortical projections. J Comp Neurol 177:473–502.

Graham J, Lin C-S, Kaas JH. 1979. Subcortical projections of six visual cortical areas in the owl monkey, *Aotus trivirgatus*. J Comp Neurol 187:557–580.

Harting JK, Updyke BV, Van Lieshout DP. 1992. Corticotectal projections in the cat—anterograde transport studies of 25 cortical areas. J Comp Neurol 324:379–414.

Harvey AR, Worthington DR. 1990. The projection from different visual cortical areas to the rat superior colliculus. J Comp Neurol 298:281–292.

Hoffer ZS, Arantes HB, Roth RL, Alloway KD. 2005. Functional circuits mediating sensorimotor integration: quantitative comparisons of projections from rodent barrel cortex to primary motor cortex, neostriatum, superior colliculus, and the pons. J Comp Neurol 488:82–100.

Hollander H. 1974. On the origin of the corticotectal projections in the cat. Exp Brain Res 21:433–439.

Imig TJ, Irons WA, Samson FR. 1990. Single-unit selectivity to azimuthal direction and sound pressure level of noise bursts in cat high-frequency primary auditory cortex. J Neurophysiol 63:1448–1466.

Innocenti GM, Manger PR, Masiello I, Colin I, Tettoni L. 2002. Architecture and callosal connections of visual areas 17, 18, 19 and 21 in the ferret (*Mustela putorius*). Cereb Cortex 12:411–422.

Jay MF, Sparks DL. 1987. Sensorimotor integration in the primate superior colliculus. I. Motor convergence. J Neurophysiol 57:22–34.

Jiang H, Guitton D. 1995. Eye, head and forelimb movements evoked from the anterior ectosylvian cortex of the unrestrained cat. Soc Neurosci Abstr 21:1899.

Kanaseki T, Sprague JM. 1974. Anatomical organization of pretectal nuclei and tectal laminae in the cat. J Comp Neurol 158:319–337.

Kassel J. 1982. Somatotopic organization of SI corticotectal projections in rats. Brain Res 231:247–255.

Kawamura K, Konno T. 1979. Various types of corticotectal neurons of cats as demonstrated by means of retrograde axonal transport of horseradish peroxidase. Exp Brain Res 35:161–175.

Kawamura K, Brodal A, Hoddevik G. 1974. The projection of the superior colliculus onto the reticular formation of the brain stem. An experimental anatomical study in the cat. Exp Brain Res 19:1–19.

Kawamura K, Konno T, Chiba M. 1978. Cells of origin of corticopontine and corticotectal fibers in the medial and lateral banks of the middle suprasylvian sulcus in the cat. An experimental study with the horseradish peroxidase method. Neurosci Lett 9:129–135.

Kelly JP, Gilbert CD. 1975. The projections of different morphological types of ganglion cells in the cat retina. J Comp Neurol 163:65–80.

King AJ. 2004. The superior colliculus. Curr Biol 14:R335–338.

Künzle H. 1995. Regional and laminar distribution of cortical neurons projecting to either superior or inferior colliculus in the hedgehog tenrec. Cereb Cortex 5:338–352.

Lee CC, Winer JA. 2011. Convergence of thalamic and cortical pathways in cat auditory cortex. Hear Res 274:85–94.

Leichnetz GR, Spencer RF, Hardy SGP, Astruc HJ. 1981. The prefrontal corticotectal projection in the monkey: an anterograde and retrograde horseradish peroxidase study. Neuroscience 6:1023–1041.

Lock TM, Baizer JS, Bender DB. 2003. Distribution of corticotectal cells in macaque. Exp Brain Res 151:455–470.

Lomber SG, Payne BR. 2004. Cerebral areas mediating visual redirection of gaze: cooling deactivation of 15 loci in the cat. J Comp Neurol 474:190–208.

Lomber SG, Payne BR, Rosenquist AC. 1994a. The spatial relationship between the cerebral cortex and fiber trajectory through the corpus callosum of the cat. Behav Brain Res 64:25–35.

Lomber SG, Cornwell P, Sun JS, MacNeil MA, Payne BR. 1994b. Reversible inactivation of visual processing operations in middle suprasylvian cortex of the behaving cat. Proc Natl Acad Sci U S A 91:2999–3003.

Lomber SG, Malhotra S, Hall AJ. 2007a. Functional specialization in non-primary auditory cortex of the cat: areal and laminar contributions to sound localization. Hear Res 229:31–45.

Lomber SG, Malhotra S, Sprague JM. 2007b. Restoration of acoustic orienting into a cortically deaf hemifield by reversible deactivation of the contralesional superior colliculus: the acoustic "Sprague Effect". J Neurophysiol 97: 979–993.

Lomber SG, Payne BR, Cornwell P. 2001. Role of the superior colliculus in analyses of space: superficial and intermediate layer contributions to visual orienting, auditory orienting, and visuospatial discriminations during unilateral and bilateral deactivations. J Comp Neurol 441:44–57.

Lomber SG, Payne BR, Hilgetag CC, Rushmore J. 2002. Restoration of visual orienting into a cortically blind hemifield by reversible deactivation of posterior parietal cortex or the superior colliculus. Exp Brain Res 142:463–474.

Lui F, Gregory KM, Blanks RHI, Giolli RA. 1995. Projections from visual areas of the cerebral cortex to pretectal nuclear complex, terminal accessory optic nuclei, and superior colliculus in macaque monkey. J Comp Neurol 363:439–460.

Magalhães-Castro HH, Saraiva PE, Magalhães-Castro B. 1975. Identification of corticotectal cells of the visual cortex of cats by means of horseradish peroxidase. Brain Res 83: 474–479.

Malhotra S, Hall AJ, Lomber SG. 2004. Cortical control of sound localization in the cat: unilateral cooling deactivation of 19 cerebral areas. J Neurophysiol 92:1625–1643.

Malhotra S, Stecker GC, Middlebrooks JC, Lomber SG. 2008. Sound localization deficits during reversible deactivation of primary auditory cortex and/or the dorsal zone. J Neurophysiol 99:1628–1642.

Manger PR, Engler G, Moll CK, Engel AK. 2005. The anterior ectosylvian visual area of the ferret: a homologue for an enigmatic visual cortical area of the cat? Eur J Neurosci 22:706–714.

Manger PR, Restrepo CE, Innocenti GM. 2010. The superior colliculus of the ferret: cortical afferents and efferent connections to dorsal thalamus. Brain Res 1353:74–85.

Martinich S, Pontes MN, Rocha-Miranda CE. 2000. Patterns of corticocortical, corticotectal, and commissural connections in the opossum visual cortex. J Comp Neurol 416: 224–244.

May PJ. 2006. The mammalian superior colliculus: laminar structure and connections. Prog Brain Res 151:321–378.

McHaffie JG, Kruger L, Clemo HR, Stein BE. 1988. Corticothalamic and corticotectal somatosensory projections from the anterior ectosylvian sulcus (SIV cortex) in neonatal cats: an anatomical demonstration with HRP and ^{3}H-leucine. J Comp Neurol 274:115–126.

McHaffie JG, Thomson CM, Stein BE. 2001. Corticotectal and corticostriatal projections from the frontal eye fields of the cat: an anatomical examination using WGA-HRP. Somatosens Mot Res 18:117–130.

Meredith MA, Allman BL. 2009. Subthreshold multisensory processing in cat auditory cortex. Neuroreport 20:126–131.

Meredith MA, Clemo HR. 1989. Auditory cortical projection from the anterior ectosylvian sulcus (Field AES) to the superior colliculus in the cat: an anatomical and electrophysiological study. J Comp Neurol 289:687–707.

Meredith MA, Keniston LR, Dehner LR, Clemo HR. 2006. Crossmodal projections from somatosensory area SIV to the auditory field of the anterior ectosylvian sulcus (fAES) in cat: further evidence for subthreshold forms of multisensory processing. Exp Brain Res 172:472–484.

Mesulam MM. 1978. Tetramethyl benzidine for horseradish peroxidase neurohistochemistry: a non-carcinogenic blue reaction-product with superior sensitivity for visualizing neural afferents and efferents. J Histochem Cytochem 26:106–117.

Middlebrooks JC, Pettigrew JD. 1981. Functional classes of neurons in primary auditory cortex of the cat distinguished by sensitivity to sound location. J Neurosci 1: 107–120.

Norita M, McHaffie JG, Shimizu H, Stein BE. 1991. The corticostriatal and corticotectal projections of the feline lateral suprasylvian cortex demonstrated with anterograde biocytin and retrograde fluorescent techniques. Neurosci Res 10:149–155.

Ogasawara K, McHaffie JG, Stein BE. 1984. Two visual corticotectal systems in cat. J Neurophysiol 52:1226–1245.

Olucha F, Martinez-Garcia F, Lopez-Garcia C. 1985. A new stabilizing agent for the tetramethyl benzidine (TMB) reaction product in the histochemical detection of horseradish peroxidase (HRP). J Neurosci Methods 13:131–138.

Palmer LA, Rosenquist AC, Tusa RJ. 1978. The retinotopic organization of lateral suprasylvian visual areas in the cat. J Comp Neurol 177:237–256.

Pandya DN, Karol EA, Heilbronn D. 1971. The topographical distribution of interhemispheric projections in the corpus callosum of the rhesus monkey. Brain Res 32:31–43.

Paula-Barbosa MM, Sousa-Pinto A. 1973. Auditory cortical projections to the superior colliculus in the cat. Brain Res 50:47–61.

Payne BR, Lomber SG. 1996. Age dependent modification of cytochrome oxidase activity in the cat dorsal lateral geniculate nucleus following removal of primary visual cortex. Vis Neurosci 13:805–816.

Payne BR, Siwek DF. 1991. The visual map in the corpus callosum of the cat. Cereb Cortex 1:173–188.

Powell TP. 1976. Bilateral cortico-tectal projection from the visual cortex in the cat. Nature 260:526–527.

Rajan R, Aitkin LM, Irvine DR. 1990a. Azimuthal sensitivity of neurons in primary auditory cortex of cats. II. Organization along frequency-band strips. J Neurophysiol 64:888–902.

Rajan R, Aitkin LM, Irvine DR, McKay J. 1990b. Azimuthal sensitivity of neurons in primary auditory cortex of cats. I. Types of sensitivity and the effects of variations in stimulus parameters. J Neurophysiol 64:872–887.

Ramsay AM, Meredith MA. 2004. Multiple sensory afferents to ferret pseudosylvian sulcal cortex. Neuroreport 15: 461–465.

Rauschecker J, Grunau M, Poulin C. 1987. Centrifugal organization of direction preferences in the cat's lateral suprasylvian visual cortex and its relation to flow field processing. J Neurosci 7:943–958.

Recanzone GH, Cohen YE. 2010. Serial and parallel processing in the primate auditory cortex revisited. Behav Brain Res 206:1–7.

Sanides F. 1969. Comparative architectonics of the neocortex of mammals and their evolutionary interpretation. Ann N Y Acad Sci 167:404–423.

Schurr PH, Merrington WR. 1978. The Horsley-Clarke stereotaxic apparatus. Br J Surg 65:33–36.

Sefton AJ, Mackay-Sim A, Baur LA, Cottee LJ. 1981. Cortical projections to visual centres in the rat: An HRP study. Brain Res 215:1–13.

Segal RL, Beckstead RM. 1984. The lateral suprasylvian corticotectal projection in cats. J Comp Neurol 225:259–275.

Smith PH, Populin LC. 2001. Fundamental differences between the thalamocortical recipient layers of the cat auditory and visual cortices. J Comp Neurol 436:508–519.

Sparks DL. 1988. Neural cartography: sensory and motor maps in the superior colliculus. Brain Behav Evol 31:49–56.

Sprague JM, Levitt M, Robson K, Liu CN, Stellar E, Chambers WW. 1963. A neuroanatomical and behavioral analysis of the syndromes resulting from midbrain lemniscal and reticular lesions in the cat. Arch Ital Biol 101:225–295.

Stecker GC, Harrington IA, Macpherson EA, Middlebrooks JC. 2005. Spatial sensitivity in the dorsal zone (area DZ) or cat auditory cortex. J Neurophysiol 94:1267–1280.

Stein BE. 1978. Nonequivalent visual, auditory, and somatic corticotectal influences in cat. J Neurophysiol 41:55–64.

Stein BE. 1984. Development of the superior colliculus. Annu Rev Neurosci 7:95–125.

Stein BE. 1998. Neural mechanisms for synthesizing sensory information and producing adaptive behaviors. Exp Brain Res 123:124–135.

Stein BE, Clamann HP. 1981. Control of pinna movements and sensorimotor register in cat superior colliculus. Brain Behav Evol 19:180–192.

Stein BE, Spencer RF, Edwards SB. 1983. Corticotectal and corticothalamic efferent projections of SIV somatosensory cortex in cat. J Neurophysiol 50:896–909.

Stein BE, Wallace MT, Meredith MA. 1995. Neural mechanisms mediating attention and orientation to multisensory cues. In: Gazzaniga MA, editor. The cognitive neurosciences. Cambridge, MA: MIT Press. p 683–702.

Tamai M. 1973. Inflows from the somatosensory cortex in the cat's superior colliculus. J Exp Med 109:7–11.

Thong IG, Dreher B. 1986. The development of the corticotectal pathway in the albino rat. Dev Brain Res 25:227–238.

Tigges J, Tigges M. 1981. Distribution of retinofugal and corticofugal axon terminals in the superior colliculus of squirrel monkey. Invest Ophthalmol Vis Sci 20:149–158.

Tortelly A, Reinoso-Suarez F, Llamas A. 1980. Projections from non-visual cortical areas to the superior colliculus demonstrated by retrograde transport of HRP in the cat. Brain Res 188:543–549.

Updyke BV. 1977. Topographic organization of the projections from cortical areas 17, 18, and 19 onto the thalamus, pretectum and superior colliculus in the cat. J Comp Neurol 173:81–121.

Updyke BV. 1986. Retinitopic organization within the cat's posterior suprasylvian sulcus and gyrus. J Comp Neurol 246:265–280.

Van Der Gucht E, Vandesande F, Arckens L. 2001. Neurofilament protein: a selective marker for the architectonic parcellation of the visual cortex in adult cat brain. J Comp Neurol 441:345–68.

Wallace MT, Meredith MA, Stein BE. 1993. Converging influences from visual, auditory, and somatosensory cortices onto output neurons of the superior colliculus. J Neurophysiol 69:1797–1809.

Wickelgren BG, Sterling P. 1969. Influence of visual cortex on receptive fields in the superior colliculus of the cat. J Neurophysiol 32:16–23.

Wilkinson LK, Meredith MA, Stein BE. 1996. The role of anterior ectosylvian cortex in cross-modality orientation and approach behavior. Exp Brain Res 112:1–10.

Winer JA, Prieto JJ. 2001. Layer V in cat primary auditory cortex (AI): cellular architecture and identification of projection neurons. J Comp Neurol 434:379–412.

Winer JA, Larue DT, Diehl JJ, Hefti BJ. 1998. Auditory cortical projections to the cat inferior colliculus. J Comp Neurol 400:147–174.

Wise SP, Jones EG. 1977. Somatotopic and columnar organization in the corticotectal projection of the rat somatic sensory cortex. Brain Res 133:223–235.

Brain and Cognition 83 (2013) 271–278

Contents lists available at ScienceDirect

Brain and Cognition

journal homepage: www.elsevier.com/locate/b&c

Brief pitch-priming facilitates infants' discrimination of pitch-evoking noise: Evidence from event-related potentials

Blake E. Butler [a], Laurel J. Trainor [a,b,*]

[a] Psychology, Neuroscience and Behaviour, McMaster University, Hamilton, Ontario L8S 4K1, Canada
[b] Rotman Research Institute, Baycrest Centre, University of Toronto, Toronto, Ontario M6A 3E1, Canada

ARTICLE INFO

Article history:
Accepted 10 September 2013

Keywords:
Pitch
Development
Event-related potentials
Mismatch negativity
Iterated rippled noise (IRN)

ABSTRACT

Pitch is derived by the auditory system through complex spectrotemporal processing. Pitch extraction is thought to depend on both spectral cues arising from lower harmonics that are resolved by cochlear filters in the inner ear, and on temporal cues arising from the pattern of action potentials contained in the cochlear output. Adults are capable of extracting pitch in the absence of robust spectral cues, taking advantage of the temporal cues that remain. However, recent behavioral evidence suggests that infants have difficulty discriminating between stimuli with different pitches when resolvable spectral cues are absent. In the current experiments, we used the mismatch negativity (MMN) component of the event related potential derived from electroencephalographic (EEG) recordings to examine a cortical representation of pitch discrimination for iterated rippled noise (IRN) stimuli in 4- and 8-month-old infants. IRN stimuli are pitch-evoking sounds generated by repeatedly adding a segment of white noise to itself at a constant delay. We created IRN stimuli (delays of 5 and 6 ms creating pitch percepts of 200 and 167 Hz) and high-pass filtered them to remove all resolvable spectral pitch cues. In experiment 1, we did not find EEG evidence that infants could detect the change in the pitch of these IRN stimuli. However, in Experiment 2, after a brief period of pitch-priming during which we added a sine wave component to the IRN stimulus at its perceived pitch, infants did show significant MMN in response to pitch changes in the IRN stimuli with sine waves removed. This suggests that (1) infants can use temporal cues to process pitch, although such processing is not mature and (2) that a short amount of pitch-priming experience can alter pitch representations in auditory cortex during infancy.

1. Introduction

Pitch perception is central to musical development (see Trainor & Corrigall, 2010 for review), and conveys a wealth of semantic and prosodic information that is crucial for language acquisition (see Moore, 2008 for review). Additionally, pitch provides information vital to the identification of environmental sounds, and aids in the perceptual separation of co-occurring sounds (Bregman, 1990). Stimuli with pitch are typically complex tones with energy at a fundamental frequency, and at integer multiples of that frequency, known as harmonics. The basilar membrane of the cochlea is responsible for translating the mechanical energy of sound waves into a pattern of action potentials. Physical characteristics of this membrane, such as width and rigidity, differ along its length, such that high frequencies cause maximal displacement at the basal end, while lower frequencies cause maximal displacement at the apex of the membrane (Von Bekesy, 1960). This is referred to as tonotopic organization, and it is this arrangement that gives rise to spectral, or place cues to pitch. A complex tone with many harmonics is heard as a single entity, and its pitch is derived from the fundamental frequency and/or the relations between the harmonics present. This is evidenced by the fact that removing the fundamental from a complex tone does not alter its pitch, a phenomenon known as hearing the pitch of the missing fundamental.

The basilar membrane can be thought of as a series of bandpass filters (e.g., Carney & Yin, 1988; Evans, 1977). In contrast to harmonics, which are linearly spaced, basilar membrane filters are logarithmically spaced (Fletcher, 1938) such that at low frequencies, individual harmonics fall into separate filters and are thus individually resolved. However, at higher harmonics, the bandwidth of cochlear filters exceeds harmonic spacing and multiple harmonics fall into the same filterband, causing interfering patterns on the basilar membrane. These harmonics are thus unresolved, and place cues cannot provide an accurate pitch estimate (Plomp, 1964). A second, temporal mechanism is thought to

* Corresponding author. Address: McMaster University, Department of Psychology, Neuroscience and Behaviour, Auditory Development Lab, 1280 Main Street West, Hamilton, Ontario L8S 4L8, Canada. Fax: +1 (905) 529 6225.
E-mail address: ljt@mcmaster.ca (L.J. Trainor).

0278-2626/$ - see front matter © 2013 Published by Elsevier Inc.
http://dx.doi.org/10.1016/j.bandc.2013.09.002

compensate by taking advantage of temporal regularity in the pattern of action potentials in the cochlear output. Because action potentials are generated at the point of maximal displacement of the basilar membrane, the pattern of potentials across a population of auditory nerve fibers approximates the frequency of an auditory stimulus (e.g., Cariani & Delgutte, 1996; Delgutte & Cariani, 1992; Meddis & O'Mard, 1997). Current models of pitch perception typically include contributions from both spectral and temporal cues (e.g., Cedolin & Delgutte, 2007; Larsen, Cedolin, & Delgutte, 2008).

A number of studies have demonstrated that infants perceive pitch-evoking stimuli with resolved spectral content in much the same way as adults. While the limits of complex tone discrimination have not been reported, 8-month-old infants have been shown to discriminate behaviorally between complex stimuli, with and without energy at the fundamental frequency, that differ in pitch by 20% (e.g., 160 and 200 Hz; Clarkson & Clifton, 1985). Montgomery and Clarkson (1997) verified that 8-month-old infants' discrimination of missing-fundamental stimuli is not impaired by the addition of a low-frequency noise masker covering the region of the fundamental; this suggests that, like adults, infants discriminate these stimuli based on integration of harmonic content into a pitch percept, rather than based on low-frequency combination tones resulting from non-linearities of the inner ear. Furthermore, He, Hotson, and Trainor (2009) used event-related potentials (ERPs) to demonstrate that a cortical representation of the pitch of the missing fundamental emerges between 2 and 4 months of age, suggesting that by this age infants are able to integrate harmonics into a single percept with pitch. Finally, Clarkson and Clifton (1995) have demonstrated that 7-month-old infants can discriminate pitch changes in inharmonic complexes (where spectral content is resolved, but the harmonics do not fit exactly to the expected template of a complex tone), and that their performance is related to the degree of inharmonicity in a manner qualitatively similar to adult performance.

While infant pitch discrimination may be adult-like for stimuli containing robust spectral pitch cues, infants appear to be significantly impaired relative to adults when discriminating stimuli that do not contain such cues to pitch. This is consistent with Werner's (1992) suggestion that spectral mechanisms mature earlier in development than temporal mechanisms. Understanding how infants perform in the absence of resolved spectral information is important to the study of auditory development in general, and language acquisition in particular, because low frequency components are often masked in everyday noisy environments, such that only higher frequency, unresolved components remain as cues to vocal pitch. When presented with complex stimuli containing only higher, unresolved harmonics, infants do not appear to be able to successfully categorize them according to pitch in a behavioral conditioned head turn paradigm in which infants are rewarded for turning their head in response to a change in pitch (Clarkson & Rogers, 1995). Consistent with this, we (Butler, Folland, & Trainor, 2013) found that without any pitch-priming (i.e., training on how to perceive the pitch of such stimuli), 8-month-old infants did not show behavioral (conditioned head turn) discrimination of changes in the pitch of iterated rippled noise (IRN) stimuli.

IRN stimuli are created by repeatedly adding a sample of frozen white noise to itself following a short, fixed delay. In this way, temporal regularity is introduced, and a (weak) pitch percept is created that is equal to the inverse of the delay (e.g., a delay of 5 ms produces a perceived pitch of 200 Hz; Yost, 1996). The stimuli used in Butler et al. (2013) were high pass filtered so as to contain no resolved spectral cues, so the sensation of pitch was predominantly dependent on the temporal mechanism.

Interestingly, Butler et al. (2013) found that if given a period of training in which a sine tone was added to the IRN stimulus at the frequency of its perceived pitch, infants were able to behaviorally discriminate a pitch change from 167 Hz to 200 Hz above change levels. However, performance was still quite poor (d' = .69) under conditions where adults were 100% correct. It is therefore important to gather converging evidence that infants are able to process the pitch of IRN stimuli, and to investigate how pitch-priming affects representations for pitch in the infant nervous system. In the present paper, we look for evidence using ERPs that (1) infants 4 months and 8 months of age can use temporal cues to process IRN stimuli, and (2) that pitch representations in auditory cortex are enhanced after pitch-priming experience.

Exactly how and where pitch percepts are formed in auditory cortex is not entirely clear. However, functional imaging studies in adults suggest that a common pitch-processing center is located beyond primary auditory cortex, along the lateral aspect of Heschl's gyrus (Griffiths, Buchel, Frackowski, & Patterson, 1998; Hall, Barrett, Akeroyd, & Summerfield, 2005; Patterson, Uppenkamp, Johnsrude, & Griffiths, 2002; Penagos, Melcher, & Oxenham, 2004; Puschmann, Uppenkamp, Kollmeier, & Thiel, 2010). Moreover, an event-related potential study in adults has shown that pitch changes in IRN stimuli similar to those used in the current study elicit a mismatch negativity (MMN) component, the source of which is consistent with these imaging studies (Butler & Trainor, 2012). The MMN reflects automatic detection of an infrequent deviant stimulus, and can be recorded from both adults and infants. For example, an MMN-like deflection is elicited by changes in the frequency of synthesized piano tones in 2-month-old infants, which increases amplitude and decreases latency in the months that follow (He, Hotson, & Trainor, 2007; He et al., 2009). A number of other studies have also successfully used the MMN to study deviation in pure tone frequency (e.g., Alho, Sainio, Sajaniemi, Reinkainen, & Näätänen, 1990; Cheour et al., 1999; Čeponiené et al., 2000; Hirasawa, Kurihara, & Konishi, 2003; Leppänen, Guttorm, Pihko, Takkinen, & Lyytinen, 2004; Leppänen, Pihko, Eklund, & Lyytinen, 1999) and the pitch of harmonic tones (e.g., Čeponiené et al., 2002; Fellman et al., 2004; Kushnerenko et al., 2002).

No study to date has demonstrated evidence of a cortical basis for pitch discrimination in infants when the pitch-evoking stimuli contain no resolved spectral cues. Experiments 1 and 2 examine whether pitch changes in high-pass filtered IRN stimuli elicit a mismatch response in 4- and 8-month-old infant listeners. Experiment 2 asks whether brief priming of the pitch of IRN stimuli can enhance the representation of pitch in auditory cortex.

2. Experiment 1

2.1. Materials and methods

2.1.1. Participants

Fifteen 4-month old infants (8 males; mean age = 19.7 ± .17 weeks) and fifteen 8-month old infants (5 males; mean age = 36.0 ± .36 weeks) participated. All infants were born within 2 weeks of full term, were healthy at the time of testing, and no parent reported a history of chronic ear infection or hearing impairment. An additional 13 infants were unable to complete the minimum number of trials due to fussiness, while four infants were excluded from data analysis because excessive movement during testing left too few artifact-free trials.

2.1.2. Stimuli

The IRN stimuli used in this experiment were created by generating a sample of frozen white noise and adding it to itself following a delay equal to the inverse of the desired pitch. The standard stimulus had a perceived pitch of 167 Hz (corresponding to a 6 ms delay) and was presented on 85% of trials. The deviant stimulus

was presented on the remaining 15% of trials and had a perceived pitch of 200 Hz (corresponding to a 5 ms delay). The delay-and-add process was performed a total of 16 times, as the strength of the pitch percept has been shown to plateau following 16 iterations (Patterson, Handel, Yost, & Datta, 1996). Following this many iterations, some peaks appear in the power spectra of IRN stimuli. In order to eliminate the contribution of resolvable spectral pitch cues, IRN stimuli were high-pass filtered at 2600 Hz (high-order Butterworth filter), representing the 13th harmonic of the 200 Hz stimulus. Within a complex tone, individual harmonics with numbers below 5 appear well-resolved, while resolvability decreases between 5 and 8, such that harmonics above 8 are at best poorly resolved (see Moore and Gockel, 2011 for a review). Thus, this filter cutoff served to limit the spectral information in the IRN stimuli to the region of unresolved harmonics. Stimuli were 450 ms in length, had 10 ms onset and offset ramps, and were presented with a stimulus onset asynchrony (SOA) of 800 ms at 70 dBA. Sometimes high-pass filtered stimuli are presented in white noise in order to mask any potential low frequency distortion products arising from nonlinearities in the inner ear. However, these distortions depend on simplistic phase relationships between components (Pressnitzer & Patterson, 2001) that are weak, or not present in the IRN stimuli used in the present experiment (Sayles & Winter, 2008). Moreover, Winter, Wiegrebe, and Patterson (2001) have suggested that if IRN produces audible distortion products, they are at such a low level as to be essentially negligible. Thus, a white noise masker was not used in the present experiment to avoid creating any further ambiguity in an already weak pitch percept.

2.1.3. Procedure

Experimental procedures were explained to parents, who gave informed consent to have their child participate. Each infant was seated on his or her parent's lap in a sound-attenuated room, facing a loudspeaker and a computer monitor. In order to keep the infant still and awake during the experiment, he or she watched a silent movie and a puppet show provided by an experimenter seated in the room. Sounds were presented using E-Prime software through a loudspeaker located 1 m in front of the infant. The experiment consisted of 1600 trials and lasted approximately 21 min. Stimuli were presented in a quasi-random fashion, such that at least two standard stimuli were presented between deviant stimuli.

EEG data were recorded at a sampling rate of 1000 Hz from 124-channel HydroCel GSN nets (Electrical Geodesics, Eugene, OR) referenced to Cz. Impedance at each electrode was maintained below 50 kΩ during recording. EEG data were band-pass filtered offline between .5 and 20 Hz using EEProbe software to remove slow wave activity. Data were then resampled at 200 Hz and artifacts resulting from muscle activity such as eye blinking and head movements were removed using an Artifact Blocking paradigm in MATLAB (Mourad, Reilly, De Bruin, Hasey, & MacCrimmon, 2007). Finally, the data were re-referenced off-line to an average reference, and then segmented into 500 ms epochs that included a 100 ms baseline.

2.1.4. Analysis

Responses to standard and deviant stimuli were averaged, and difference waveforms were computed for each participant by subtracting their response to the standard stimulus from their response to the deviant stimulus. Grand average standard and deviant waveforms and difference waveforms (deviant-standard) were then computed for each age group. Subsequently, for statistical analysis, 90 electrodes were selected and divided into five groups for each hemisphere representing frontal, central, parietal, occipital, and temporal scalp regions (see Fig. 1). Electrodes near the face and periphery of the net were excluded in order to further reduce the impact of muscle artifacts from the eyes, face, and neck. Midline electrodes were excluded to allow for comparisons between hemispheres.

In both age groups, when the waveforms were averaged across all infants (grand average waveforms) a small negative-going component resembling the MMN response was observed at the frontal and central electrode sites (with reversing polarity at occipital and temporal electrodes). This component was not present at parietal sites, consistent with the inversion of morphology typically observed between frontal/central regions and occipital regions for responses generated in auditory cortex. Thus, parietal responses were eliminated from further analysis. To analyze the amplitude of the mismatch response, the latency of the component peak at the frontal electrode regions was determined from the grand average difference waveforms for each age group. The mean amplitudes of the standard and deviant waveforms were calculated for each subject and each region across a 50 ms window centered at this latency. A repeated-measures analysis of variance (ANOVA) was conducted to examine effects of stimulus type (standard, deviant), age (4 months, 8 months), scalp region (frontal, central, occipital, temporal), and hemisphere (left, right). Greenhouse–Geisser corrections were applied where necessary. The amplitudes in occipital and temporal regions were inverted in polarity for the analysis to ensure that any region effects represented true amplitude differences rather than polarity inversions.

2.2. Results

Figs. 2 and 3 show the grand average responses to the standard (solid lines) and deviant (dashed lines) stimuli for the 4-month-olds and 8-month-olds, respectively. Fig. 4 shows the grand average difference waves recorded from 4-month-old (solid lines) and 8-month-old listeners (dashed lines) in response to a change in the pitch of IRN stimuli. An ANOVA with stimulus type, age, scalp region, and hemisphere as within-subject factors, and age

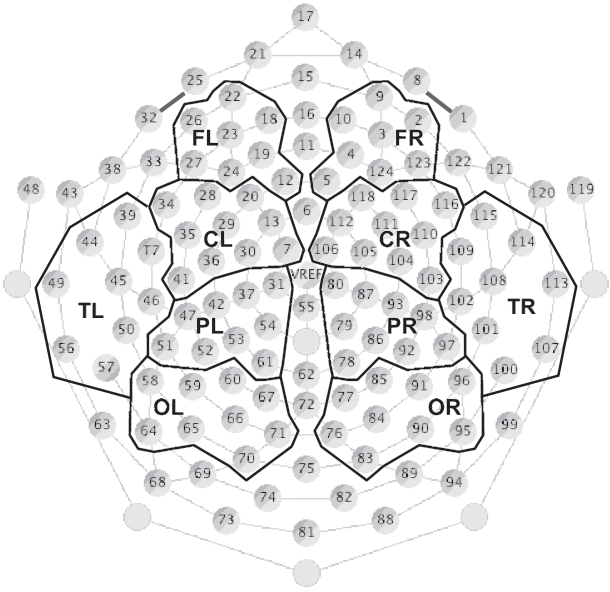

Fig. 1. Electrode groupings (see Section 2.1 for details). Ninety of 124 electrodes were divided into five groups (frontal, central, parietal, occipital, and temporal) for each hemisphere. Each group contained between 8 and 10 electrodes that were averaged together to represent EEG responses from that scalp region. The remaining channels around the perimeter of the net were excluded from analysis to avoid artifacts resulting from muscle activity in the face and neck, and channels along the midline were removed to allow for comparison between hemispheres.

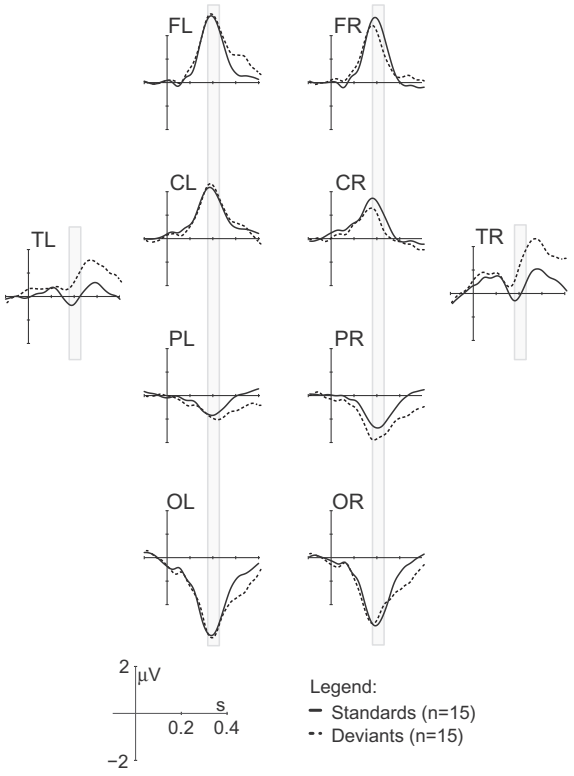

Fig. 2. Grand average responses to the standard, 167 Hz IRN stimulus (solid lines) and deviant, 200 Hz IRN stimulus (dashed lines) recorded from 4-month-old listeners in Experiment 1. Responses from each of the 10 electrode regions are presented. Vertical bars represent the temporal window over which the mean amplitude of the waveform was calculated for statistical analysis.

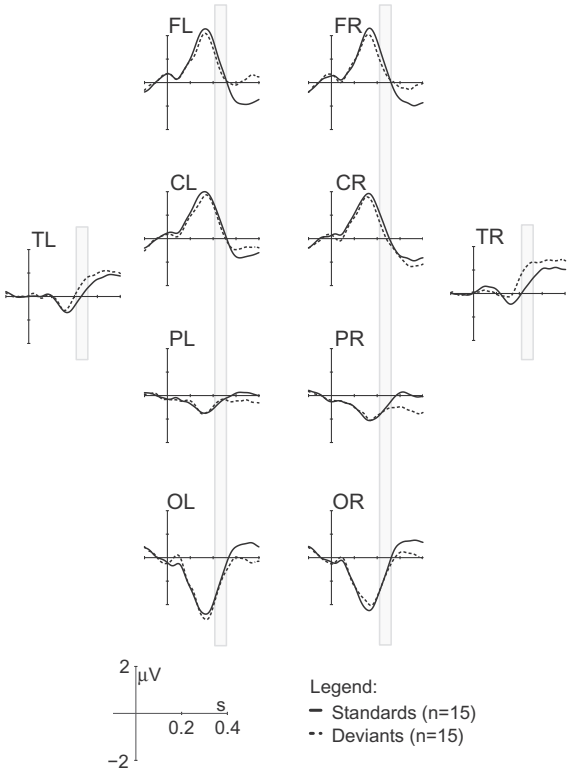

Fig. 3. Grand average responses to the standard, 167 Hz IRN stimulus (solid lines) and deviant, 200 Hz IRN stimulus (dashed lines) recorded from 8-month-old listeners in Experiment 1. Responses from each of the 10 electrode regions are presented. Vertical bars represent the temporal window over which the mean amplitude of the waveform was calculated for statistical analysis.

as a between-subjects factor revealed only a significant interaction between stimulus type and electrode region ($F[1.5, 40.6] = 9.54$, $p = 0.001$). As a result, separate repeated-measures ANOVAs were conducted for each region with stimulus type (standard, deviant), and hemisphere (left, right) as within-subject factors, and age (4 months, 8 months) as a between-subjects factor. These follow-up ANOVAs revealed that the MMN failed to reach significance (simple main effect of stimulus type) in the frontal ($F[1,28] = 3.17$, $p = 0.09$), central ($F[1,28] = 2.06$, $p = 0.2$), and occipital ($F[1,28] = 0.28$, $p = 0.6$) electrode regions, and was significantly different from zero only in the temporal regions ($F[1,28] = 26.95$, $p < 0.001$). No other main effects or interactions were significant.

In Experiment 2 we investigated whether infants' representations of the pitch of IRN stimuli could be changed and their performance improved with a brief priming of the pitches for which they were listening.

3. Experiment 2

3.1. Materials and methods

3.1.1. Participants

Fifteen, 4-month-old infants (5 males; mean age = 20.0 ± .17 weeks) and fifteen, 8-month old infants (12 males; mean age = 36.5 ± .27 weeks) participated. All infants were born within 2 weeks of full term, were healthy at the time of testing, and no parent reported a history of chronic ear infection or hearing impairment. An additional eight infants were unable to complete the minimum number of trials due to fussiness, while five infants were excluded from data analysis because excessive movement during testing left too few artifact-free trials.

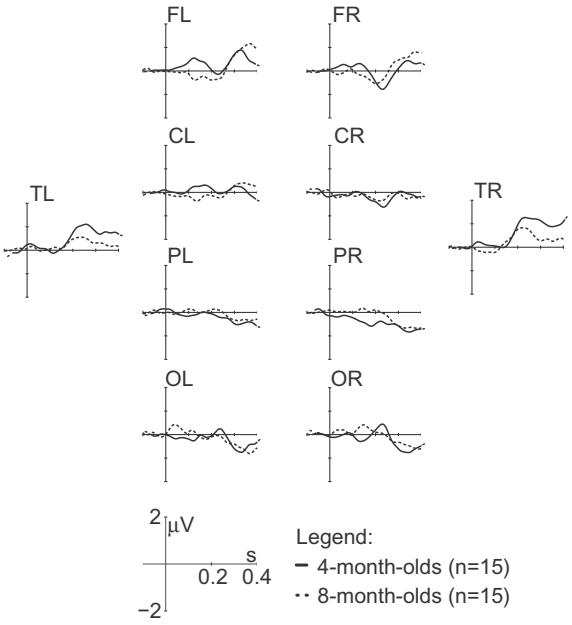

Fig. 4. Grand average difference waveforms (deviant-standard) for pitch changes recorded in Experiment 1. Responses from each of the 10 electrode regions are presented for both 4-month-olds (solid lines) and 8-month-olds (dashed lines).

3.1.2. Stimuli

Two types of stimuli were used in this experiment. The priming phase consisted of high-pass filtered IRN stimuli with a pure tone

of equivalent pitch added. The experimental phase consisted of the high-pass filtered IRN stimuli alone and was identical to Experiment 1. As in Experiment 1, in both the priming and experimental phases, the standard stimulus had a perceived pitch of 167 Hz and was presented on 85% of trials. The deviant stimulus was presented on the remaining 15% of trials and had a perceived pitch of 200 Hz. All stimuli were 450 ms in length, had 10 ms onset and offset ramps, and were presented with a stimulus onset asynchrony (SOA) of 800 ms at 70 dBA.

3.1.3. Procedure

The experimental procedure was identical to that of Experiment 1 with the following exceptions. The experiment included a priming phase consisting of 600 trials (lasting approximately 8 min), followed by the experimental phase consisting of 1600 trials (lasting approximately 21 min) that was identical to that of Experiment 1.

EEG data collected during the experimental phase were recorded, filtered, resampled, artifact blocked and re-referenced as in Experiment 1. Data collected during the priming phase were not analyzed as there were too few trials.

3.1.4. Analysis

Data were analyzed as in Experiment 1.

3.2. Results

Figs. 5 and 6 show the grand average responses to the standard (solid lines) and deviant (dashed lines) stimuli for the 4-month-olds and 8-month-olds, respectively. Fig. 7 shows the grand average difference waves recorded from 4-month-old (solid lines)

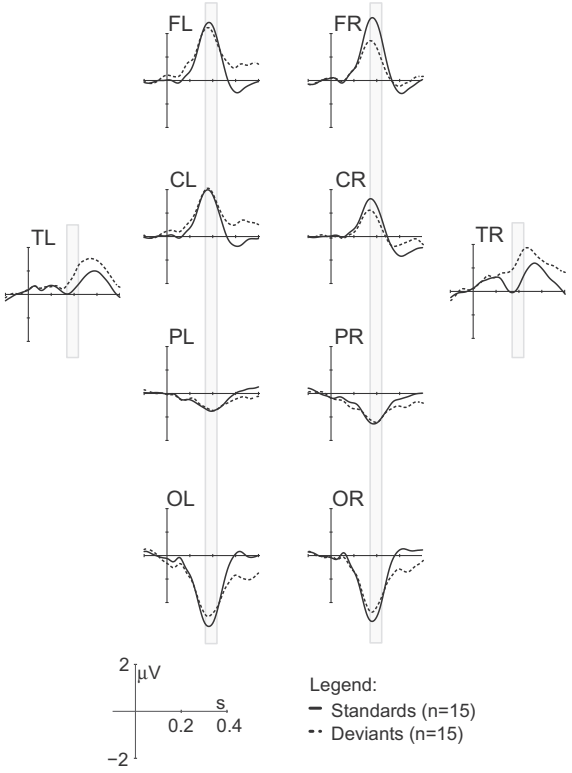

Fig. 5. Grand average responses to the standard, 167 Hz IRN stimulus (solid lines) and deviant, 200 Hz IRN stimulus (dashed lines) recorded from 4-month-old listeners in Experiment 2. Responses from each of the 10 electrode regions are presented. Vertical bars represent the temporal window over which the mean amplitude of the waveform was calculated for statistical analysis.

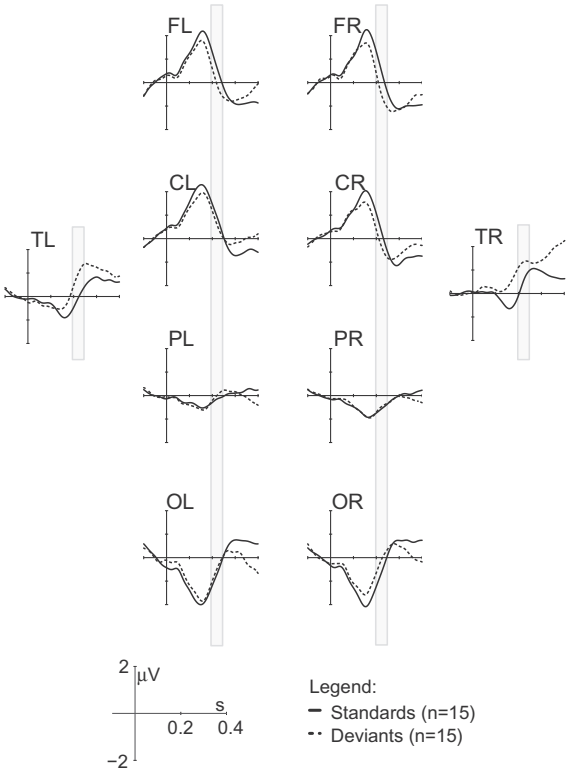

Fig. 6. Grand average responses to the standard, 167 Hz IRN stimulus (solid lines) and deviant, 200 Hz IRN stimulus (dashed lines) recorded from 8-month-old listeners in Experiment 2. Responses from each of the 10 electrode regions are presented. Vertical bars represent the temporal window over which the mean amplitude of the waveform was calculated for statistical analysis.

and 8-month-old listeners (dashed lines) in response to a change in the pitch of IRN stimuli. An ANOVA with stimulus type, age, scalp region, and hemisphere as within-subject factors, and age as a between-subjects factor revealed significant interactions between stimulus type and hemisphere ($F[1,28] = 7.05$, $p = 0.01$; MMN was larger in the right hemisphere than in the left across electrode regions), and between stimulus type and electrode region ($F[1.4, 38.2] = 31.09$, $p < 0.001$). No other interaction or main effect reached significance. Separate follow-up repeated-measures ANOVAs were conducted for each region with stimulus type (standard, deviant), and hemisphere (left, right) as within-subject factors, and age (4 months, 8 months) as a between-subjects factor. These follow-up ANOVAs revealed that the MMN measured across the 50 ms window was significantly different from zero (simple main effect of stimulus type) in the frontal ($F[1,28] = 18.85$, $p < 0.001$), central ($F[1,28] = 7.29$, $p = 0.01$), occipital ($F[1,28] = 4.43$, $p = 0.04$), and temporal ($F[1,28] = 55.20$, $p < 0.001$) electrode regions. Consistent with the initial ANOVA, a significant main effect of hemisphere was observed in the ANOVA for each electrode region (all ps equal to or less than 0.05). No other interactions or main effects reached significance in these follow-up ANOVAs.

In order to compare the amplitude of the MMN response across experiments, a mixed-model ANOVA was conducted with region (frontal, central, occipital, temporal), hemisphere (left, right), and stimulus type (standard, deviant) as within-subject factors, and with age and listening condition (unprimed, primed) as between-subjects factors. Although the average MMN amplitude was larger across all electrode regions in Experiment 2 than in Experiment 1, this difference (stimulus type X listening condition) approached, but failed to reach significance ($F[1,56] = 2.15$, $p = 0.1$). No other interactions involving listening condition were significant.

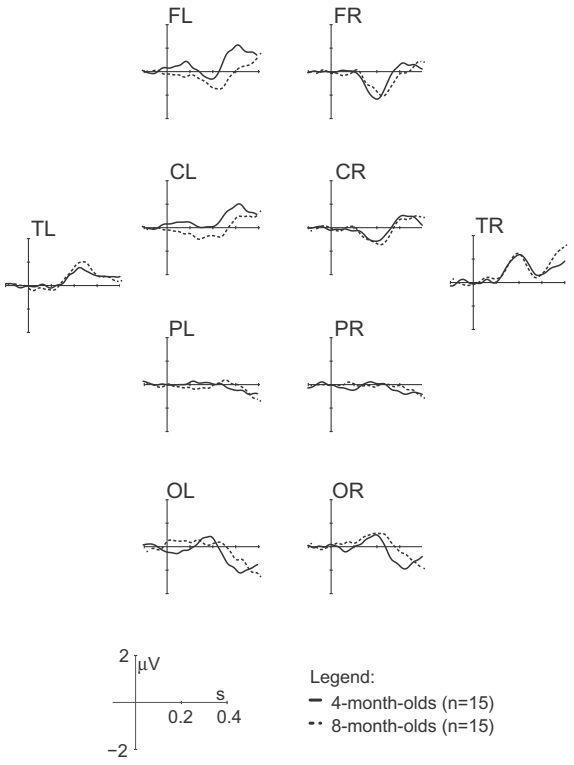

Fig. 7. Grand average difference waveforms (deviant-standard) for pitch changes recorded in Experiment 2. Responses from each of the 10 electrode regions are presented for both 4-month-old (solids lines) and 8-month-olds (dashed lines).

4. Discussion

A previous behavioral study found that 8-month-old infants showed no evidence of the ability to discriminate the pitch of IRN stimuli that contained no resolvable harmonics, unless previously primed with IRN stimuli with added sine tones at the frequencies of the pitch percepts (Butler et al., 2013). The electrophysiological evidence presented here corroborates this behavioral evidence. In Experiment 1, infants showed a small, negative-going deflection in response to a pitch change in IRN stimuli, but that response failed to reach significance in the frontal, central, or occipital electrode regions where MMN is typically seen, although it did reach significance in temporal regions. In Experiment 2, after pitch-priming, a significant negative response was seen across all regions tested, specifically, at frontal, central, occipital, and temporal sites. While the difference in response amplitudes between Experiments 1 and 2 failed to reach significance, there was a trend in this direction, suggesting that a brief period of pitch-priming may be sufficient to increase the electrophysiological response to a pitch-change in IRN stimuli. These results are consistent with those of the behavioral study of Butler et al. (2013), which found that infants failed to show pitch discrimination of IRN stimuli prior to priming, but did show clear discrimination after pitch-priming. The present study suggests that infants' failure to discriminate IRN pitch is not due to attentional processes because MMN is a preattentive component that is evoked regardless of whether the person is aware of or attending to the pitch change. Rather, the present results suggest that prior to pitch-priming, there is a lack of differential representations in auditory cortex for IRN stimuli of different pitches. However, after a brief period of pitch- priming, the larger MMN deflections generated in response to IRN stimuli of different pitch appear to provide a sufficient basis for behavioral discrimination. Thus, pitch-priming can successfully modulate both preattentive electrophysiological responses and behavioral responses to changes in the pitch of IRN stimuli. To our knowledge, the current study is the first to demonstrate that infants as young as 4 months of age can discriminate pitch-evoking auditory stimuli that contain no resolvable spectral cues.

Infants have been shown to process pitch-evoking stimuli in an adult-like manner in the presence of robust spectral cues (Čeponienė et al., 2002; Fellman et al., 2004; He et al., 2007; Kushnerenko et al., 2002). For deviations in the pitch of the missing fundamental, an MMN-like negativity emerges by 4 months of age (He & Trainor, 2009). This suggests that 4-month-old infants are capable of integrating the harmonic structure of pitch-evoking stimuli into a single pitch percept. Moreover, it suggests that the cortical generators of the MMN are in place by 4 months of age for stimuli that contain resolved spectral content.

While resolved spectral information may provide the most salient cues to pitch, temporal cues also make a functionally important contribution to pitch perception. For example, the ability to extract pitch in the absence of resolved spectral cues allows one to communicate over the telephone, where band-pass filters often remove resolvable harmonics, or to understand speech against a noisy background that often masks those same harmonics. Thus, in situations where spectral cues to pitch are unavailable, both infants and adults, rely more heavily on temporal information. The fact that behavioral performance is low for discriminating pitch-evoking stimuli without resolved spectral cues (Butler et al., 2013; Clarkson & Rogers, 1995), and that electrophysiological responses are only significant after priming, suggests that the temporal mechanism for pitch is slower to mature than the spectral mechanism. This is consistent with the literature on infant pure tone frequency discrimination, which suggests a similar pattern of development (see Werner, 1992 for review). However, the presence of a significant MMN response in the difference wave of the infants in the present study provides evidence that infants can extract pitch from stimuli where spectral cues are limited to the unresolvable region.

The pitch-priming phase of Experiment 2 provided resolved spectral pitch cues (a pure tone at the fundamental frequency of the IRN stimulus) in an effort to make clear to infants the basis on which the different stimuli could be most easily discriminated. Following this priming period, the mismatch response recorded during the test period (where pure tones were removed) reached significance in both 4- and 8-month-old listeners. The MMN is thought to reflect the passive updating of auditory memory traces. Thus, it appears that the experience acquired during the pitch-priming phase impacts the formation of these auditory traces in the subsequent testing phase. Similar effects of learning on evoked components have been observed previously in adults. MMN responses to unattended deviants have been shown to emerge slowly across blocks in a single experimental session (Näätänen, Schröger, Karakas, Tervaniemi, & Paavilainen, 1993). However, in this case, passive listening blocks were interspaced with blocks requiring active discrimination; repeated, unattended exposure to the stimuli alone was insufficient to affect passive discrimination. This suggests that, in adults, the process of attending to, and/or actively discriminating stimuli sharpens encoding in auditory memory such that the representation of the standard stimulus is precise enough to allow for the passive discrimination of a deviant. In a related study, Schulte, Knief, Seither-Preisler, and Pantev (2001) demonstrated that adults learn to use complex pitch cues following repeated exposure to a melody. Learning was indexed by an increase in evoked gamma band responses, suggesting increased neural synchrony and/or an enlargement of the cortical network generating the response. Both of these studies demonstrate an effect of exposure on cortically-evoked responses. However, each

depends to some extent on attention to the stimuli being discriminated. Attention is not easily manipulated in infant listeners, as it can be difficult to capture and maintain. Moreover the maturational states of attentional networks and working memory during early infancy are poorly understood. However, the present study demonstrates that a short amount of passive exposure may be sufficient to modulate cortically-evoked, processing-related ERP components in infants aged 4–8 months, and thus that learning may be qualitatively different early in development.

Across ages in the current study, mismatch responses to a change in IRN pitch were much larger in amplitude in right hemisphere electrodes than in left hemisphere electrodes. This is in agreement with recent imaging studies in adults suggesting that the right hemisphere is selectively activated in tasks related to pitch perception (Hyde, Peretz, & Zatorre, 2008), and production (Perry et al., 1999). Moreover, lesion studies suggest that the right hemisphere dominates perception of the pitch of the missing fundamental (Zatorre, 1988), processing of complex spectral structures (Sidtis & Volpe, 1988), and discrimination of melodic pitch patterns (Zatorre, 1985, 1988). Functional lateralizations have been previously demonstrated in infants in response to a variety of acoustic properties including: speech signals (e.g., Dehaene-Lambertz et al., 2010), pitch accents (Sato, Sogabe, & Mazuka, 2010), and temporal structures (Telkemeyer et al., 2009). In many cases, these asymmetries resemble those recorded from adult listeners. Thus, the hemisphere effect observed in the present study may represent an early right-hemisphere specialization for pitch processing.

Behavioral evidence suggests that spectral cues dominate pitch perception in infancy (Butler et al., 2013; Clarkson & Rogers, 1995); discrimination is drastically impaired in the absence of resolved spectral pitch cues. However, the present study demonstrates that, following a period of pitch-priming, infants as young as 4-months-old produce a significant mismatch component in response to a pitch change in IRN stimuli that lack resolvable spectral information. This represents the first evidence for a cortical representation of pitch discrimination by infant listeners in the absence of spectral cues. In future studies, it would be of interest to use ERPs to examine infant pitch discrimination for other types of auditory stimuli that evoke a pitch sensation in the absence of resolved spectral cues (e.g., high-pass filtered complex tones, Huggins pitch, click trains, etc.) and whether priming can similarly lead to better pitch processing for such stimuli in infancy.

Acknowledgments

This research was supported by grants to LJT from the Natural Sciences and Engineering Research Council of Canada (NSERC) and the Canadian Institutes of Health Research (CIHR) and an NSERC graduate scholarship to BEB. The authors wish to thank Elaine Whiskin and Cathy Chen for assisting with data collection.

References

Alho, K., Sainio, K., Sajaniemi, N., Reinkainen, K., & Näätänen, R. (1990). Event-related brain potentials of human newborns to pitch change of an acoustic stimulus. *Electroencephalography and Clinical Neurophysiology/Evoked Potentials Section, 77*, 151–155.

Bregman, A. S. (1990). *Auditory scene analysis: The perceptual organization of sound*. Cambridge: MIT Press.

Butler, B. E., & Trainor, L. J. (2012). Sequencing the cortical processing of pitch-evoking stimuli using EEG and source estimation. *Frontiers in psychology, 180*, 1–13.

Butler, B. E., Folland, N. A., & Trainor, L. J. (2013). Development of pitch processing: Infants' discrimination of iterated rippled noise stimuli with unresolved spectral content. *Hearing Research, 304*, 1–6.

Cariani, P. A., & Delgutte, B. (1996). Neural correlates of the pitch of complex tones. I. Pitch and pitch salience. *Journal of Neurophysiology, 76*, 1698–1716.

Carney, L. H., & Yin, T. C. T. (1988). Temporal coding of resonances by low-frequency auditory nerve fibers: Single-fiber responses and a population model. *Journal of Neurophysiology, 60*, 1653–1677.

Cedolin, L., & Delgutte, B. (2007). Spatio-temporal representation of the pitch of complex tones in the auditory nerve. In B. Kollmeier, V. Hohmann, U. Langemann, M. Mauermann, S. Uppenkamp, & J. Verhey (Eds.), *Hearing – From sensory processing to perception* (pp. 61–70). Berlin: Springer-Verlag.

Čeponiené, R., Hukki, J., Cheour, M., Haapanen, M. L., Koskinen, M., Alho, K., et al. (2000). Dysfunction of the auditory cortex persists in infants with certain cleft types. *Developmental Medicine and Child Neurology, 42*, 258–265.

Čeponiené, R., Kushnerenko, E., Fellman, V., Renlund, M., Suominen, K., & Näätänen, R. (2002). Event-related potential features indexing central auditory discrimination by newborns. *Brain Research, 13*, 101–113.

Cheour, M., Čeponiené, R., Hukki, J., Haapanen, M. L., Näätänen, R., & Alho, K. (1999). Brain dysfunction in neonates with cleft palate revealed by the mismatch negativity. *Clinical Neurophysiology, 110*, 324–328.

Clarkson, M. G., & Clifton, R. K. (1985). Infant pitch perception: Evidence for responding to pitch categories and the missing fundamental. *Journal of the Acoustical Society of America, 77*, 1521–1528.

Clarkson, M. G., & Clifton, R. K. (1995). Infants' pitch perception: Inharmonic tonal complexes. *Journal of the Acoustical Society of America, 98*, 1372–1379.

Clarkson, M. G., & Rogers, C. (1995). Infants require low-frequency energy to hear the pitch of the missing fundamental. *Journal of the Acoustical Society of America, 98*, 148–154.

Dehaene-Lambertz, G., Montavont, A., Jobert, A., Allirol, L., Dubois, J., Hertz-Pannier, L., et al. (2010). Language or music, mother or Mozart? Structural and environmental influences on infants' language networks. *Brain and Language, 114*, 53–65.

Delgutte, B., & Cariani, P. (1992). Coding of the pitch of harmonic and inharmonic complex tones in the interspike intervals of auditory nerve fibers. In M. E. H. Schouten (Ed.), *The processing of speech* (pp. 37–45). Berlin: Mouton-De Gruyter.

Evans, E. F. (1977). Frequency selectivity at high signal levels of single units in cochlear nerve and nucleus. In E. F. Evans & J. P. Wilson (Eds.), *Psychophysics and physiology of hearing* (pp. 185–192). New York: Academic.

Fellman, V., Kushnerenko, E., Mikkola, K., Čeponiené, R., Leipala, J., & Näätänen, R. (2004). Atypical auditory event-related potentials in preterm infants during the first year of life: A possible sign of cognitive dysfunction? *Pediatric Research, 56*, 197–291.

Fletcher, H. (1938). The mechanism of hearing as revealed through experiment on the masking effect of thermal noise. *Proceedings of the National Academy of Sciences of the United States of America, 24*, 265–274.

Griffiths, T. D., Buchel, C., Frackowski, R. S. J., & Patterson, R. D. (1998). Analysis of temporal structure in sound by the human brain. *Nature Neuroscience, 1*, 422–427.

Hall, D. A., Barrett, D. J. K., Akeroyd, M. A., & Summerfield, A. Q. (2005). Cortical representations of temporal structure in sound. *Journal of Neurophysiology, 94*, 3181–3191.

He, C., Hotson, L., & Trainor, L. J. (2007). Mismatch responses to pitch changes in early infancy. *Journal of Cognitive Neuroscience, 19*, 878–892.

He, C., Hotson, L., & Trainor, L. J. (2009). Maturation of cortical mismatch responses to occasional pitch change in early infancy: Effects of presentation rate and magnitude of change. *Neuropsychologia, 47*, 218–229.

He, C., & Trainor, L. J. (2009). Finding the pitch of the missing fundamental in infants. *Journal of Neuroscience, 29*, 7718–7722.

Hirasawa, K., Kurihara, M., & Konishi, Y. (2003). The relationship between mismatch negativity and arousal level. Can mismatch negativity be an index for evaluating the arousal level in infants? *Sleep Medicine, 3*, 45–48.

Hyde, K. L., Peretz, I., & Zatorre, R. J. (2008). Evidence for the role of the right auditory cortex in fine pitch resolution. *Neuropsychologia, 46*, 632–638.

Kushnerenko, E., Čeponiené, R., Balan, P., Fellman, V., Huotilainen, M., & Näätänen, R. (2002). Maturation of the auditory change detection response in infants: A longitudinal ERP study. *NeuroReport, 13*, 1843–1848.

Larsen, E., Cedolin, L., & Delgutte, B. (2008). Pitch representation in the auditory nerve: Two concurrent complex tones. *Journal of Neurophysiology, 100*, 1301–1319.

Leppänen, P. H. T., Guttorm, T. K., Pihko, E., Takkinen, S., & Lyytinen, H. (2004). Maturational effects on newborn ERPs measured in the mismatch negativity paradigm. *Experimental Neurology, 190*, 91–101.

Leppänen, P. H. T., Pihko, E., Eklund, K. M., & Lyytinen, H. (1999). Cortical responses of infants with and without a genetic risk for dyslexia: II. Group effects. *NeuroReport, 10*, 969–973.

Meddis, R., & O'Mard, L. (1997). A unitary model of pitch perception. *Journal of the Acoustical Society of America, 102*, 1811–1820.

Montgomery, C. R., & Clarkson, M. G. (1997). Infants' pitch perception: Masking by low- and high-frequency noises. *Journal of the Acoustical Society of America, 102*, 3665–3672.

Moore, B. C. J. (2008). *An introduction to the psychology of hearing* (5th ed.). London: Emerald Group Publishing.

Moore, B. C. J., & Gockel, H. E. (2011). Resolvability of components in complex tones and implications for theories of pitch. *Hearing Research, 276*, 88–97.

Mourad, N., Reilly, J. P., De Bruin, H., Hasey, G., & MacCrimmon, D., (2007). A simple and fast algorithm for automatic suppression of high amplitude artifacts in EEG data, In IEEE international conference on acoustics, speech and signal processing – proceedings ICASSP, Honolulu, pp. 1393–1396.

Näätänen, R., Schröger, E., Karakas, S., Tervaniemi, M., & Paavilainen, P. (1993). Development of a memory trace for a complex sound in the human brain. *NeuroReport, 4*, 503–506.

Patterson, R. D., Handel, S., Yost, W. A., & Datta, A. J. (1996). The relative strength of the tone and noise components in iterated rippled noise. *Journal of the Acoustical Society of America, 100*, 3286–3294.

Patterson, R. D., Uppenkamp, S., Johnsrude, I. S., & Griffiths, T. D. (2002). The processing of temporal pitch and melody information in auditory cortex. *Neuron, 36*, 767–776.

Penagos, H., Melcher, J. R., & Oxenham, A. J. (2004). A neural representation of pitch salience in nonprimary human auditory cortex revealed with functional magnetic resonance imaging. *Journal of Neuroscience, 24*, 6810–6815.

Perry, D. W., Zatorre, R. J., Petrides, M., Alivisatos, B., Meyer, E., & Evans, A. C. (1999). Localization of cerebral activity during simple singing. *NeuroReport, 10*, 3979–3984.

Plomp, R. (1964). The ear as a frequency analyzer. *Journal of the Acoustical Society of America, 36*, 1628–1636.

Pressnitzer, D., & Patterson, R. D. (2001). Distortion products and the perceived pitch of complex tones. In D. J. Breebart, A. J. M. Houtsma, A. Kohlrausch, V. F. Prijs, & R. Schoonhoven (Eds.), *Physiological and psychophysical bases of auditory function* (pp. 97–104). Masstricht, The Netherlands: Shaker.

Puschmann, S., Uppenkamp, S., Kollmeier, B., & Thiel, C. M. (2010). Dichotic pitch activates pitch processing centre in Heschl's gyrus. *Neuroimage, 49*, 1641–1649.

Sato, Y., Sogabe, Y., & Mazuka, R. (2010). Development of hemispheric specialization for lexical pitch-accent in Japanese infants. *Journal of Cognitive Neuroscience, 22*, 2503–2513.

Sayles, M., & Winter, I. M. (2008). Ambiguous pitch and the temporal representation of inharmonic iterated rippled noise in the ventral cochlear nucleus. *Journal of Neuroscience, 28*, 11925–11938.

Schulte, M., Knief, A., Seither-Preisler, A., & Pantev, C. (2001). Gestalt recognition in a virtual melody experiment. In J. Nenonen, R. Ilmoniemi, & T. Katila (Eds.), *Biomag 2000, proceedings of the 12th international conference on biomagnetism* (pp. 107–110). Espoo, Finland: Helsinki University of Technology.

Sidtis, J. J., & Volpe, B. T. (1988). Selective loss of complex-pitch of speech discrimination after unilateral lesion. *Brain and Language, 34*, 235–245.

Telkemeyer, S., Rossi, S., Koch, S. P., Nierhaus, T., Steinbrink, J., Poeppel, D., et al. (2009). Sensitivity of newborn auditory cortex to the temporal structure of sounds. *Journal of Neuroscience, 29*, 14726–14733.

Trainor, L. J., & Corrigall, K. A. (2010). Music acquisition and effects of musical experience. In M. Riess-Jones & R. R. Fay (Eds.), *Springer handbook of auditory research: Music perception* (pp. 89–128). Heidelberg: Springer.

Von Bekesy, G. (1960). *Experiments in hearing*. New York: McGraw-Hill.

Werner, L. A. (1992). Interpreting developmental psychoacoustics. In L. A. Werner & E. W. Rubel (Eds.), *Developmental psychoacoustics* (pp. 47–88). Washington: American Psychological Association.

Winter, I. M., Wiegrebe, L., & Patterson, R. D. (2001). The temporal representation of the delay of iterated rippled noise in the ventral cochlear nucleus of the guinea-pig. *Journal of Physiology, 537*, 553–566.

Yost, W. A. (1996). Pitch strength of iterated rippled noise. *Journal of the Acoustical Society of America, 100*, 3329–3335.

Zatorre, R. J. (1985). Discrimination and recognition of tonal melodies after unilateral cerebral excisions. *Neuropsychologia, 23*, 31–41.

Zatorre, R. J. (1988). Pitch perception of complex tones and human temporal-lobe function. *Journal of the Acoustical Society of America, 84*, 566–572.